DOCTOR OF PHILOSOPHY

Flexural Behaviour of Reinforced Concrete Beams with Recycled Aggregates and Steel Fibres

Anike, Emmanuel Ejiofor

Award date:
2021

Awarding institution:
Coventry University

DOCTOR OF PHILOSOPHY

Flexural Behaviour of Reinforced Concrete Beams with Recycled Aggregates and Steel Fibres

Anike, Emmanuel Ejiofor

Award date:
2021

Awarding institution:
Coventry University

Flexural Behaviour of Reinforced Concrete Beams with Recycled Aggregates and Steel Fibres

By

Emmanuel Ejiofor Anike

A thesis submitted in partial fulfilment of the University's requirements for the Degree of Doctor of Philosophy

August 2020

Certificate of Ethical Approval

Applicant:

Emmanuel Anike

Project Title:

Flexural behaviour of reinforced concrete beams with recycled aggregates and steel fibres

This is to certify that the above named applicant has completed the Coventry University Ethical Approval process and their project has been confirmed and approved as Low Risk

Date of approval:

25 February 2020

Project Reference Number:

P103848

Dedication

To the memory of my father, Mr. Shedrack Anike Nsude, who humorously called me Headmaster when I was still five years old.

Acknowledgement

My profound gratitude goes to my amiable Director of Studies, Associate Professor Messaoud Saidani, for his contributions in many ways and understanding of human frailties, from the commencement of my study through the preparation of this work. He was, indeed, exceptional.

I deeply appreciate the rest members of my supervisory team—Dr. Adegoke Olubanwo, Professor Eshmaiel Ganjian, and Professor Mark Tyrer—for their great input and encouragements. It was an absolute pleasure working with them.

Dr. Ucheowaji Ogbologugo was helpful during the numerical analysis aspect of this work, and I am grateful. The university's Civil Engineering department technicians: Ian Breakwell, Kieran Teeling, and Tim Griffiths were instrumental during the laboratory experiments, and I thank them. The assistance offered by Laith Alhelalat, Henry Tachie-Menson, Ayodeji Bamgbelu, and Karandeep Sohal who had their undergraduate and postgraduate final-year projects under my supervision is worth mentioning. My heartfelt thanks to my mentor, Engr. Dr. Uchechukwu C. Anya and Dr. Justin Okoli for their invaluable support. I wish to thank in a special way, Professor Don Harris for his encouragement during the preparation of this work.

Special thanks to the managements of Litecast Homefloor Limited, Nuneaton, United Kingdom and Dalian HARVEST Metal Fibres Co. Limited, Zhongshan Dist., China for supplying all the raw materials used for experimentation, free of charge.

Furthermore, I remain indebted to the Centre for Low Impact Buildings, Coventry University, for awarding me a PhD studentship. Throughout my PhD journey, considerable guidance and assistance were received from the management and staff of Coventry University starting from Doctoral College to the Faculty of Engineering, Environment and Computing, Library, Registry, Student Centre, IT, etc. To them I pay tribute.

Finally, the love, prayers, and encouragement of my dearest wife, Mirian, to this feat cannot be overemphasized and I thank her a great deal. My precious kids: Neriah, Esther, and David, who required much attention, motivated me. My sweet mother, Beatrice, and my siblings—Onyenma, Eric, Charles, Daniel, Ngozi, Isaiah and Joshua—were supportive in numerous ways. Consistent prayers were said on my behalf by Pastor Blessing Nkwocha of which I greatly appreciate. Also, I sincerely appreciate the assistance and prayers of the following: Pastor Praise Kayode, Rev & Mrs. Patrick Nwachukwu, Mr. & Mrs. Rowland Ohiagu, Mr. Joshua Nwachukwu, and Mr. and Mrs. Desmond Etukudo. Additionally, I enjoyed the company of my pal, Obiajulu Iweka (PhD), and I am very thankful.

Above all, I owe it all to God for wisdom, knowledge, understanding, and good health throughout my programme. To Him alone be the glory.

Abstract

The use of recycled aggregate concrete is on the increase but the remnant of mortar clinging to the aggregate, typically lightweight and porous, is responsible for its downsides when compared to normal concrete. This presence of mortar makes the recycled aggregate (RA) a heterogeneous substance (as opposed to the homogeneity of the natural aggregate). Consequently, the mix design method appropriate to RA reuse for structural purposes, has long been debated.

In this work, conventional and unconventional mix design methods were investigated to determine the flexural performance of reinforced concrete beams produced with RA obtained from a precast waste concrete and steel fibres. Both experimental and numerical investigations were employed in this research. The experimental study involved: characterization of the aggregates, design of the concrete mixes, set of trial mixes to attain mixtures of comparable workability and to optimize steel fibre content appropriate to the design methods, and the production, curing, and testing of concrete specimens for mechanical and durability properties.

Two conventional methods—absolute volume method given by the American Concrete Institute (ACI) and the British Department of Environment (DoE) guidelines—were examined experimentally for the production of recycled aggregate concrete. The rationale was to ascertain which of the two traditional methods would manage resources better without compromising strength all the same. Eventually, five principal mixes were developed and investigated experimentally as follows: natural aggregate concrete (NAC), recycled aggregate concrete (RAC) composed of 100% RA, steel fibre-reinforced recycled aggregates concrete (SFRRAC) made of 100% RA and 1% steel fibre content by volume of concrete, blended aggregate concrete (BAC) which consisted of 60% RA and 40% normal aggregates, and steel fibre-reinforced blended aggregate concrete (SFRBAC) constituting of the BAC mix with 0.5% steel fibre volume ratio. Whereas the NAC, RAC, and SFRRAC mixes were designed using the ACI approach, the BAC and SFRBAC mixes were proportioned according to the *extended* Equivalent mortar volume (EMV) technique. Then, the flexural behaviour of the reinforced concrete beams was simulated using commercial ANSYS Mechanical APDL 2019 R1 software, with the aid of finite element model, for the numerical investigation.

The results of the experiments showed that the oven-dry specific gravity of recycled fine aggregates (RFA) and recycled coarse aggregates (RCA) were respectively 23% and 12% lower than those of their corresponding natural aggregates. The average water absorption capacity of RFA and RCA were 13% and 5.3%, while those of their comparable natural aggregates were 1.0% and 0.8%, respectively. The mortar content of the RCA was 52%. Comparatively, the ACI mix design method used about 11% lesser amount of cement to produce RAC of a higher strength than its DoE counterpart. With over 28% reduction in cement content, the BAC mix produced a concrete of comparable compressive strength to that of the NAC mix and of a higher compressive strength relative to those of RAC and SFRRAC mixes. In spite of mix design methods, all

concretes composed of RA showed a substantially higher tensile splitting strength than the conventional concrete. The flexural strength of the concrete mixes was not dependent on both RA and RA content.

The flexural behaviour of the tested beams revealed that the SFRRAC had the most load bearing capacity. Although both BAC and NAC beams gave the same load capacity, the former showed a fewer crack, the least crack width (at the fracture), and visually the least deflected at failure compared to the other beams. The greatest effect of steel fibres was on the tensile splitting strength, moment capacity, and ductile failure mode of the SFRRAC beams. Finally, all the concretes containing RA and prepared in the conventional way, exhibited a higher water absorption capacity up to a degree of 49% than the normal concrete. Nevertheless, the use of the EMV procedure reduced this gap to just 8.8%.

This research necessitates that the ACI and DoE mix design methods be revised for concrete containing RA. This is essential to encourage the use of the actual properties of the RA (particularly their water absorption capacity) instead of adopting the tables of values and curves developed from the results of the experiments conducted using natural aggregates. Also, the extended application of the EMV mix design technique has, in this research, been proven adequate for the production of recycled aggregate concrete fit for structural purposes.

Publications

◊ **Anike, E.E.**, Saidani, M., Ganjian, E., Tyrer, M., Olubanwo, A.O. Evaluation of conventional and equivalent mortar volume mix design methods for recycled aggregate concrete. *Mater Struct* **53,** 22 (2020). https://doi.org/10.1617/s11527-020-1457-3

◊ **E. E. Anike**, M. Saidani, A. O. Olubanwo, M. Tyrer and E. Ganjian. Effect of mix design methods on the mechanical properties of steel fibre-reinforced concrete prepared with recycled aggregates from precast waste, *Structures,* 27 (2020) pp. 664–672, https://doi.org/10.1016/j.istruc.2020.05.038

◊ **Anike, E.E.**, Saidani, M., Ganjian, E., Tyrer, M. and Olubanwo, A. (2019), "The potency of recycled aggregate in new concrete: a review", *Construction Innovation*, Vol. 19 No. 4, pp. 594-613. https://doi.org/10.1108/CI-07-2018-0056

◊ **E. E. Anike**, M. Saidani, A. O. Olubanwo and M. Tyrer (2020) Extended application of the Equivalent Mortar Volume mix design method for recycled aggregate concrete. *5th World Congress on Civil, Structural, and Environmental Engineering (CSEE'20).* Virtual Conference. Paper No. ICSECT 132. DOI:10.11159/icsect20.132.

◊ **Anike, E. E.**, Saidani, M., Ganjian, E. & Tyrer, M. (2018). Recycled Concrete Aggregate and its Prospects in Structural Concrete. Young Researchers' Forum IV Innovation in Construction Materials. Newcastle-Upon-Tyne, UK. pp. 75-78.

Table of Contents

Appendices

List of Tables

List of Figures

List of Abbreviations

ACI – American Concrete Institute
ACPA – American Concrete Pavement Association
ACS – average compressive strength
AP – apparent
ASTM – American Society for Testing and Materials
BAC – blended aggregate concrete
BS – British standard
CC – conventional concrete (or control concrete where stated)
CDW – construction and demolition waste
CS – compressive strength
DoE – Department of Environment
EMV – equivalent mortar volume
FEA – finite element analysis
FS – flexural strength
ITZ – interfacial transition zone
LVDT – linear variable displacement transducer
NA – natural aggregate
NAC – natural aggregate concrete
NCA – natural coarse aggregate
NFA – natural fine aggregate
OD – oven-dry
PPM – Particle Packing Method
RA – recycled aggregate
RAC – recycled aggregate concrete
RCA – recycled coarse aggregate
RFA – recycled fine aggregate
RMC – residual mortar content
SF – steel fibre
SFRBAC – steel fibre-reinforced blended aggregate concrete
SFRC – steel fibre-reinforced concrete
SFRRAC – steel fibre-reinforced recycled aggregate concrete
SP - superplasticizer
SSD – saturated surface-dry density
STS – splitting tensile strength
TSMA – two-stage mixing approach
US – United States
WBCSD – World Business Council for Sustainable Development

List of Symbols

a – shear span

A_c – cross-sectional area of specimen

A_s – cross-sectional area of steel reinforcement

b – width of specimen

d – average depth of specimen (or diameter of specimen or effective depth where stated)

D – density of specimen

E_c – elastic modulus of concrete

E_M – experiment ultimate moment

E_P – experimental ultimate load

E_s – elastic modulus of steel reinforcement

E_s' – tangent modulus of steel reinforcement

E_δ – experimental mid-span deflection

f_c– compressive strength

f_{ct} – tensile splitting strength

f_f – flexural strength (or modulus of rupture)

f_{f1} – first-peak strength

f_{fp} – peak strength

f_{f600}^D – residual strength at net deflection of L/600

f_{f150}^D – residual strength at net deflection of L/150

f_y – yield strength of steel reinforcement

I – second moment of area about the neutral axis

L – span length (or length of the line of contact of the specimen where stated)

m – mass of specimen

m_a – mass of specimen in air

M_a – mass of recycled coarse aggregate after treatment

M_b – mass of recycled coarse aggregate before treatment

m_w – apparent mass of immersed specimen

M_R – moment of resistance

M_{ult} – ultimate moment

n – modular ratio

N_P – numerical ultimate load

N_δ – numerical mid-span deflection

P – load

P_1 – first-peak load

P_p – peak load

P_{600}^D – residual load at net deflection of L/600

P_{150}^D – residual load at net deflection of L/150

P_{ult} – ultimate load

r – rate of loading

RMC_{max} – maximum residual mortar content

T_M – theoretical ultimate moment

T_P – theoretical ultimate load

V – volume of specimen

v – Poisson's ratio of concrete or steel

W/C – water-to-cement ratio

y – neutral axis depth

β_c – closed shear transfer coefficient

β_o – open shear transfer coefficient

ρ – density of steel reinforcement

$R^D_{T,150}$ – equivalent flexural strength ratio

T^D_{150} – toughness (area under the load vs net deflection curve 0 to L/150)

μ – rate of increase in maximum stress on the tension face (taken as 1.0MPa/s)

δ_1 – net deflection at first-peak load

δ_p – net deflection at peak load

π – Pi (a constant assigned the value of 3.142)

V^{NAC}_{DR-NA} – dry-rodded volume of natural aggregate in natural aggregate concrete

SG^{NCA}_b – bulk specific gravity of natural coarse aggregate

SG^{RCA}_b – bulk specific gravity of recycled coarse aggregate

Chapter 1

1 INTRODUCTION

1.1 Background

Demolition of infrastructures is on the increase worldwide as a result of the obsolete nature of some existing structures and the drive to attain modern designs and specifications. A number of structures are approaching their design life (Tabsh and Abdelfatah 2009), hence the need for major repairs or outright replacement. Other reasons evolved due to perceived impending structural failure, development, change of purpose for structures, fire or other incidences including natural disasters. However, when concrete structures are demolished for any cause, recycling the used materials, and deriving aggregates from them is a more sustainable solution than dumping them in landfills for disposal.

In developed countries like Europe and the United States (US), recycled aggregate (RA) is used in a wide range of civil engineering works. Countries like the Netherlands and Taiwan have hit above 90 percent recovery rate of their construction and demolition waste (CDW). According to the Federal Highway Authority (FHWA) (2005) and the World Business Council for Sustainable Development (WBCSD) (2012), 11 states in the US recycle waste concrete into new concrete while 38 states use it as an aggregate for road base or sub-base. Figure 1.1 and Figure 1.2 provide useful information on the global use of RA.

Essentially, RA is produced by crushing concrete rubble from CDW (Etxeberria, Marí, and Vázquez 2007) which originally comprised of mixed materials of wood, reinforcements, concrete, soil, polymers, etc. Alternatively, RA can be sourced from generated waste concrete at a precast production facilities and unused fresh concrete from ready-mix (Silva, de Brito, and Dhir 2017, WBCSD 2012, BRE Digest 433 1998). It can also be obtained from concrete specimens used for laboratory experiments (Pradhan, Kumar, and Barai 2017) and old concrete pavements such as sidewalks, curb, parking lots, gutter, etc. (ACPA 2009). However, the production of RA requires a series of steps and special technology, although the process is similar to that of crushed natural aggregate (NA) procuring (Gagan and Agam 2015).

A typical plant for producing RA, as shown in Figure 1.3, consists of crushers, screens, transfer equipment and apparatus for removing foreign material (Hansen 1986). The main products obtained are 10mm and 20mm aggregates (about 35 % of the input material) and fine sand (from the remaining input material), obtained as a by-product of

the recycling process (Tam et al. 2014). Generally for RA, sizes from 0–5mm are considered fine aggregate and those with sizes in the range of 5–20mm as coarse aggregate (Duan and Poon 2014).

(b)

Figure 1.1: Some examples of what is happening around the world (WBCSD 2012).

Figure 1.2: States recycling concrete as aggregate base in the US (FHWA 2005).

According to Duan and Poon (2014) and Sagoe-Crentsil et al. (1996), the quality of the RA plays an important role in the new concrete. The latter authors suggested that quality and consistency of RA supply is the responsibility of the concrete recyclers who must classify and separate incoming concrete into strength grades to be appropriately applied to specific grades of recycled aggregate concrete (RAC). Tests such as ten percent fine value, flakiness index and water absorption help in this classification. According to Silva et al. (2014), four classifications of RA exist and these include: “Recycled concrete aggregates, recycled masonry aggregates, mixed recycled aggregates, and construction and demolition recycled aggregates.” They maintain that all the categories vary in composition and that the first class, which is RA comprising of 100% concrete waste, is of a better quality than the others. This variation, and its effects on the overall performance of RAC of varied strengths, has become a subject of investigation (Duan and Poon 2014).

Figure 1.3: Rubble Master Compact Crusher 70Go!^{TM}.

The effective use of RA for structural purpose would result in resource and energy savings and preservation of the environment (Sato et al. 2007). An experimental study

on the flexural performance of reinforced concrete beams under short-term loading, using coarse RA derived from demolished old concrete bridge and discarded laboratory concrete samples, showed that RAC beams are satisfactory for both service and ultimate loading compared with natural aggregate concrete (NAC) beams (Ignjatović et al. 2013). In terms of crack pattern and morphology, there was no significant difference between reinforced beams of NAC and RAC (Pradhan, Kumar, and Barai 2018), although the RAC beam samples exhibited an increased number of cracks. The structural performance of RAC beams is enhanced when unconventional mix design methods such as Particle Packing Method (PPM) (Pradhan, Kumar, and Barai 2017, 2018) and Equivalent mortar volume (EMV) technique (Fathifazl et al. 2009a, 2009b) are used.

Nevertheless, a greater use of RA is limited to non-structural applications for pavement base, sub-base, and backfill for retaining wall (Ignjatović et al. 2013, Choi and Yun 2012, Sato et al. 2007, Hansen 1986). This is because RA is perceived to be inferior to its corresponding NA since the mechanical properties of RAC are either slightly or largely lower than those of the conventional concrete. This is owing to the residual mortar from the original concrete present in the RA. As the residual mortar is generally rough and porous (Ravindrarajah 1996), it causes an increase in water absorption and a decrease in density of the material. Also, modulus of elasticity of RA is reduced while its drying shrinkage and creep are increased. Shear resistance is likewise affected by the high water absorption capacity of RA (Schubert et al. 2012). Notwithstanding, if the water absorption capacity of any RA is less, the mechanical properties of RAC obtained are comparable to those of the control mix made of NA (Yang, Chung, and Ashour 2008).

But it should be noted that the recycling process, quality of the source material, and particles size, all influence the quality of RA (Ossa, García, and Botero 2016, Malešev, Radonjanin, and Broćeta 2014, Silva, De Brito, and Dhir 2014). The first two factors determine the amount of impurity present in RA. For instance, CDW is defined by Thomas, Setién, and Polanco (2016) as “Waste generated in new construction, repair, remodelling, renovation, and demolition.” These activities would generally produce a more contaminated RA than those obtained from an equivalent precast waste concrete, which is of a superior quality and free from impurities (Soares et al. 2014, Thomas et al. 2013). In the writer’s opinion, precast waste concrete at a production facilities site has not undergone any deterioration and should be seen as having the potential to replicate similar results as NA in concrete.

Thus, the motivation for the present research is driven by the purity and quality of RA obtained from a precast waste concrete. It is believed that RA derived from concrete

alone, would present a better mechanical properties than those of CDW or other origins (Soares et al. 2014, Etxeberria, Marí, and Vázquez 2007). In addition, this research attempts to adapt a combination of techniques (discussed in the next two sections), proven to improve the performance of RA in concrete production.

1.2 Problem Statement

The usefulness of concrete in civil engineering projects cannot be over-emphasized, as such, its annual global demand is on the increase. Concrete has been described as the world's most consumed material next to water (De Brito and Silva 2016, Arezoumandi et al. 2014, WBCSD 2012) with up to 6 billion tonnes production each year, globally (Damtoft et al. 2008). In other words, concrete is the most consumed man-made substance worldwide (Arezoumandi et al. 2015a). Consequently, there is a corresponding growing need for cement and construction aggregates required for concrete manufacture. According to the U.S. Geological Survey in 2015 (Kurad et al. 2017), the overall production of cement worldwide in 2014 was approximately 4.045 billion tonnes. This amount, they said, was expected to reach 5.2 billion tonnes in 2020 and 6 billon tonnes in 2025, following an average 5% increase on global demand for cement on a yearly basis. On the other hand, aggregates account for ¾ of concrete volume and cannot be compromised (Omary, Ghorbel, and Wardeh 2016). As a result, it was projected that concrete industries worldwide will require NA of about 8–12 billion tonnes every year beginning from 2011 (Tu, Chen, and Hwang 2006). In 2007, the Freedonia group estimated world's construction aggregates requirement per annum to be 26.8 billion metric tons by 2012 (Freedonia 2007). This value was predicted by Behera et al. (2014) to double in the next two to three decades. A later report by Freedonia (2012), showed that the global aggregates for construction would rise at a rate of 5.2% through 2015 to reach 48.3 billion metric tons. With the same rate, it was reported that the demand for construction aggregates would rise to 51.79 billion metric tons in 2019 (Kurad et al. 2017).

It is therefore evident that natural resources are heavily exploited in order to meet the current demand for concrete, as a result of the high volume of construction activities around the world. Aggregates obtained from stone mining lead to the depletion of non-renewable resources and consumption of a high amount of energy (Oikonomou 2005). According to Anike et al. (2019), the procurement of cement and aggregates is the reason why the production of concrete is not environmentally friendly. To them, the associated ecological concerns have become overwhelming and require immediate attention to secure posterity. Otherwise, if the pressure on natural resources is sustained

unabated, we all would be exposed to the harmful effects of climate change and resource depletion.

Not only are natural resources depleted, in the near future, most existing concrete structures would be demolished, resulting in generation of more CDW (Wang et al. 2017). This is already the case as shown in Figure 1.4(a)–(c).

(a)

(b)

(c)

Figure 1.4: Ongoing demolition of "healthy" structures in and around Coventry University.

Currently, developed countries are facing scarcity of land, especially in their cities. This is apparent in the increasing rate of high-rise buildings in those countries to meet the accommodation needs for shelter and business activities for their populace. As such, incessant destruction of low-capacity buildings has become commonplace. Developing countries at the same time are experiencing massive demolition of structures, some of which may have been unlawfully situated. Chakradhara Rao, Bhattacharyya, and Barai (2011) pointed out that CDW generation is higher in the developing countries and that the demolitions have emerged from new zoning bye-laws, migration to the urban areas following industrial development, reconstruction, and modernization of old roads and bridges to suit the immediate and future growing traffic and other social amenities. Effects of natural disasters like earthquakes, tsunamis, and eruptions as well as fire and war incidences are other reasons structures are destroyed.

Juxtaposing the above circumstances for both developed and developing nations, enormous concrete rubble is generated yearly, globally. At the moment, there is no world's available data on waste generation as CDW is only estimated with wide variation

across regions due to different construction traditions (WBCSD 2012, ETC/SCP 2009). However, a report by WBCSD (2012) estimated the amount of concrete contained in CDW to range between 20–80%. In a similar report by ETC/SCP (2009), 31% of the overall waste generated in the European Union annually, is made of about 850 million tonnes of waste from CDW. Asserting that concrete debris is too valuable to be landfilled, the FHWA (2005) report projected that by year 2020, the 2 billion tonnes of aggregate produced every year in the US would amount to 2.5 billion. Rahal (2007) reported that between year 2001 and 2002, concrete debris in municipal landfills in Kuwait was estimated at 58%, of which concrete and masonry were the majority of the total waste disposed.

The account continues with recent reports. Waste concrete in mainland China is estimated to be 200 million tonnes per annum (Xiao et al. 2012). According to the WBCSD (2012) report, more than 900 million tonnes of concrete waste is generated in Europe, the US, and Japan alone, each year. In India, a total of 25% of the solid waste generated annually are from construction industry (Chakradhara Rao, Bhattacharyya, and Barai 2011) and 65% of the overall CDW is concrete (Gagan and Agam 2015). Kang et al. (2014) reported daily construction waste generated in Korea to be 100,000 tonnes and affirmed that 7 years projection to year 2021 resulted in 90 million tonnes of concrete rubble, per annum. Thus, one of the world's largest waste flows is actually CDW (Wang et al. 2017). Presently, the high rate of waste production emerging from CDW is not just environmentally unbearable but has also led to both economic and social issues. This is due to the inability of waste managers to quantify and classify CDW, as such, a large amount that could be recycled is deposited in landfill (Silva, de Brito, and Dhir 2017, Ismail and Ramli 2013).

"The common practice is to discard CDW in designated dumping areas" (Anike et al. 2019). But landfills are nearing their threshold as a result of ongoing demolition of dilapidated infrastructures (Huda and Alam 2014). Consequently, local production of coarse aggregate is prohibited in some countries (Rahal 2007), others impose levies on NA and taxes or fees on the deposition of construction debris in landfills (WBCSD 2012, Malešev, Radonjanin, and Marinković 2010). Hence, we are confronted with the challenges of the best way to manage construction waste generated, at the same time reduce the exploitation of the diminishing natural resources.

An alternative to the diminishing natural resources and viable solution to the overwhelming environmental pollution induced by a large generation of construction waste lies in the recycling of concrete rubble into aggregates to be used in new concrete.

But this initiative has been hampered by the variability in properties of RA for wider engineering applications (Pedro, de Brito, and Evangelista 2017, Younis et al. 2014). As RA is composed of mortar and the original aggregate, this variation in RA properties is induced by the difference in quality and quantity of mortar present in RA. According to Belin et al. (2013), the content of dry mortar in RA is dependent on the strength of the concrete from which the RA is obtained. Therefore, the basis for research in this subject area is hinged on the mortar adhering to the RA. Mortar is a lightweight material characterized by high water absorption capacity due to its high porosity. Thus, concrete manufactured using RA is subject to increased absorption capacity, low density, and has shown lower mechanical properties compared to that prepared with NA (Pedro, de Brito, and Evangelista 2017, Etxeberria et al. 2007). Nonetheless, the use of certain percentages of RA was proposed by some researchers (Behera et al. 2014, Etxeberria, Marí, and Vázquez 2007, Xiao, Li, and Zhang 2005), to serve as a measure to the devastating effect of the material on the mechanical properties of concrete. Although the idea of partial substitution of NA limits the full-scale integration of concrete waste in the production of concrete (Liu and Chen 2008).

Furthermore, the use of recycled fine aggregate (RFA) in concrete has been criticized (Schubert et al. 2012, Etxeberria, Marí, and Vázquez 2007, Hansen 1986). This is because of its negative impact on concrete durability and workability issue due to its higher absorption capacity compared to recycled coarse aggregate (RCA). But since the amount of RFA obtained when concrete rubble is crushed, is twice that of RCA (Anike et al. 2020a), RFA needs to be integrated in recycled concrete to relief the pressure on landfills and natural resources. However, Etxeberria et al. (2007) argued that RA has not been proven unfit for structural uses by any of the results published in the literature. The major problem with RA is not inherent in the raw material but lies in the mix design of its concrete (Abbas et al. 2009). Gupta and Bhatia (2013) noted that the lack of globally accepted mix proportioning method for RAC is the main factor that has limited its field implementation. Current codes of practice have imposed restrictions on the use of RA based on structural requirements (BS EN 12620:2002+A1 2008, BS 8500-2 2006, DIN 4226-100 2002).

It is generally known that the properties of concrete are greatly influenced by the proportions of the constituents which are a product of the mix design method adopted. When a conventional method is used in the formulation of RAC mix in which NA is partially or completely replaced with RA, the overall mortar content in the concrete mix increases and the proportion of coarse aggregate reduces because of the dry mortar

adhering to the RA. This normally leads to the production of concrete with poor mechanical and durability properties. To overcome this challenge and the misrepresentation of RA properties imposed by the conventional mix design method, a new mix proportioning approach dubbed “Equivalent mortar volume” (EMV) technique was proposed by Fathifazl et al. (2009a). The EMV method regards the dry mortar clinging to the RA as mortar and considers the original aggregate (in the RA) as aggregate in the new concrete. Hence, the mortar content in the conventional concrete and the total mortar content (new mortar plus attached mortar) in the EMV concrete are made equal, and the aggregate content in the conventional concrete is made equal with the total aggregate content (NA plus original aggregate in the RA) in the EMV concrete.

It is also interesting to note that concrete is remarkable for its compression and durability properties (Kang et al. 2010), but its major challenge is poor tensile and flexural capacities, making it brittle and susceptible to cracking. Obviously, concrete consisting of RA would require a strengthening material to compensate for strength loss. Steel fibre (SF) has been on focus for this purpose (Kang et al. 2017, Gao, Zhang, and Nokken 2017a, 2017b, Afroughsabet, Biolzi, and Ozbakkaloglu 2017, Vaishali and Rao 2012, Akinkurolere 2010). Additionally, it is important to devise a mix design approach that would utilize the properties of RA rather than using design methods developed for conventional concrete. Such method should be able to take into account, the quantity of dry mortar (which induces the unwanted characteristics of RA) present in RA and this was the proposition of the EMV provisions. Based on these requirements, the present study adapted to the inclusion of SF in concrete prepared with RA using both conventional and the “extended” EMV methods.

1.3 Research Gap

The recycling of demolition waste is dated back to the end of World War II (Malešev, Radonjanin, and Broćeta 2014, Ebrahim Abu El-Maaty Behiry 2013, Wagih et al. 2013, Olorunsogo and Padayachee 2002). Since then, RA has strongly been investigated by researchers, to ensure its use as not only a construction material, but a structural component.

1.3.1 State of the Art in Recycled Aggregate and Recycled Aggregate Concrete

The first state of the art in RA and the ensued concrete was published in Hansen (1986) and the following conclusions are drawn:

- Recycled concrete fines decrease workability of the new concrete considerably but have little influence on the compressive strength. On the other hand, the workability of the concrete made of RCA is close to that of the reference mix consisting of NA.
- When RAC fails, it is the weakest link, which is the mortar attached to the RA that induces the failure.
- The variation in the elastic moduli of RAC and NAC is very little.
- With unpolluted concrete as RA source, there is no concerns with regard to concrete resistance to freeze-and-thaw.
- Drying shrinkage is higher for RAC than NAC.

There was a limited data in the first state of the art, and it was noted that most of the studies reported were carried out using RA obtained by crushing concrete used for laboratory tests. The RA obtained by crushing concrete specimens used for laboratory experiments are not contaminated when compared to those obtained from demolition waste. Such version of RA will definitely show a composition and properties at variant with those obtained from CDW which are highly polluted (Silva, de Brito, and Dhir 2017, Bravo et al. 2015a, Rodrigues et al. 2013). In the second state of the art, Hansen (1986) gave a more detailed information on the developments which had taken place from 1978 to 1985 regarding the use of RA. In summary, according to the author, the cement paste adhering to the RA is the major problem with the material (in concrete manufacture) and could be technically resolved.

A similar study was conducted by Silva et al. (2014) in which 236 publications published from 1978 to 2014 were reviewed, with focus on the physical and compositional properties of RA. According to the authors, the success of obtaining RA from CDW begins with a selective demolition approach rather than the conventional method, to ensure a raw material of reduced impurity. The following remarks are drawn from the report:

- The variety of contaminants associated with CDW are detrimental to strength properties of concrete produced with RA.
- Both type of crusher and number of crushing stages affect aggregates size and shape, however, the best gradation is achieved using the jaw crusher.
- Mechanical properties of RA are influenced by recycling procedure, quality of the parent material, and size.

- Recycled concrete aggregates made of 100% concrete are of better quality than the class containing masonry and blends of construction and demolition recycled aggregates.
- Natural aggregates have a higher density and a lower water absorption compared with RA. This is due to the high porosity of the mortar adhering to the RA.
- There exist two transition zones in RAC as opposed to one in NAC as a result of the residual mortar. One is formed between the original NA and the adhering mortar while the second is formed as result of the interaction between the new and old mortar.

Overall, Silva et al. (2014) maintain that a high mortar content in RA would lead to concrete of inferior properties and they advocate that the knowledge of RA composition as well as its physical properties prior to use in concrete, is essential. They concluded that if RA is well processed and classified, it can be likened to a normal aggregate and globally accepted.

1.3.2 Techniques for Improving the Properties of Recycled Aggregate and Recycled Aggregate Concrete

1.3.2.1 Removal of Mortar Adhering to the Recycled Aggregate

From the foregoing, the first reasonable step that comes to mind on how to improve the performance of RA would be to remove the attached mortar. Thus, different techniques have been employed in the past to address the effect of the clinging mortar. One method was described as a thermal process (Akbarnezhad et al. 2011, Mulder, de Jong, and Feenstra 2007, Shima et al. 2005, Katz 2004) and the other a chemical process (Wang et al. 2017, Ismail and Ramli 2013, Tam, Tam, and Le 2007). But it is worth to note that, whereas the former uses a high amount of thermal energy as well as results in the emission of Carbon (IV) Oxide, the latter introduces Chloride and Sulphate ions that are detrimental to the aggregates and can be harmful to workers. Altering the water-to-cement ratios of the concrete mix to improve the compressive strength of RAC was an alternative means suggested (Topcu and Sengel 2004, Dhir, Limbachiya, and Leelawat 1999).

1.3.2.2 Moisture Condition of Recycled Aggregate

With reference to the high absorption capacity of RA, different propositions regarding the moisture condition of RA prior to use in concrete production have emerged. Hansen (1992) proposed that RA be used in its saturated surface-dry form as opposed to NA which can be used in its dry state for concrete production. Silva et al. (2016) upheld that

this is to prevent the available water intended for the workability of the RAC mix from being soaked by the RA while aiming to achieve a similar workability as the conventional concrete. Leite (2001) suggested that, with free water volume being kept constant, an amount of water corresponding to that absorbed by RA be added during mixing. This is regarded as 'Mixing water compensation' method. Wetting of RCA using a sprinkler system was also recommended, to be applied 24 hours before use and ensuring that a humidity of about 80% of the overall absorption of the RCA is maintained by covering the material with a plastic sheet (Etxeberria, Marí, and Vázquez 2007). The authors discourage the use of saturated RCA due to its effect on the interfacial transition zone (ITZ) between the new cement mortar and saturated RA. Also, saturation point may result in bleeding of the concrete which would affect the bond strength as a result of the affected ITZ (Poon et al. 2004). Later, the mixing water compensation and pre-saturation methods were investigated by Ferreira, de Brito, and Barra (2011) and the authors found both methods adequate in regulating the water absorption of RCA to obtain a desirable technological control in concrete production. Ultimately, the use of RA in its oven dried form is not recommended for concrete production.

1.3.2.3 Mix Design and Mixing Methods

Until 2009, the conventional mix proportioning method developed for concrete consisting of NA has been used to design RAC mixes in most research (if not all). But according to Fathifazl et al. (2009a), using the normal mix design approach for concrete constituting the heterogeneous material, would imply treating RA as its analogous NA which is homogeneous in nature. The implication is that the overall mortar content of the RAC mix is found higher than that of its equivalent NAC designed with the same method (Abbas et al. 2009). So, Fathifazl et al. (2009a) in their EMV technique proposed that the residual mortar in RA should be treated as part of the total mortar content of RAC. This method eliminates the use of *trial-and-error* method recommended in the literature, and uses the real properties of the RA, to obtain the right replacement ratio. Additionally, this approach remedies the risk of any undesirable properties of RA with no history data or from variety of sources as pointed out by Bravo et al. (2015a). In a recent study, Pradhan et al. (2017) proposed the PPM for the production of RAC. This is an optimization-based approach which aims to minimize void content in RAC by maximizing packing density of RCA.

Also, different mixing methods such as: two-stage mixing approach (TSMA), mortar mixing approach, and sand enveloped mixing approach (Liang et al. 2013, Tam and Tam 2008, Tam, Gao, and Tam 2006) have been studied for RAC mixes. These mixing

approaches emerged because, RA as already mentioned, is considered a hybrid substance needs to be treated differently from its comparable NA, in order to enhance its performance in concrete. This, in the writer's opinion, implies therefore that the preparation of RAC mixes should differ from those of companion NAC, from the design mechanism to production. Also, these methods can be selectively combined to offer a greater effect on the properties of both wet and hardened concretes.

1.3.2.4 Addition of Fibres

The incorporation of fibres in RAC mixes has become a recent practice (Kang et al. 2017, Afroughsabet, Biolzi, and Ozbakkaloglu 2017, Gao, Zhang, and Nokken 2017b, Senaratne et al. 2016, Vaishali and Rao 2012). Generally, the response of concrete to compressive, flexural, and tensile forces, and crack development are influenced by the presence of fibres. In terms of compressive strength however, there appears to be a conflicting opinion in the literature regarding the effect of fibre in concrete. While an improvement in compressive strength of fibre-reinforced concrete was recorded (Younis et al. 2014, Graeff 2011, Pilakoutas, Neocleous, and Tlemat 2004, Tlemat 2004, Lim and Oh 1999), other authors reported a significant reduction in this property of concrete with the introduction of fibres (Boulekbache et al. 2012, 2010, Erdem, Dawson, and Thom 2011, Altun, Haktanir, and Ari 2007, Lee and Barr 2004). It should be noted, however, that the contrasting results observed by the different researchers may be attributed to varied fibre contents adopted. This is because, a high fibre volume ratio would engender balling effect in concrete, thus impairing with concrete strength (Anike et al. 2019). However, other strength properties of concrete relating to flexure and tension are improved by the inclusion of fibres. Vaishali and Rao (2012) who investigated the performance of common fibres in concrete, assert that SF performed best compared to their analogous glass and polypropylene fibres and that the effects of fibres are more in RAC than NAC. They even recommended the use of both recycled fine and coarse aggregates in high performance concrete provided that the volume of SF is restricted to 1%.

Although SF improves the structural performance of concrete, limited study is available on its use in the production of RAC (Senaratne et al. 2016). Mostly material testing has been carried out in a few studies that adopted the use of SF in RAC production, thereby lacking proofs of structural integrity of the composite material. To this end, the current study investigates the combined effect of SF and the EMV mix proportioning technique on the properties of RAC. To the best of the writer's knowledge, no previous study has

incorporated recycled fine aggregates and SF to investigate the impact of this non-conventional mix design mechanism on RAC.

Hence, the following specific research questions will be addressed in this work:

- Is it possible to incorporate recycled fine aggregate into concrete proportioned using the EMV guidelines without any devastating effects on the properties of both concrete and the reinforced concrete beams?
- Is it possible to completely replace NA with the RA from a precast waste in accordance with the EMV mix design principles?
- Can SF further improve the properties of recycled aggregate concrete prepared with the EMV method?
- Does the presence of SF increase or decrease the compressive strength of RAC?
- Does a change of mix design method influence the optimum SF content?

The following are the hypotheses:

- The RA derived from a precast waste concrete is pure, containing very little or no impurities, and capable of replacing normal aggregates.
- The use of TSMA and the EMV mix proportioning technique improves the microstructure of the cement matrix, thus enhancing the properties of the concrete.

1.4 Aim and Objectives

The overall aim of the present research is to investigate the flexural performance of reinforced concrete beams produced using RA and SF as well as determine the suitability of incorporating RFA in the concrete mixes and extent of replacement ratio for both RCA and RFA. This is to be determined through a series of laboratory tests on standard cube, cylinder, and beam specimens to study both material and structural performance of RAC. The following specific objectives are set:

- Optimize the water-to-cement ratio of all concrete mixes designed using either conventional method or the extended Equivalent mortar volume (EMV) method.
- Ascertain the optimum steel fibre content and which of the common steel fibre shapes (straight, hooked-ended, and undulated) that performs best in improving the compressive strength of RAC.
- Investigate experimentally the flexural performance of reinforced RAC beams prepared with conventional method and compare them with those prepared with the extended EMV design method.

- Study whether the replacement ratio of recycled coarse aggregate obtained using the EMV proportioning technique can be applied to recycled fine aggregate from the same source, without having any devastating effects on concrete properties.
- Carry out numerical modelling on the reinforced concrete beams with the aid of finite element analysis (FEA) and compare the results with those obtained from the experimental investigation.

1.5 Research Significance

Waste management by way of recycling is an environmental conservative approach (Ibrahim 2016) and it brings beneficiation in cost of building projects through reduction in purchase and disposal costs (EPA 2000). Hence, the broad benefits of this research provided by the use of RA as the aggregate in new concrete can be summarised as follows:

- ◊ Decrease in the consumption of valuable landfill spaces.
- ◊ Reduction in environmental pollution.
- ◊ Preservation of diminishing natural resources and
- ◊ Possible low-cost building units.

As pointed out in the preceding sections, the major issue with RA is its high-water absorption capacity caused by the adhering mortar. But this problem is not intrinsic and can be fixed, technically. Specifically, work by Fathifazl et al. (2009a) showed that by the use of the EMV mix design method, cement content as well as fine aggregate required for RAC mix can be considerably reduced with no significant influence on both fresh and hardened properties of the concrete compared to its parallel NAC made of NA. It is important, however, to note that only natural coarse aggregate (NCA) was replaced in their work.

This research seeks to employ an extended EMV mix proportioning technique and the addition of SF in the production of RAC. The extension of the EMV method ensures the utilization of RFA, as such, offers a holistic solution to the problems currently faced by CDW generation. Therefore, this research would solve the environmentally related problems arising from precast waste concrete and the exploitation of NA, thereby protecting the entire ecosystem. That is, the preservation of the diminishing non-renewable natural resources and the relief in the sustained pressure on landfills. Also, the successful application of the extended EMV mix design method would lead to reduction in the amount of cement required for concrete production, thus reducing carbon footprint. Moreover, concrete industries who are currently selling their generated

concrete waste for "*peanuts*" in order to maintain a safe and clean working environment, will benefit from this study.

1.6 Research Scope

The subject of RA has gained popularity. As a result, plenty of study has been carried out already on RA and its resulting concrete by various scholars. However, this work covers both experimental and numerical studies. The experimental study involved characterization of all the aggregates employed, design of concrete mixes using both conventional and the EMV mix proportioning techniques, optimization of steel fibre and the determination of the best performing type (straight, hooked-ended and undulated), production of concretes from the developed mixes, curing of samples, and the structural testing of the specimens. On the other hand, the numerical study involved a finite element analysis carried out using the commercial computer application software (ANSYS Mechanical APDL 2019 R1). The FEA was deemed necessary to study the linear and non-linear analyses of the reinforced concrete beams. Specifically, crack, strain, and stress developments, deflection at the mid-span, ultimate load capacity, and the failure mode were evaluated with the model to investigate the flexural responses of the beams prepared from different mixes studied. Eventually, a comparison was undertaken between the experimental and numerical results, leading to the conclusions and recommendations for future research. The methodological framework for this research is given in Figure 1.5.

1.7 Layout of Thesis

Chapter 1: The general introduction of this thesis is presented in sections of background, problem statement, research gap, aim and objectives, research significance, and research scope.

Chapter 2: Review of works done by previous researchers was extensively carried out, to determine the state of affairs of the materials investigated. This revealed the extent of adaptation of recycled aggregate globally and some factors that have limited its usage to secondary purposes. Through the review, it was established that recycled aggregate can be used for structural applications, and that the inclusion of steel fibre would improve the properties of the formed steel fibre-reinforced recycled aggregate concrete.

Chapter 3: Here, the materials and method adopted to actualize the set objectives are spelt out. This includes sequence of activities and the description of all materials employed in this research. Also, full descriptions of both experimental procedures (with

references to the relevant codes) and numerical programme carried out in the laboratory and ANSYS application software respectively, are explained.

Chapter 4: Results from experimental studies are presented and discussed. Comparisons of results are made with those obtained by previous researchers.

Chapter 5: Results analyses from numerical studies are presented and discussed. Correlations between the two studies are established to draw relevant conclusions.

Chapter 6: Conclusions are drawn from both experimental and numerical studies and answers to the research questions posed in Chapter 1 of this thesis are proposed. Limitations of study are stated, and recommendations are made for future studies. Also, the contributions to knowledge from the research are highlighted.

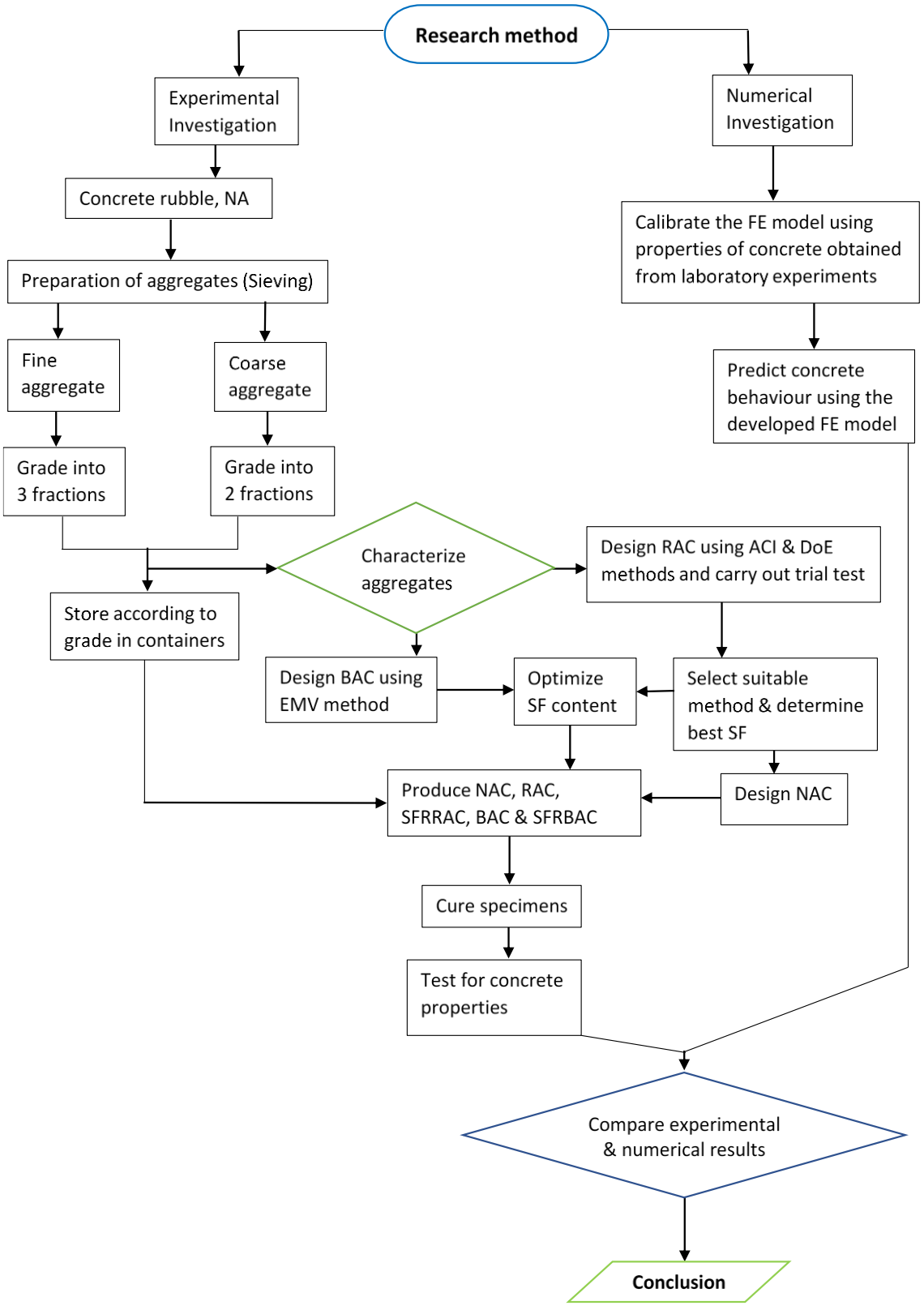

Figure 1.5: Methodological framework.

Chapter 2

2 LITERATURE REVIEW

2.1 Introduction

Concrete is used all over the world for different purposes. Some of the areas of its applications include frames, bridges, tunnels, silos, retaining walls, dams, pavements, etc. The reasons for its vast use are: availability of raw materials, ease of handling, possession of good strength and durability (Damtoft et al. 2008). Generally, concrete is made of cement (binder), water, and aggregates (fine and coarse) combined in a specific proportion. However, other materials classified as admixture are added to these basic concrete ingredients to achieve certain desirable characteristics (e.g., colour, flowability, etc.).

Over the years, the breakthrough by researchers has led to the replacement of cement to an extent in concrete production, with no devastating effects on the concrete properties. So, such materials like fly ash and ground granulated blast-furnace slag (GGBS) have become popular in the concrete industry. But aggregates, which occupy the highest volume of all the concrete constituents, are hardly substituted without a devastating effect on the properties of the resulting concrete. Therefore, the quest for a sustainable material that can relief the pressure on the diminishing natural aggregates (NA), has been on. The feasible solution, however, lies in the reuse of concrete rubble as aggregates in new concrete. Hence, recycled aggregate (RA) has been a subject of serious investigation in the past few decades.

The use of RA in concrete has been identified to be sustainable with some economic and environmental benefits (Gagan and Agam 2015, Chakradhara Rao, Bhattacharyya, and Barai 2011, Tabsh and Abdelfatah 2009, Sato et al. 2007). However, only the developed countries of the world with a few fast-developing countries, especially from Asia, have grasped this measure as revealed in Table 2.1 and Table 2.2. According to the report by WBCSD (2012), both American Society for Testing and Materials (ASTM) and American Association of State Highway and Transportation Officials agree to the use of RA as aggregate in new concrete. From the report, other bodies that have followed suit, although at varied degrees include numerous Municipalities, the Federal Aviation Administration, Environmental Protection Agency, Army Corps of Engineers, and State Departments of Transportation.

Table 2.1: Recovery Data for Construction and Demolition Waste in Some Countries. Adapted from (WBCSD 2012).

Country	Total C&DW (Mt)	Total C&DW Recovery (Mt)	% C&DW Recovery
Australia	14	8	57
Belgium	14	12	86
Canada	—	8[d]	—
Czech Republic	9[a]	1[d]	45[e]
England	90	46	50 - 90
France	309	195	63
Germany	201	179	89
Ireland	17	13	80
Japan	77	62	80
Netherlands	26	25	95
Norway	—	—	50 - 70
Portugal	4	Minimal	Minimal
Spain	39	4	10
Switzerland	7[b]	2	Near 100
Taiwan	63	58	91
Thailand	10	—	—
United States	317[c]	127[d]	82

[a]includes 3 of concrete; [b]includes 2 of concrete; [c]includes 155 of concrete; [d]recycled concrete; [e]concrete; Mt = Million tonne.

These information notwithstanding, further investigations are required over the fitness of RA, especially for structural uses. This is as a consequence of the documented gap in knowledge yet to be addressed (De Brito and Silva 2016) and a lack of specification which has hampered the application of quality control on RA (Silva, de Brito, and Dhir 2017, De Brito and Silva 2016, Fathifazl et al. 2009a, BRE Digest 433 1998). Initially, researches on RA were limited to mechanical properties (Schubert et al. 2012), but recent studies have progressed to the structural applicability of the material and that is the hub of the present study.

This chapter therefore explores such development concerning the adaptation of RA, specifically for concrete production, as available in the literature. The account was considered under the following headings: production of RA, composition of RA, properties of RA, recycled aggregate concrete (RAC), properties of RAC, fibre-reinforced concrete, and success story summarized.

Table 2.2: Recycling of Construction and Demolition Waste in Percentage of Generated Amount in the EU and Norway. Adapted from (ETC/SCP 2009).

Country	1995 – 1999	2000 – 2003	2004	2005 – 2006
Austria	–	–	60.2%	59.5%
Belgium	73.8%	–	67.5%	–
Cyprus	–	–	0.7%	–
Czech Republic	–	3.6%	17.0%	23.0%
Denmark	89.0%	89.4%	94.1%	94.9%
Estonia	–	81.0%	92.7%	91.9%
Finland	26.3%	–	–	–
France	–	–	62.3%	–
Germany	86.7%	85.3%	83.6%	86.3%
Hungary	–	–	3.1%	15.5%
Ireland	43.3%	48.2%	85.2%	79.5%
Latvia	–	1.8%	64.6%	45.8%
Lithuania	–	–	–	59.7%
Netherlands	91.40%	95.5%	97.8%	98.1%
Norway	–	–	61.0%	–
Poland	–	–	–	28.3%
Spain	–	–	–	13.6%
United Kingdom	–	63.5%	74.6%	64.8%

2.2 Production of Recycled Aggregate

The processing of RA is similar to that of NA and it involves crushing, grading, and washing which ensures that impurities are removed (Gagan and Agam 2015). The plants used in manufacturing RA are not quite at variant with those used in producing normal (crushed) aggregates obtained from other sources (Silva, de Brito, and Dhir 2017). It has also been established from the literature that different crushers exist for various needs. However, the use of jaw crusher is easier for the production of well-graded recycled coarse aggregate (RCA), although the fines produced were out of range of ASTM and British Standard (BS) grading provisions (Hansen 1986, Silva, De Brito, and Dhir 2014).

For the production of RA from construction and demolition waste (CDW), Hansen (1986) highlighted two crucial precautions that can improve the process as follows:

- Consulting record history of the concrete structure to be demolished. This would reveal important information like composition, quality, mix proportions, and performances (strengths) of the old concrete.

- Separation of large contaminants such as pieces of iron, wood, plastics, paper, glasses, ceramics, etc.

These recommendations are important because, according to Waste & Resources Actions Programme (2007), the rate of material recovery from waste is almost a function of the extent of waste separation achieved on construction sites for various material. On this account, Ravindrarajah (1996) and Silva et al. (2017) proposed that the reuse of demolished concretes should be borne in mind during demolition and segregation of the included contaminants is necessary. Likewise, management problem associated with recycling concrete waste is no less important and ought to be given attention like the technical aspect (Xiao et al. 2012). Both Figure 2.1 and Figure *2.2* are flow charts showing the recycling processes for CDW.

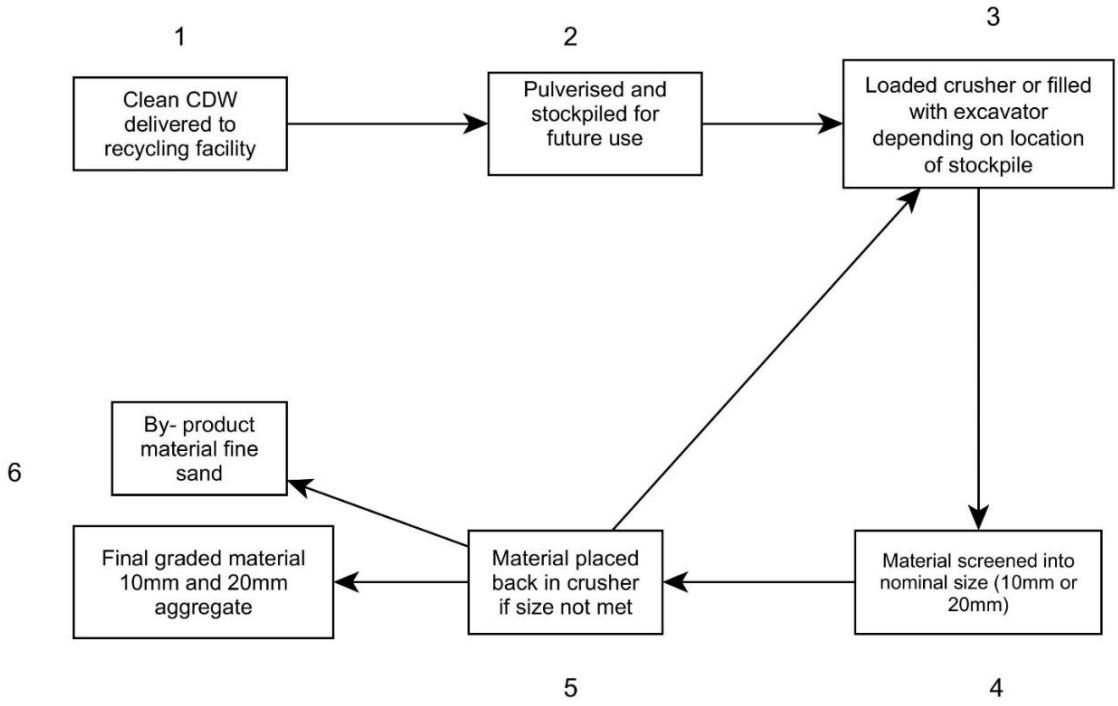

Figure 2.1: Recycling aggregate process. Adapted from (Senaratne et al. 2016).

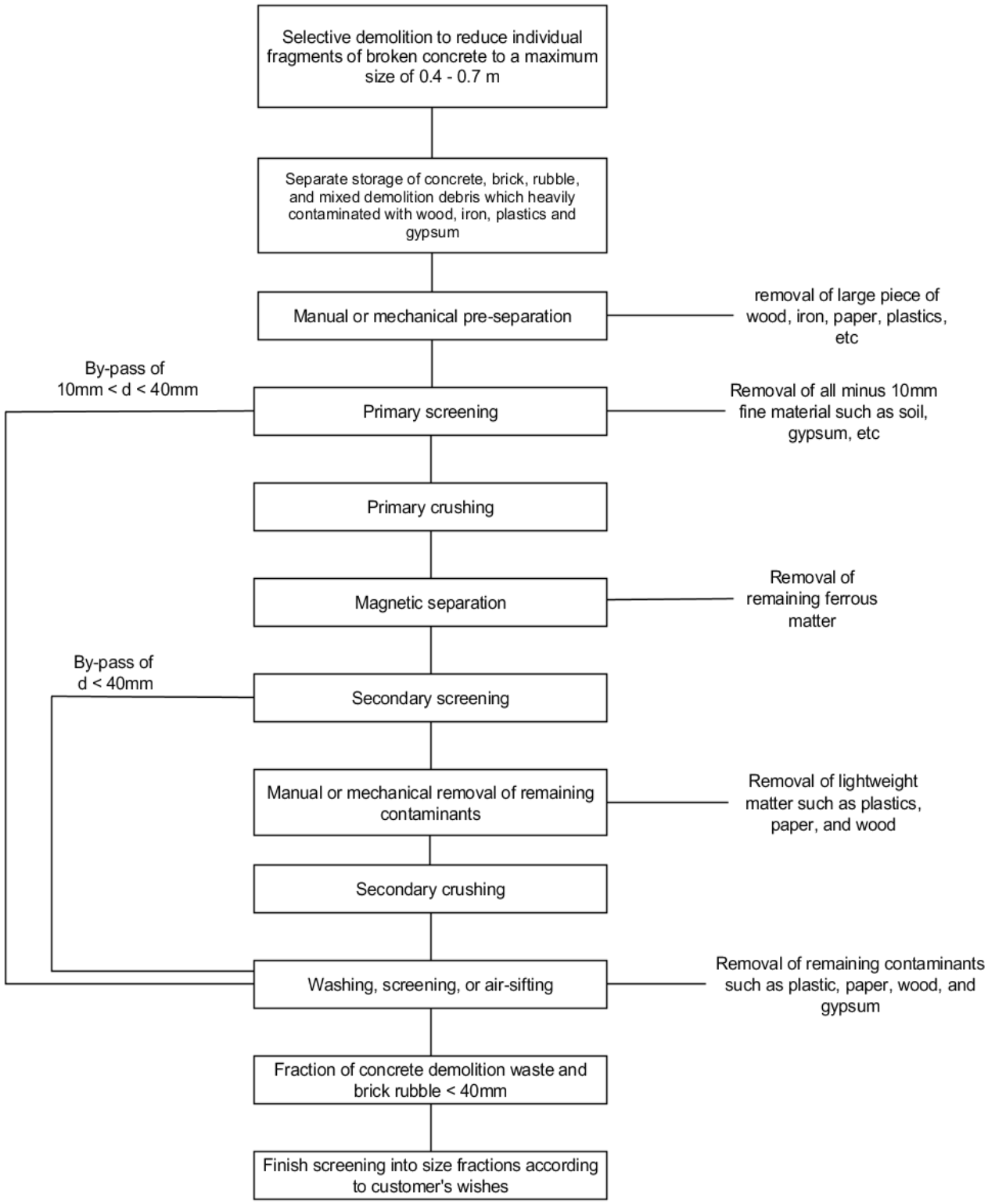

Figure 2.2: Processing procedure for building and demolition waste. Adapted from (Hansen 1986)

2.3 Composition of Recycled Aggregate

Composite material whose texture is rough and porous, consisting of hardened mortar, unbound stones, NA, and some impurities held together by a weak bond is regarded as RA (Duan and Poon 2014, Ravindrarajah 1996). A group of other researchers maintain that RA is a two-phase material made up of residual mortar and the original aggregates (Fathifazl et al. 2009a). However, in some situations, a reasonable amount of NA and impurities that need to be separated are found in RA (BRE Digest 433 1998). From the foregoing, the composition of RA using mathematical relationship can be summarized as shown in Equation 2.1 thus,

$$RA = NA + Dry\ mortar + Impurities \qquad Equation\ 2.1$$

The source from which RA was derived mainly determines the level of impurity in Equation 2.1 (Silva, De Brito, and Dhir 2014). According to Soares et al. (2014) and Thomas et al. (2016), the RA obtained from a precast waste concrete has no contaminants, and of a very good and better quality when compared with those derived from other sources. Another source of RA recognised to be of good quality and having no impurities common in CDW is concrete pavements (ACPA 2009). Thus, Equation 2.1 can be reduced as shown in Equation 2.2 (Anike et al. 2020b) for a purer RA obtained from a precast waste concrete or concrete pavements. That is,

$$RA = NA + Dry\ mortar \qquad Equation\ 2.2$$

Therefore, it can be stated that the composition of RA depends on the source material which in turn determines the number and quantity of included contaminants discussed here.

2.3.1 Contaminants

The presence of impurities influences the quality of concrete and there exists a range of contaminants with varied degree of influence. Extensive work on this regard was compiled by Hansen (1986), enumerating those impurities and their associated effects. They are discussed in the following sections.

2.3.1.1 Soil

No doubt, RA most times consists of organic soil or clay, but its harmful effect in the new concrete can be mitigated by adopting already set standards such as limits on organic contaminants, clay lumps, coal, and lignite, with the rejection of particles tinier than ASTM recommended 0.075µm size.

2.3.1.2 Chlorides

Presence of chlorides in concrete causes corrosion of the reinforcement bars. The limits of chlorides content in aggregate and concrete is inconclusive, however, the following recommendations (Hansen 1986) are proposed:

(i) 0.06% content for pre-stressed concrete

(ii) 0.10% content for normal reinforced concrete exposed to chloride and in a moist environment.

(iii) 0.15% content for normal reinforced concrete shielded to chloride but in a moist environment.

(iv) No limits for building construction above ground level where concrete remains dry.

With regards to concrete incorporating RA, both chloride penetration rate and chloride binding capacity increase, and water soluble chloride contents in normal concrete and RAC have similar values (Villagrán-Zaccardi, Zega, and Di Maio 2008).

2.3.1.3 Metals

The likelihood of having significant number of metals (e.g., steel) remaining in RA is minimal, however any small amount can stain or mar the surface of the RAC due to rust, especially when chloride is present. Also, pieces of steel if unnoticed, can damage the crusher during recycling process. This can be remedied using magnetic separation technique before feeding the crusher.

2.3.1.4 Particles Damaged by Weathering or Fire

If the source of RA was damaged by alkali or sulphate reactions, frost or other weathering agents like fire, it renders the aggregate unfit for use in the manufacture of RAC based on the requirements for mechanical properties.

2.3.1.5 Industrial Chemicals and Radioactive Substances

While RA should be void of oil- or water-soluble chemicals, RAC is to be free of stinking, toxic or radioactive substances. Existence of common contaminants such as chlorides, humus and sulphates in NA can be accommodated in standard specifications for aggregate used in concrete production. However, undesirable soluble impurities from

demolished concrete of industrial plants source can influence the properties of the RAC thereof.

Other contaminants include glass, organic substances, chemical and mineral admixtures, alkali-reactive aggregate particles, particles susceptible to frost damage, high alumina cement, and fragmented brickwork and lightweight concretes. They have varied degrees of influence on the properties of RA and the ensued RAC. The effect of some is negligible, some detrimental and the other undetermined. However, RA sourced from structures of high alumina cement instead of Portland cement should not be employed in producing RAC for structural purposes. More so, fragmented bricks from refractory containing high Periclase and MgO have been reported to show a serious negative effect even when present in a very little quantity of 0.01% (Hansen 1986). Classes of RA and limits of impurities in RA are shown in Table 2.3 and Table 2.4, respectively. Further to the definition given in Table 2.3, the RA(I), RA(II), and RA(III) labels in Table 2.4 represent lowest, high, and mixed quality materials with a relatively high, low, and high impurity content, respectively.

Table 2.3: Classes of recycled aggregate. Adapted from (BRE Digest 433 1998).

Class	Original (normal circumstances)	Brick content by weight
RA (I)	Brickwork	0 - 100%
RA (II)	Concrete	1 - 10%
RA (III)	Concrete and brick	1 - 50%

2.4 Properties of Recycled Aggregate

RA exhibits varied properties from conventional aggregates due to the attached mortar. But with RA produced from a higher strength concrete, a better physical characteristics (Andreu and Miren 2014) and improved mechanical properties of RAC (Ajdukiewicz and Kliszczewicz 2002) can be obtained. Thus, RA quality and properties depend on the quality as well as amount of dry cement mortar present in the material, and this is subsequently linked to the quality of the source concrete and the recycling method adopted (Malešev, Radonjanin, and Broćeta 2014, WBCSD 2012). Some characteristics of RA are discussed here.

Table 2.4: Maximum recommended levels of impurity (by weight). Adapted from (BRE Digest 433 1998).

Impurity	Use in concrete as coarse aggregate	Use in road construction- unbound/cement bound material Sub-base type 1 or 2, or CBM 3,4 or 5: RA(II) only. Capping layer 6F1 or 6F2, CBM 1 or 2: normally RA(I), (III)	Hardcore, fill or granular (drainage) material
Asphalt and tar (as lumps, e.g. road planing, sealants)	Included in limit for other foreign material	10% in RA(I)[b] or 5% in RA(II)[b] or 10% in RA(III)[b]	10%[b]
Wood (also any material less dense than water)	1% in RA(I) or 0.5% in RA(II) or 2.5% in RA(III)[a]	Sub-base type 1 and 2: 1% or CBM (1 - 5): 2%, and capping layer 6F1 and 6F2: 2%	2%
Glass	Included in limit for other foreign material	Contents above 5% to be documented	Contents above 5% to be documented
Other foreign material (e.g. metals, plastics, clay lumps)	5% in RA(I) or 1% in RA(II) or 5% in RA(III)[a]	1% (by volume if ultra-lightweight)	1% (by volume if ultra-lightweight)
Sulfates	Concrete and CBM: 1% acid soluble SO_3[a]. Unbound material: See Digest 363 if near concrete		

[a] *No limit if physical and mechanical test criteria are satisfied.*

[b] *RA(III) must not replace more than 20% of natural aggregate. Limits on wood and other foreign matter that there will be no contribution from the natural aggregate. Similarly, a limit of 1% acid soluble SO_3 should apply to 1:4 mixtures of RA(III): natural aggregate.*

2.4.1 Shape, Sieve Analysis, Los Angeles Abrasion, and Surface Texture

These characteristics of RA depend on type and extent of crushing of the raw materials from which they are obtained (ACPA 2009). Particle size is a consequence of the crushing operations and according to Chakradhara Rao, Bhattacharyya, and Barai (2011), RA is relatively finer, hence possesses a lower fineness modulus compared with NA. More so, the content of mortar adhering to RA increases with decreasing particles size (Anike et al. 2020a, de Juan and Gutiérrez 2009). The source of the RA contributes to these features in addition to method and extent of crushing. RA from concrete origin tend to be largely angular with a rough texture. Also, the amount of fines included in RA after the recycling process depends on the quality of the old concrete (Wagih et al. 2013). Generally, RA has a lower impact resistance and a higher loss in abrasion resistance than its parallel NA. The result of different RA investigated showed that impact value and abrasion index range from 21–38% and 31–47% respectively (Wagih et al. 2013). An

average of about 34% higher loss in abrasion was reported for RA relative to NA (Tabsh and Abdelfatah 2009). These properties can be improved if the RA is derived from a higher strength concrete as given in Table 2.5, however, the improvement does not apply to abrasion index here.

Table 2.5: Physical and mechanical properties of RA compared with NA. Adapted from (Andreu and Miren 2014).

Type of aggregates	Physical and mechanical properties			
	Oven dried density (kg/m^3)	Water absorption (%)	Flakiness index (%)	LA index (%)
River gravel	2.61	1.29	17.71	19.61
Dolomitic gravel	2.68	2.13	7.81	24.77
RCA 40MPa	2.30	5.91	9.59	24.31
RCA 60MPa	2.39	4.90	13.57	25.24
RCA 100MPa	2.47	3.74	16.53	24.01

2.4.2 Specific Gravity

The specific gravity of aggregates is directly related to the density of concrete and aggregate type influences it (Gameiro, De Brito, and Correia da Silva 2014, Duan and Poon 2014). From the information available in the literature (Verian, Ashraf, and Cao 2018, Kurda, Brito, and Silvestre 2017, Younis et al. 2014, Wagih et al. 2013, Chakradhara Rao, Bhattacharyya, and Barai 2011, Fathifazl et al. 2009b, Rahal 2007, Hansen 1986), the specific gravity of RA is generally lower than that of NA. This gap is caused by the mortar adhering to the RA (Kurda, Brito, and Silvestre 2017, de Juan and Gutiérrez 2009) and higher porosity of the RA than the NA (Wagih et al. 2013). According to Verian, Ashraf, and Cao (2018), whereas the specific gravity of normal aggregates ranges from 2.4–2.89, that of RA ranges from 1.91–2.70. Concrete grade (from which RA is obtained) and particles size significantly affect the specific gravity of RA as shown in Table 2.5 and Table 2.6.

2.4.3 Water Absorption Capacity

RA is expected to have higher absorption capacity than the conventional aggregates owing to the fragments of dry mortar present in the former. Albeit, the source and particles size of RA contribute to this property (Kisku et al. 2012, Nováková and Mikulica 2016). The absorption capacity of RA obtained from fifteen different sources was found to range from 2.15%–7.15% (Wagih et al. 2013). Senaratne et al. (2016) found an absorption capacity of aggregates of sizes 10mm and 20mm to be 5.9% and 4.3% for

RA and 1.2% and 0.7% for NA respectively. Similar study reported about 64% higher absorption capacity for RA relative to NA (Chakradhara Rao, Bhattacharyya, and Barai 2011). However, the degree of absorption reduces as particle size increases. This was demonstrated in the work by Hansen and Narud (1983) in which absorption was found to be 8.7% and 3.7% for RCA in the range of 4–8mm and 16–32mm respectively. Further justification is provided in the investigation carried out by Pepe et al. (2014) as shown in Table 2.6.

Table 2.6: Effects of size fraction on properties of RA compared with NA. Adapted from (Pepe et al. 2014).

Aggregate type	Size, d (mm)	Specific mass (kg/m^3)	Water absorption (%)
Natural sand	$d < 4.75$	2690	1.2
Natural aggregates - N1	$4.75 < d < 9.5$	2690	0.5
Recycled aggregates - R1	$4.75 < d < 9.5$	2310	8.7
Natural aggregates - N2	$9.5 < d < 19$	2690	0.4
Recycled aggregates - R2	$9.5 < d < 19$	2440	6.6

2.5 Recycled Aggregate Concrete

Both RAC and NAC are similar in production, but not in composition following the mortar adhering to the RA. This presence of residual mortar has formed the basis for research over the years. Of the many concerns identified with RA, the mix design appropriate to RAC is the major. While some researchers maintain that the conventional mix proportioning method would suffice for RAC (Sato et al. 2007), others are of the view that the mix design method for RAC needs entirely different approach (Gupta and Bhatia 2013, Fathifazl et al. 2009a, Topcu and Sengel 2004, Ray and Venkateswarlu 1991). The reason behind the opinion of the latter group is in connection with the element of mortar adhering to the RA which makes it a hybrid material compared to pure NA. This attached mortar raises the total mortar volume of RAC higher than that of its parallel NAC (Fathifazl et al. 2009a) leading to the production of inferior concrete.

2.5.1 Mix Design of Recycled Aggregate Concrete

Currently, there exists no universally accepted mix design for RAC due to the lack of consistency in the characteristics of RA obtained from variety of sources (Younis et al. 2014, Gupta and Bhatia 2013, Tam, Gao, and Tam 2006). Nevertheless, different techniques have been employed by different authors in the past for the production of

RAC mixes. The list includes, but is not limited to, replacement by volume of aggregate method, replacement by weight of aggregate method, equivalent mortar volume (EMV) method, particle packing method (PPM), compressible packing method, and various modified mixing technique such as two-stage mixing approach (TSMA), TSMA plus silica fume and cement, mortar mixing approach, etc.

Generally, the use of conventional method impacts negatively on the properties of RAC. Whereas the conventional method regards RA as a single-phase material, the EMV mechanism treats RA as a binary component (Pradhan, Kumar, and Barai 2017, Fathifazl et al. 2009a). Furthermore, simply substituting certain percentages of RA (either by volume or weight) does not entirely solve the problems associated with RA. Hence, the idea of the EMV technique is using the properties of both NA and RA to determine the substitution ratio with RA, which is an absolute solution. This is because the quality of the source material mainly determines the quality of the RA which subsequently should determine the substitution level of NA.

The PPM uses the optimization of the aggregates packing to improve the RAC properties. With an optimal packing system, voids in the concrete are reduced. This is because, in concrete technology, the matrix comprising of water, air and powder defined by particles smaller than 125µm interact to fill the voids (Hunger and Brouwers 2009). The microscopic properties of the concrete are improved by this mechanism depending on such factors as particles shape and size distribution, reactivity, water-cement ratio etc. According to Van Der Putten et al. (2017), the concrete mixes prepared with crushed aggregate are less compacted and possess more voids than those made with rounded aggregate due to the angularity of the crushed aggregates. Also, a higher water-cement ratio engenders a less dense packing, resulting in a more permeable paste (Moosberg-Bustnes, Lagerblad, and Forssberg 2004). The authors pointed out that superplasticizer was instrumental in achieving a low water-cement ratio with proper homogenisation of the cement and the filler. They also maintain that the efficiency of superplasticizer in a denser particulate system is higher than in a porous less dense system. This could be the reason why the properties of RAC prepared with 100% RA are still inferior to those of comparable NAC even though the RAC mixes require superplasticizer to match the workability of the conventional concrete. However, RAC of good quality is achievable using a suitable mix proportioning technique and RA of well-defined properties.

2.5.2 Properties of Recycled Aggregate Concrete

2.5.2.1 Workability

Additional water is required for the concrete mixes containing RA to obtain a comparable workability with those of NAC and such alteration may impact on the mechanical properties of the RAC (Wardeh, Ghorbel, and Gomart 2015). Ultimately, the workability issue of RAC mixes ensues due to the porosity of the RA (Butler, West, and Tighe 2013, Rahal 2007). Up to 13% increase in water content was required to match the workability of RAC and NAC and the attached mortar, rough surface texture and more angularity in shape of the RA were responsible for this gap (Wagih et al. 2013). However, the desired fluidity of the concrete can be achieved using a water-reducing admixture, without any devastating effects on the properties of the hardened concrete. Wagih et al. (2013) reported that full replacement of NA with RA required about 10% additional water to attain similar workability when no superplasticizer was used. The authors recorded an average reduction of 12% in water-to-cement ratio when both superplasticizer and silica fume was added and 15% with solely superplasticizer. With the same amount of superplasticizer in RAC and NAC, Chakradhara Rao, Bhattacharyya, and Barai (2011) who used slump value to measure workability recorded about 6% lower slump for RAC in relation to NAC. Malešev, Radonjanin, and Marinković (2010) observed no significant difference in workability after 30 minutes, for the three types of concrete produced using 0%, 50%, and 100% RA. Recycled concrete fines decrease the workability of concrete considerably (Hansen 1986). In spite of a higher content of superplasticizer, workability of RAC containing steel fibre (SF) was substantially reduced (Afroughsabet, Biolzi, and Ozbakkaloglu 2017, Gao, Zhang, and Nokken 2017a).

2.5.2.2 Hardened Density

The density of RA has a direct effect on the density of the resulting concrete. When compared with the concrete made of NA, the density of hardened RAC produced using 100% RCA was reduce by about 3.6% (Rahal 2007). A comparable reduction of 3% in the density of RAC was noted by both Malešev, Radonjanin, and Marinković (2010) and Chakradhara Rao, Bhattacharyya, and Barai (2011) who separately investigated 100% and 25% substitution ratios with RA. The density of RAC depends on the porosity of both concrete and aggregate which in turn depends on the replacement level with RA (Omary, Ghorbel, and Wardeh 2016). Overall, the density of RAC has been found lower compared to that of NAC following the mortar adhering to the RA. Nonetheless, the fresh and hardened density of RAC proportioned using the EMV method and incorporating blast furnace slag were found greater than those of the corresponding NAC (Fathifazl et

al. 2009a). Addition of SF marginally increased the density of RAC (Erdem, Dawson, and Thom 2011).

2.5.2.3 Compressive strength

Compressive strength is regarded as the most important mechanical properties of the concrete as it relates with other properties and always shows the general quality of the cement composite (Wagih et al. 2013). With regard to RAC, both quantity and quality of RA affect its mechanical properties. A group of researchers observed no substantial reduction in compressive strength when RAC prepared using up to 30% substitution ratio with RCA was compared with normal concrete (Behera et al. 2014, Tam, Gao, and Tam 2005, Xiao, Li, and Zhang 2005). But by using 30% RA replacement of NA, Corinaldesi (2011) recorded 20% loss in the 28 days cube compressive strength despite the type of cement used. Using a replacement ratio above 30%, a notable reduction in the compressive strength of the resulting RAC was observed (Wagih et al. 2013, Corinaldesi 2011). An appreciable reduction of about 28% was reported for the compressive strength of RAC produced with more than 50% RA replacement ratio (Wagih et al. 2013). There was up to 30% loss in the compressive strength of RAC at full replacement with RCA when compared with the NAC (Behera et al. 2014, Xiao, Li, and Zhang 2005, Hansen and Narud 1983). The major reason for the gap between the compressive strength of NAC and RAC is in the quality of their paste and interfacial transition zone (ITZ) (Fathifazl et al. 2009a).

According to Malešev, Radonjanin, and Marinković (2010), the cube compressive strength of the concrete developed with RA remains unaffected in spite of the substitution level if a good quality RA produced maybe from a high-strength old concrete is used. For example, using a RA obtained from a concrete of 30MPa strength, 30% decrease in compressive strength of cylindrical specimens for the resulting RAC was recorded (Tabsh and Abdelfatah 2009). Whereas the authors achieved a RAC of a comparable strength to that of NAC using a RA derived from concrete of 50MPa strength. With RCA derived from a concrete of 100MPa strength, Andreu and Miren (2014) recorded a higher strength even with 100% RCA compared with concrete made entirely of NA. However, the compressive strength of the concrete developed with RA is not limited to the strength of the old concrete even though the strength and water–cement ratio of the old concrete affect the compressive strength of RAC.

Recycled fine aggregate (RFA) is not widely recommended for concrete production. There is even a serious constraint or ban in some cases in the use of RFA for

manufacturing concrete (Pedro, de Brito, and Evangelista 2017). This is because RFA contains a higher amount of mortar than its parallel RCA (Hansen and Narud 1983). Compressive strength of cube samples of RAC consisting RFA was reduced by 16% when compared with the conventional concrete (Pedro, de Brito, and Evangelista 2017). At all ages of high-strength concrete incorporating RFA, Liu and Chen (2008) observed a loss in compressive strength of cylinder specimens. In a similar investigation into high-performance concrete using RA obtained from a demolished concrete of strength 35–70MPa, Ajdukiewicz and Kliszczewicz (2002) concluded that a high-strength concrete can be produced with RA but opposed the use of RFA. Tu, Chen, and Hwang (2006) also confirmed that RA could be employed in producing a high-strength concrete provided the physical properties of the RA meet the requirements for such class of concrete.

Khatib (2005) noticed a higher rate of strength development for the concrete made with RFA following a further cementing action after 28 days of curing in comparison with NAC. Corinaldesi and Moriconi (2009) upheld that concrete of satisfactory properties can be attained with 100% RA provided a suitable mix proportioning method is adopted. By replacing coarse aggregate with RCA using the EMV mix proportioning approach, Fathifazl et al. (2009a) observed up to 13% higher compressive strength for cylinder specimens when compared to conventional concrete. With the same mix design mechanism and replacement with RCA, cube compressive strength improved by approximately 7% relative to concrete made with NA (Gupta and Bhatia 2013). Using the PPM for both NAC and RAC mixes, RAC showed a higher compressive strength at the 7 and 28 days strengths, however, after 90 days the compressive strength of RAC decreased by over 17% compared with that of NAC (Pradhan, Kumar, and Barai 2017). There was over 13% and 24% increase in compressive strength at 28 and 56 days respectively when RAC made of 100% RCA was prepared with TSMA compared to the normal mixing procedure (Tam, Gao, and Tam 2006). The TSMA is effective in improving the ITZ around the RCA and in filling up the pores and cracks thereof, thus a greater strength when compared with the orthodox mixing approach (Tam, Gao, and Tam 2005).

There seem to be a mixed opinion over the use of fibres in concrete production in terms of compressive strength. On one hand, some scholars found that the cube compressive strength of fibre-reinforced concrete was decreased by up to 7% (Erdem, Dawson, and Thom 2011, Boulekbache et al. 2010, Lee and Barr 2004). On the other hand, inclusion of fibre in concrete had up to 25% improvement (Afroughsabet, Biolzi, and Ozbakkaloglu 2017, Younis et al. 2014, Graeff 2011, Lim and Oh 1999). The gap in the performance

of fibre under compression can be ascribed to fibre volume fraction adopted by researchers.

2.5.2.4 Tensile Strength

Concrete is generally weak in tension and steel reinforcements are used to overcome this weakness. Tensile strength is negatively affected by the use of RA in concrete production and both quality and content of the RA contribute to this effect. The 28 days splitting tensile strength of RAC showed about 9–24% reduction when compared to corresponding NAC (Wagih et al. 2013). Tensile strength decreased by 10–15% when a lower grade concrete (30MPa) was used as the RA source compared with NAC (Tabsh and Abdelfatah 2009). Chakradhara Rao, Bhattacharyya, and Barai (2011) observed up to 23% decrease in split tensile strength of the concrete made with 100% RA.

Conversely, the effect of RA on splitting tensile strength does not largely depend on the RA volume but on its quality, according to Malešev, Radonjanin, and Marinković (2010). They found that splitting tensile strength was slightly higher for RAC manufactured with 100% RCA (obtained from a concrete of 50MPa strength) compared with traditional concrete. RCA sourced from a concrete of good grade produced a RAC of similar or greater tensile strength even at 100% replacement ratio in comparison with conventional concrete produced with NA as shown in Figure 2.3 (Andreu and Miren 2014).

A collection of studies by different researchers is presented in Figure 2.4 (Anike et al. 2019). It should be noted that only the substitution ratios of RCA (0, 50, and 100%) common to the studies were compared and presented here. The work by Afroughsabet, Biolzi, and Ozbakkaloglu (2017) was conducted using RCA obtained from a parent concrete of 80MPa strength (relatively higher than those of other studies) and the mixes were designed for higher strength. From Figure 2.4, the splitting tensile strength of RAC at all replacements was found lower than that of NAC just for the work by Bravo et al. (2015a). This could be because their RCA was derived from a mixed source while the other authors utilized a single source of RCA. However, the studies demonstrate that RCA can completely replace its conventional counterpart in concrete with no devastating effects from tensile strength perspective, provided a single source of good aggregate is used. The presence of SF has proved efficient in enhancing the tensile strength of the concrete. Tensile strength was significantly improved when SF was added to concrete (Akinkurolere 2010), to the extent that the value without SF was doubled with 2% SF content (Lim and Oh 1999). Afroughsabet, Biolzi, and Ozbakkaloglu (2017) noticed up to 60% improvement in RAC made with 1% volume ratio of hooked-ended SF.

Approximately 39% improvement in tensile strength was reported when superplasticizer was added to concrete mix (Soares et al. 2014).

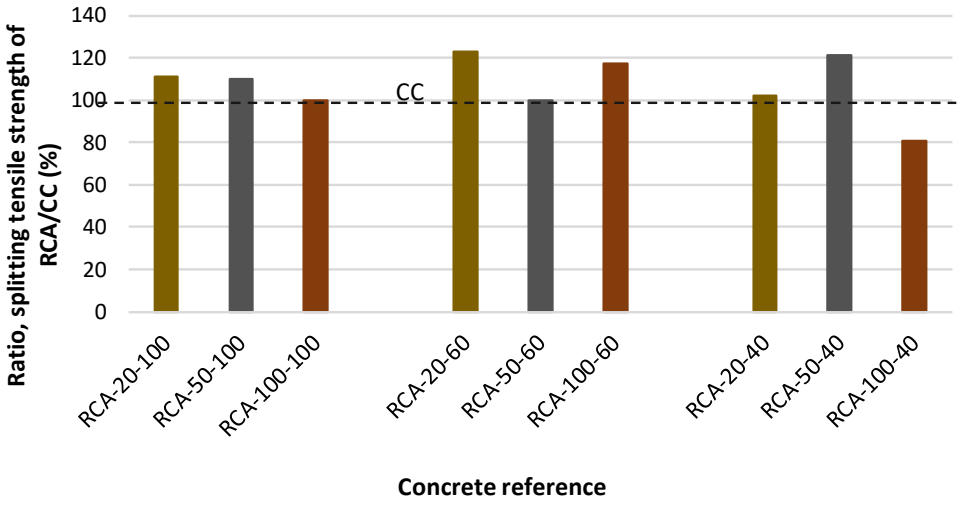

Figure 2.3: Splitting tensile strength of RAC in comparison with that of conventional concrete (CC) at 28 days of age. Adapted from (Andreu and Miren 2014). [RCA–20–100 represents RCA–substitution ratio by volume–strength of the old concrete from which RCA was produced].

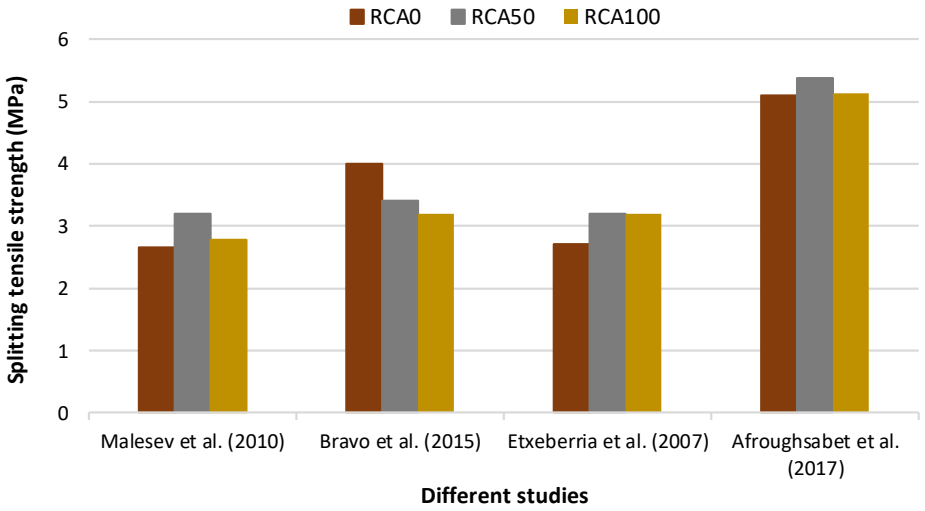

Figure 2.4: Comparison of the splitting tensile strength of RAC compiled from different studies.

2.5.2.5 Flexural Strength

The resistance offered by a body subjected to bending stresses is referred to as flexural strength or modulus of rupture. Flexural strength of RAC relates inversely to replacement ratio with RA (Malešev, Radonjanin, and Marinković 2010, Padmini, Ramamurthy, and Mathews 2009, Heeralal, Kumar Rathish, and Rao 2009, Topcu and Sengel 2004, Katz

2003). On the other hand, the effect of RA on modulus of rupture of the developed RAC beams was found negligible even with up to 100% replacement RCA (Ignjatović et al. 2013, Choi, Yun, and Kim 2012).

Some studies investigated the impact of regulating RA content on this property of concrete. For RAC prepared with 50% and 100% RCA, flexural strength was found to increase and reduce by 5% and 4% respectively relative to conventional concrete (Malešev, Radonjanin, and Marinković 2010). One study considered a series of substitution ratios (0%, 20%, 50%, and 100%) with a RCA derived from concretes of 40MPa, 60MPa, and 100MPa strength on modulus of rupture (Andreu and Miren 2014). Another study evaluated the effect of 0%, 30%, 50%, and 100% substitution levels with RCA for concretes of different design strength (Limbachiya, Leelawat, and Dhir 2000). The results of both studies show that a comparable or even higher flexural strength can be achieved with RCA compared with normal aggregate (Figure 2.5). Also, the effect of RCA content is inconsequential on flexural strength.

Furthermore, the flexural behaviour of RAC beam was similar to that of the NAC beam and elastic, elasto-plastic, and fracture stages were observed in the failure pattern of tested RAC beam (Qin, Chen, and Chen 2012). Similar cracking development but not crack spacing was reported for RAC and NAC beams tested in flexure (Arezoumandi et al. 2015b).

Expectedly, the inclusion of SF in RAC enhanced flexural strength (Afroughsabet, Biolzi, and Ozbakkaloglu 2017, Younis et al. 2014). Younis et al. (2014) recorded up to 15% improvement in the flexural strength of RAC using 2% (by mass of concrete) SF compared to NAC with no SF. This is possible through the ability of SF to control cracking propagation and absorbing considerable amount of energy during concrete deformation (bending).

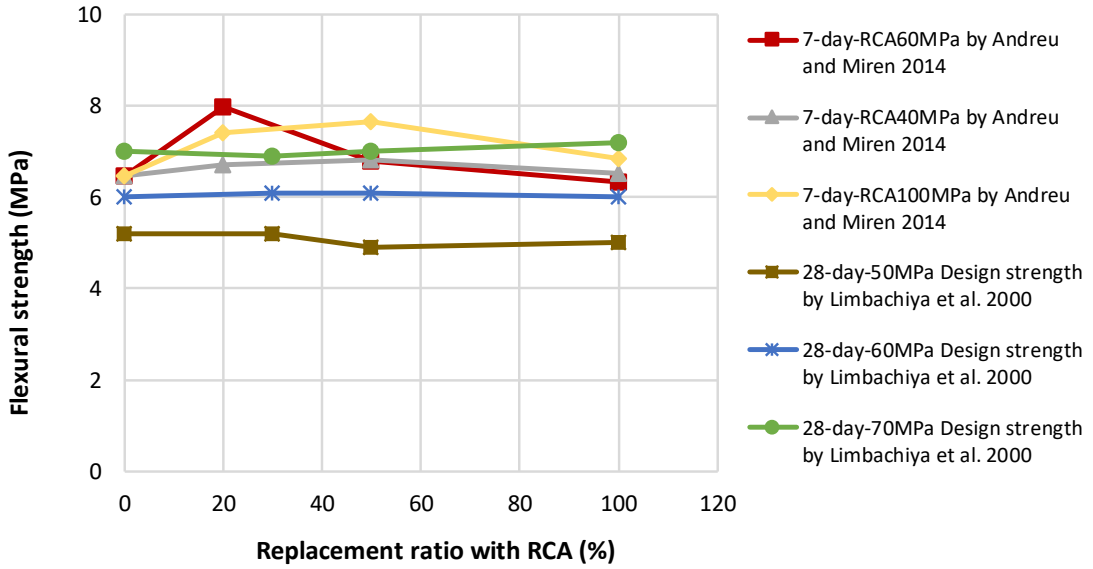

Figure 2.5: Effect of RCA substitution ratio on flexural strength. Adapted from (Anike et al. 2019).

2.5.2.6 Elastic Modulus

Elastic modulus is the ratio of normal stress to induced strain and it is directly related to compressive strength. That is, elastic modulus for concrete increases with an increase in compressive strength as given by ACI 318R (2014) in the simplified Equation 2.3.

$$E_c = 4700\sqrt{f_c} \qquad \textit{Equation 2.3}$$

Where E_c and f_c are modulus of elasticity (MPa) and compressive strength (MPa) of concrete, respectively.

The modulus of elasticity of RAC has been shown in different studies to be lower than that of the comparable NAC (Bravo et al. 2015a, Malešev, Radonjanin, and Marinković 2010, Etxeberria et al. 2007). This appears to be the most impaired property of the concrete when NA is replaced by RA. Of all the mechanical properties of concrete, modulus of elasticity is yet to be improved by different measures adopted by early authors when using RA (Fathifazl et al. 2009a). This is owing to the fact that the elastic modulus of the dry mortar clinging to RA is very low.

Nevertheless, RA derived from a high-strength parent concrete improved modulus of elasticity of RAC (Li, Xiao, and Zhou 2009). Limbachiya, Leelawat, and Dhir (2000) found that the RAC designed for a higher strength resulted in a greater value of elastic modulus compared to NAC. Ideally, modulus of elasticity of concrete depends on both elastic modulus of the aggregate and mix proportions (ACI 318R 2014).

Using 25% RCA content induced about 2.5–5% loss while 100% RCA content resulted in up to 8–15% reduction in elastic modulus compared with concrete consisting entirely of NA (Wagih et al. 2013). The authors also observed that the use of silica fume enhanced elastic modulus of concrete mix containing 100% RCA by up to 8% and this was as a result of improved ITZ formed between the old and the new mortar in the RAC. Particles gradation notwithstanding, RAC comprising of 30% RCA on one hand and 30% (RCA + RFA) on the other hand, had its elastic modulus reduced by 16% and 21% respectively in comparison with concrete made of virgin aggregate (Corinaldesi 2011). The use of fly ash, slag, and the EMV mix proportioning mechanism greatly improved the elastic modulus of RAC (Fathifazl et al. 2009a).

2.5.2.7 Drying Shrinkage

Deformation in concrete due to changes in volume (reduction) is considered as shrinkage. A number of studies proved that drying shrinkage of the concrete made of RA is proportional to the quantity of RA used (Snyder 2016, Matias et al. 2014, Beltran et al. 2014, Belin et al. 2013, Kwan et al. 2012, Kou and Poon 2012, Malešev, Radonjanin, and Marinković 2010, Sagoe-Crentsil, Brown, and Taylor 2001).

Shrinkage was found to be 10% and 20% higher respectively with 50% and 100% RCA replacements when compared with concrete made of NA (Malešev, Radonjanin, and Marinković 2010). Similar observation was made as drying shrinkage of the RAC made of 50% RCA was found to be 12% higher than that of NAC after 180 days (Domingo-Cabo et al. 2009). Replacing both fine and coarse aggregates with RA engendered up to 150% greater shrinkage than the normal concrete (Sato et al. 2007). The reason for such a whopping increment in shrinkage when all aggregates were replaced may be ascribed to a higher mortar content associated with RFA. So, absorption capacity was increased (Kwan et al. 2012) giving rise to internal hydrostatic pressure which eventually led to expansion.

2.5.2.8 Creep

Creep is as a result of increase in strain over a sustained stress in concrete (Kisku et al. 2012). Creep increases with an increase in RA content (Tam and Tam, 2007; Kou and Poon, 2012). However, Kou and Poon (2012) observed a reduction effect on creep using fly ash and a higher influence resulted with partial rather than a complete replacement of cement. Creep reduction in RAC prepared using the TSMA was up to 26% compared with the normal mixing method (Tam and Tam 2007). Introduction of fibre induced a

different response of concrete to creep depending on both type and content of fibre (Buratti and Mazzotti 2012, Mackay and Trottier 2004).

2.5.2.9 Freeze–and–Thaw

This is the ability of concrete to resist cycles of freezing and thawing and it is a concern mostly in places of extreme low temperatures. Among other factors that affect the response of RAC to freeze-and-thaw are quality and content of the RA. One of the reasons why RAC has a lower freeze-and-thaw resistance than the equivalent NAC is due to a higher porosity of RA which results in a concrete of undesirable properties (Salem, Burdette, and Jackson 2003).

Air-entrainment impacts on the freezing and thawing behaviour of concrete, as a result, air-entraining agents should be examined before being adopted for concrete production (Kisku et al. 2012). Gokce et al. (2004) found a better freeze-and-thaw resistance for RAC produced using RA obtained from air-entrained parent concrete than that incorporating RA of non-air-entrained concrete origin. However, it was reported that due to the ability of fibres to entrain air, the protection of concrete consisting of polypropylene fibres against freeze-and-thaw was enhanced compared to both plain and air-entrained concretes (Richardson, Coventry, and Wilkinson 2012).

Both strength of parent concrete from which RA was derived and mixing approach had a negligible effect on freeze-and-thaw resistance (Liu et al. 2016). Zaharieva, Buyle-Bodin, and Eric (2004) investigated the effects of different moisture state of RA and using full replacement of all aggregates on freeze-and-thaw resistance. They confirmed that the best protection was attained by replacing just the RCA. The RAC with 100% RCA and RFA performed poorly and the one prepared with all aggregates replaced by pre-soaked RA (RCA + RFA) gave the worst performance. The RAC prepared with the EMV method showed a higher resistance to freeze-and-thaw action than their comparable RAC proportioned by the traditional method (Abbas et al. 2009).

2.5.2.10 Water Absorption Capacity

This durability property of RAC depend on both quality and quantity of RA, as well as particles size. These factors determine the mortar content of RA and have a correlation with the strength of the parent concrete from which the RA is obtained. For example, completely replacing the RCA showed different water absorption capacity as follows: 68.9% (Bravo et al. 2015b), 62% (Correia, De Brito, and Pereira 2006), and 17.5% (Matias et al. 2014). Study into the effect of the original concrete strength showed that

40MPa and 80MPa as the source of the RA resulted in 57% and 27% water absorption capacity of RAC when coarse aggregate was fully replaced (Afroughsabet, Biolzi, and Ozbakkaloglu 2017).

Nevertheless, water absorption performance of RAC can therefore be improved if the microstructure of the cement matrix can be improved. This, of course, depends on a number of factors such as particles size, shape, and distribution, particles packing, water-to-cement ratio, reactivity, and the use of admixture (Anike et al. 2020a, Van Der Putten et al. 2017, Hunger and Brouwers 2009, Moosberg-Bustnes, Lagerblad, and Forssberg 2004). Afroughsabet, Biolzi, and Ozbakkaloglu (2017) observed up to 17% reduction in water absorption of RAC prepared with GGBS compared to the equivalent concrete without GGBS. This improvement was as a result of the potency of the GGBS in reducing the pores and intercepting pores connection (Kou, Poon, and Etxeberria 2014). The presence of SF in RAC resulted in up to 23% reduction in water absorption relative to corresponding concrete with no SF (Afroughsabet, Biolzi, and Ozbakkaloglu 2017).

2.5.2.11 Chloride Penetration Resistance

The depth to which chloride travels in concrete when exposed to certain chloride-prone environments is regarded as chloride penetration and the opposition to such transmission is referred to as chloride penetration resistance. The contact of chloride with the rebars in concrete causes corrosion of the rebars (Guo et al. 2018) and eventually impairs with the appearance integrity of the concrete. Overall, the resistance to chloride penetration of RAC is lower than that of NAC. However, RAC prepared with a low water-to-cement ratio offered a better resistance in a chloride environment than the corresponding NAC (Vázquez et al. 2014). It was found that chloride penetration resistance for both NAC and RAC decrease as the water-to-cement ratio increase (Tuyan, Mardani-Aghabaglou, and Ramyar 2014, Otsuki, Miyazato, and Yodsudjai 2003). Also, resistance improved with curing age for both normal and recycled concretes (Bravo et al. 2015b, Somna, Jaturapitakkul, and Amde 2012, Sim and Park 2011).

The strength of the parent concrete from which the RA is derived influence the chloride penetration resistance of the resulting concrete. This is definitely because the amount of mortar in RA is linked with the grade of the original concrete. Kou and Poon (2015) showed that RA obtained from a higher strength concrete resulted in RAC with a greater resistance than the comparable RAC made of RA obtained from a lower strength concrete. Duan and Poon (2014) investigated the response of RAC to chloride

penetration by considering three different grades (in terms of mortar content) of RA. They found that the resistance action of RAC was enhanced as the mortar content reduced. The use of fly ash or GGBS in partnership with cement for RAC mixes proportioned using the EMV technique enhanced chloride penetration resistance (Abbas et al. 2009).

2.6 Fibre-Reinforced Concrete

The use of fibres in civil engineering works has been practised over the past decades (Gettu, Zerbino, and Jose 2017) with the aim of enhancing serviceability and failure mode of concrete structures. The presence of fibres in plain concrete induces ductile behaviour, improves the mechanical properties and limits cracking propagation in the cement composites (Won et al. 2012). Also, fibre improves the ultimate shear strength and stiffness of the beam and deflection, strains, rotation, crack development, and dowel cracking are controlled, thereby preventing large crack widths and increasing aggregate interlock (Zhang et al. 2016, Swamy and Bahia 1985). Generally, there is a reduction in the rate of strength loss with the addition of SF (Markovic 2006) and greater effect of SF is on the flexural strength than the compressive or tensile strength, with more than 100% increases reported (Van Chanh 2005).

The inclusion of SF leads to the conversion of sudden failure to a ductile behaviour through resistance to crack formation and the provision of pinching forces at crack extremities to forestall cracking propagation (Won et al. 2012, Lim and Oh 1999). Toughness and ductility of concrete material are improved using fibres (Kang et al. 2010, Van Chanh 2005). According to Dinh et al. (2010), multiple diagonal cracks developed in the tested steel fibre-reinforced concrete (SFRC) beams and one or more of the cracks widened considerably, giving signal of impending failure before shear failure ultimately ensued. Increased load carrying capacity, tensile, flexural and cracking shear strengths as well as decreased crack width and deflection are all rewards for addition of SF (Won et al. 2012, Boulekbache et al. 2012, Cucchiara, La Mendola, and Papia 2004, Lim and Oh 1999, Purkiss, Wilson, and Blagojevic 1997, Swamy and Bahia 1985). Hence, fibres have successfully been applied to both high and ultra-high-performance concretes (Afroughsabet, Biolzi, and Ozbakkaloglu 2017, Vaishali and Rao 2012, Kang et al. 2010).

2.6.1 Factors Influencing the Performance of Fibres in Concrete

2.6.1.1 Fibre Aspect Ratio and Volume Content

The ratio of fibre length to its diameter known as fibre aspect ratio plays a huge role in the post-cracking capacity of FRC in a similar manner as fibre content which improves post-cracking tensile strength (Michels, Christen, and Waldmann 2013). Kang et al.

(2010) in their three-point bending test on ultra-high performance fibre-reinforced concrete (UHPFRC) beams concluded that the flexural strength for any given fibre geometry completely depends linearly on volume fraction of the fibres. On the other hand, Dinh et al. (2010) reported that longer fibres have the ability to bridge larger width cracks more effectively than their equivalent shorter ones irrespective of the fibre volume fractions. They also concluded that if fibre dosage is at least 0.75%, the three types of SF employed in their study can be used to achieve minimum shear requirement in the ACI–318 code provision. For Lim and Oh (1999), the best fibre dosage to achieve transition from shear mode to ductile mode was 1%. They recorded up to 55% improvement in the flexural strength with an exceptional ductility and energy absorption characteristics when volume fraction of SF was increased from 0 to 2%. They further stated that while tensile strength value was more than doubled, compressive strength increased by 25% with a fibre content of 2%. With respect to exposure to elevated temperatures, the effects of SF on elastic modulus became appreciable with a dosage of 1.5% (Chen et al. 2014).

Furthermore, the way FRC element responds to creep depends on type and volume fraction of fibre (Buratti and Mazzotti 2012, Mackay and Trottier 2004). Boulekbache et el. (2016) found that the cumulative energy increased notably with fibre dosage and slightly with aspect ratio.

2.6.1.2 Fibre Distribution and Orientation

To optimise fibre content, Boulekbache et al. (2012) suggest that the knowledge of fibre orientation is a key factor, and that efficiency is achieved when fibre is perpendicular to the plane of shear strength. They also reported that the alignment of fibres was influenced by the aspect ratio as fibres of larger aspect ratio were more aligned with the direction of flow. Although one disadvantage of longer fibre is its congestion which creates voids; however, Dinh et al. (2010) suggested that using the same length of fibre as the minimum clear spacing between bars can check this problem, otherwise, repair with high-strength grout into the voids would suffice. From Boulekbache et al. (2012) perspective, the most influential factors on fibre orientation in fresh concrete are the yield stress of concrete and the wall effect developed by geometry of the formwork. They maintain that fibre orientation and distribution affect the ductility property of FRC, and concretes of low yield stresses are well oriented and more homogeneously distributed. The flexural performance of FRC under cyclic loading was highly influenced by the fibre orientation (Boulekbache et al. 2016).

The consistency of concrete in fresh state, dimensions of formwork, direction of casting, technique employed for compaction, and composition of the concrete are the factors that affect fibre distribution and orientation (Michels, Christen, and Waldmann 2013). Whereas according to Boulekbache et al. (2012), the geometry of fibres and their interaction effects (that is, fibres–aggregates–formwork), concrete flowability, means of pouring and compacting the concrete, and geometry of the concrete shafts (free surface, two or four boundaries) with their dimensions are the factors that affect the two factors. However, a higher fibre efficiency results when there is a perfect alignment and in the direction of stress resulting in higher post-cracking strength compared random orientation. Theoretically, if fibre orientation is perpendicular, it will be impossible for it to contribute to strength (Michels, Christen, and Waldmann 2013).

2.6.2 Overview of Previous Experimental Investigations on Fibre Reinforced Concrete

Fibres have been used for both conventional concrete and RAC for reason already pointed out above. The findings of early researchers who investigated the use of fibres in concrete across different topics are summarized in Table 2.7.

2.7 Summary

The state of affairs in the use of RA has been examined in this chapter through the review of works by early researchers. Although RA has gained global attention, its universal acceptance is still a work in progress. Notwithstanding, some developed countries, mostly Europe and the US, have adopted the use of RA for structural purposes at various degrees. RA is considered inferior and different from its comparable NA mainly due to the adhering mortar. Among other factors, source of RA, particle size, mortar content, impurity level, and the recycling process, influence the properties of RA. Although the physical properties of RA are poor in comparison with NA, the mechanical properties of the concrete made with RA are similar or slightly lower than those of its equivalent NAC. The use of the conventional mix design method has adverse effect on RAC properties and requires further investigation. This is because the mortar content of RAC mixes proportioned with the traditional method is raised above that of the corresponding NAC. Conversely, a new mix design approach dubbed “Equivalent mortar volume” method produces RAC of similar or even higher strength compared to NAC. In fact, the only record in the literature where the elastic modulus of RAC was greater than that of NAC was with the EMV mix proportioning technique. But this method does not incorporate RFA, possibly because its mortar content cannot be measured. Incorporating the same replacement ratio of RCA obtained using the EMV guidelines for RFA could be

appropriate, and this needs to be investigated to maximize the use of RA. Using a two-stage mixing approach, RA from a high-grade concrete, and admixtures (e.g., superplasticizer, GGBS, fibres, etc.), improve the performance of RAC. Generally, introduction of fibre (especially steel fibre) and GGBS in the concrete mix enhances both mechanical and durability properties of the concrete and the improving effect of fibre is more in RAC than NAC. It is noted that aspect ratio, volume fraction, distribution, and orientation of fibre, are the factors that affect the performance of fibre in concrete. Although an aspect ratio of 60 and fibre dosage of 1% are adequate, optimization of fibre is highly recommended.

Table 2.7: Summary of some studies on fibre-reinforced concrete using RA and/or NA.

Author(s)	Description of experiment	Fibre content (%)	Fibre aspect ratio	Remarks
Lim and Oh (1999)	Effects of SF and shear stirrups contents on the mechanical properties of concrete beams	Varied from 0 to 2 by volume of concrete	60	At 2% fibre dosage there was: (i) about 25% increase in CS (ii) up to 55% increase in FS (ii) more than double in the value of STS. Cracking shear strength improved appreciably.
Akinkurolere (2010)	Influence of SF on compressive and tensile strengths of RAC produced with fly ash	1.5	N/A	(i) SF has a negligible effect on CS (ii) SF significantly influenced STS (iii) There was strength improvement with no more than 60% replacement level with RA.
Dinh et al. (2010)	The behaviour of steel fibre-reinforced concrete beams without stirrup reinforcements	Varied from 0.75 to 1.5 by volume of concrete	55, 60	(i) Longer SF showed superior performance than its shorter counterpart (ii) Multiple diagonal cracks developed due to the presence of SF, resulting in a ductile failure mode (iii) With at least 0.75% fibre dosage, minimum shear requirement by ACI-318 code can be achieved.
Erdem et al. (2011)	Impacts of SF and synthetic macro fibre on both conventional concrete and RAC	N/A	SF: 55 Synthetic fibre: 53	(i) About 20% loss in CS of RAC compared to NAC (ii) Inclusion of SF reduced the CS of RAC but marginally increased that of NAC (iii) Generally, SF improved the FS, post-cracking load, deflection and impact strength of RAC than NAC (iv) With synthetic fibre, there is a greater energy absorption capacity after the initial cracking formation than with SF.
Won et al. (2012)	Flexural responses of concretes reinforced with amorphous micro-steel fibre and conventional SF	0.2, 0.3, 0.4, 0.5, 0.7 and 1	Micro-steel fibre: 123	(i) At fibre content lower than 0.5%, conventional SF performed better than the micro-steel fibre. Reverse is the case for higher fibre contents (ii) In terms shear capacity, the conventional SF was preferred irrespective of volume fraction.

Note: CS = compressive strength, FS = flexural strength, STS = splitting tensile strength

Author(s)	Description of experiment	Fibre content (%)	Fibre aspect ratio	Remarks
Boulekbache et al. (2012)	Effects of compressive strength and yield stress on shear capacity of fibre reinforced concrete	0.5 and 1	65, 80	(i) SF slightly reduced the CS of concrete with more influence on high strength concrete (up to 10% reduction) (ii) Concrete of low yield stress produced well oriented fibres than companion high yield stress concrete (iii) SS improved by improving CS and the inclusion of SF (iv) 1% fibre content gave the best result and the effects of fibre aspect ratios of 65 and 80 do not differ significantly.
Yoo et al. (2013)	Influence of fibre contents on mechanical properties of ultra-high-performance fibre-reinforced cementitious composites	1, 2, 3, and 4	65	(i) All tested specimen failed in a brittle manner in spite of fibre content (ii) In terms of CS and elastic modulus, greatest values were recorded at 3% fibre volume ratio while the least values were at 4% (iii) Both FS and deflection increased with increasing fibre dosage (iv) Bond strength and pull-out energy values were maximum at 2% fibre ratio.
Michels et al. (2013)	Effects of aspect ratio, type and dosage of fibre on the post-cracking response of SFRC	0.2, 0.52, 0.65, 0.92, and 1.3	60 and 30	(i) Higher maximum force, post-cracking strength and total energy absorption were all achieved with SF of higher aspect ratio (ii) Even with greater volume fractions, a denser fibre had a lower efficiency compared to their longer and thinner counterparts.
Won et al. (2013)	Bonding properties of both amorphous micro-steel fibre and hooked-ended fibre in cement composites	1 and 4 (piece/s)	1034 and 60	(i) Composite made with micro-steel fibre had a higher maximum pull-out load than those reinforced with hooked-ended fibre (ii) Samples made of hooked-ended fibre had a greater bond strength and interfacial toughness than those incorporating micro-steel fibre (iii) Hooked-ended fibre composites failed by pull-out of the fibres whereas the failure of the micro-steel fibre composites was by fracture of the fibres.

Note: CS = compressive strength, FS = flexural strength, STS = splitting tensile strength

Author(s)	Description of experiment	Fibre content (%)	Fibre aspect ratio	Remarks
Vaishali and Rao (2012)	Strength and durability effects of using RA and fibres in the production of high-performance concrete. Three different types of fibre were investigated.	0 to 1.25	SF: 100 Polypropylene fibre: length = 12mm; diameter = 12 microns, Glass fibre: length = 12mm; diameter = 14 microns	(i) The best results were achieved for all the fibre types at 1% fibre dosage. Balling effects occurred in the concrete mixes at 1.25% fibre content, leading to a poor performance (ii) The contribution of SF to concrete strength was more compared to the other fibre types (iii) Fibres improved the properties of RAC more than those of the corresponding NAC. The presence of fibre reduced the Chloride ion permeability of both RAC and NAC.
Gao, Zhang and Nokken (2017a)	The compressive responses of SFRC made with RCA and designed with equivalent cube compressive strength	0.5, 1, 1.5, and 2	54.6	(i) Optimum fibre volume fraction was found to be 1.5% (ii) Cube CS improved by 11% when SF was added to RAC (iii) Elastic modulus was enhanced with the addition of SF and the effect depended on fibre ratio (iv) SF showed a greater reinforcing effects on RAC than NAC (Toughness index of RAC increased with a higher fibre dosage.
Gao, Zhang and Nokken (2017b)	Mechanical performance of reinforced concrete prepared with SF under direct shear	0.5, 1, 1.5, and 2	54.6	(i) Up to 135% improvement was recorded for RAC by considering SF volume ratio range from 0-2% (ii) The presence of SF engendered a ductile failure mode and the tested specimens maintained their integrity after shear failure.
Afroughsabet et al. (2017)	The effect of using hooked-ended SF on both mechanical and durability characteristics of high-performance concrete produced with RA	1	65	(i) CS, STS, and FS respectively improved by 12%, 60%, and 88% using 1% fibre content (ii) SF enhanced the properties of RAC more than those of comparable NAC (iii) Water absorption, shrinkage, and electrical resistivity of RAC were all reduced by adding SF.

Note: CS = compressive strength, FS = flexural strength, STS = splitting tensile strength

Chapter 3

3 RESEARCH METHOD AND MATERIALS

3.1 Introduction

This chapter explains the materials, equipment and sequence of programs employed to achieve the aim of this research. The state of the art of recycled aggregate (RA) and its resulting concrete has been reviewed in the previous chapters. Hence, both experimental and numerical investigations are required to actualize the set objectives. The success of the experimental campaign began with characterization of the aggregates used. Then, concrete mixes were designed using the normal mix design method and the equivalent mortar volume (EMV) mix design technique. Trial tests were conducted on both plain and steel fibre-reinforced concretes using the selected mix design methods, to authenticate the mixtures prior to adoption. Having obtained the best mixes, specimens for the main experiment were produced and tested appropriately. Subsequently, numerical analysis carried out on ANSYS application software was used to compare the results from experimental studies. Sections 3.2 and 3.3 respectively explain the materials and the method employed for the laboratory experiments, while Section 3.4 describes the numerical program for this research.

3.2 Materials

Fundamentally, concrete is composed of water, cement, aggregates, and sometimes admixtures. In this project, steel fibre (SF) was added to concrete mixes produced with RA, to improve the performance of recycled aggregate concrete (RAC). All constituent materials, except water and SF, used for concrete production in this study were supplied by Litecast Homefloors Ltd., a precast concrete beam company located at Nuneaton, West Midlands, United Kingdom. It is crucial to give detailed description of all materials used, as there exist a wide variety of materials with different characteristics. Thus, the following subsections are dedicated to such important details.

3.2.1 Water

Clean tap water obtained from Sir John Laing's Building where the university's Civil Engineering Laboratory is situated, was used.

3.2.2 Cement

CEMEX Rapid CEM I Portland cement was used in this research. The product which conforms to the British standard BS EN 197-1 (2011) is suitable for early strength gain.

The average of four set of tests (conducted by Rugby CEMEX UK Cement Limited) for physical, chemical, and mechanical properties of the cement is given in Table 3.1.

Table 3.1: Physical/Chemical/Mechanical properties of cement.

Physical properties									
Fineness (m^2/kg)	Initial setting time (mins)	Expansion (mm)	Loss on ignition (%)	Compressive strength (MPa)			Alkalis $(Na_2O)_e$ (%)		Chloride as Cl (%)
				2 days	7 days	28 days	Ave. of 25 data	Std dev.	Ave. of 25 data
527	96	0.8	2.86	38.9	51.5	62.7	0.65	0.03	0.05

Chemical composition by weight (%)												
SiO_2	Al_2O_3	Fe_2O_3	CaO	MgO	SO_3	$Na_2O_{(eq)}$	Cl	FL	C_3S	C_2S	C_3A	C_4AF
19.99	4.75	2.91	63.77	1.13	3.56	0.65	0.05	2.02	47.84	26.3	8.33	9.67

Note: CEM I, 52.5R; Compressive strength was determined according to BS EN 196-1.

3.2.3 Aggregates

Both natural and recycled aggregates were used in this study. The natural aggregate (NA) was gravel, and was the original aggregate used to produce the precast concrete from which RA was obtained. The RA was produced by crushing condemned precast concrete beams produced at Litecast Homefloors' facilities site, Nuneaton. Furthermore, it is worth mentioning that the mean cube compressive strength (measured after 24 hours) of all concretes produced by the company was approximately 40N/mm^2 and the age of the condemned beams was less than a year.

3.2.3.1 Preparation of Aggregates

The concrete rubble was crushed to small fragments using Rubble Master Compact Crusher 70Go!^{TM} which has the capacity to separate steel wires from the concrete; and delivered in containers (see Figure 3.1). However, the RA was delivered unsorted and there were pieces of steel wires and contaminants like paper, wood, plastic, and other lightweight materials as shown in Figure 3.2. Hence, the rubble was sieved to remove the impurities and graded as described in Sections 3.2.3.2 and 3.2.3.3 to obtain the fine and coarse aggregates, respectively. The graded aggregates were then stored according to grades in a 60-Litre Plastic Barrels until the day concretes were produced. Moisture content of the aggregates in each container was determined and used for the mix designs, accordingly. Samples used for characterization of the aggregates were obtained using the quartering method in accordance with ASTM C702/C702M–18 (2018) standards. Other standards adopted for the description of the distinct features of all aggregates used in this investigation are shown in Table 3.2.

Figure 3.1: Concrete rubble supplied by Litecast Homefloors Ltd., Nuneaton, West Midlands, UK.

Figure 3.2: Typical impurities in a precast concrete rubble.

Table 3.2: Standards used for characterization of aggregates.

Property	Standard
Sieve analysis of fine and coarse aggregates	ASTM C136/C136M–14 (2014)
Bulk density and voids in aggregate	ASTM C29/C29M–17a (2009)
Specific gravity and absorption of fine aggregate	ASTM C128–15 (2015)
Specific gravity and absorption of coarse aggregate	ASTM C127–15 (2015)

3.2.3.2 Fine Aggregates

All aggregates that passed through 4.75mm sieve were regarded as fine aggregates (sand) for both NA and RA as shown in Figure 3.3 and Figure 3.4 respectively. The fine

aggregates were further sieved through three (3) sets of wire mesh (arranged in decreasing order of size as shown in Figure 3.5) of nominal apertures of 2.47mm, 0.57mm, and 0.075mm with particles passing the 0.075mm sieve being discarded. The sieved fine aggregates were combined in the ratio 1:2:3 (in the order of size fractions presented in Table 3.3), to obtain a medium range fineness modulus for both natural fine aggregate (NFA) and recycled fine aggregate (RFA). The characteristics of the fine aggregates used in this study are presented in Table 3.3. While the sieve analyses of NFA and RFA are presented in

Table 3.4 and Table 3.5 respectively, their particles size distributions are shown in Figure 3.6.

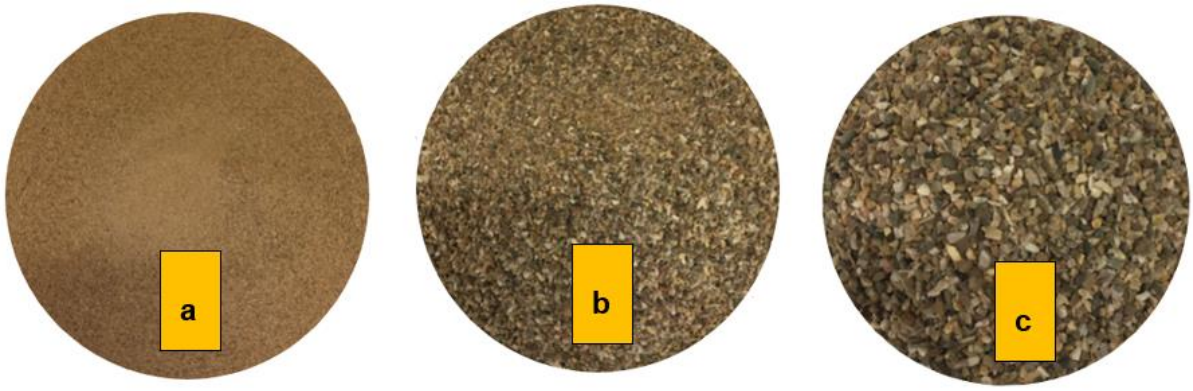

Figure 3.3: Natural fine aggregates of grades: (a) 0.075–0.57mm, (b) 0.57–2.47mm, and (c) 2.47–4.75mm.

Figure 3.4: Recycled fine aggregates of grades: (d) 0.075–0.57mm, (e) 0.57–2.47mm, and (f) 2.4–4.75mm.

Figure 3.5: A set of wire mesh for grading of fine aggregates.

Table 3.3: Properties of the natural and recycled fine aggregates.

Aggregate type	Size fraction (mm)	Specific gravity			Absorption (%)	Fineness modulus
		OD	SSD	AP		
NFA	4.750 - 2.470	2.48	2.52	2.57	1.4	2.87
	2.470 - 0.570	2.57	2.60	2.65	1.1	
	0.570 - 0.075	2.62	2.63	2.66	0.6	
RFA	4.750 - 2.470	2.15	2.34	2.66	8.9	2.71
	2.470 - 0.570	1.96	2.20	2.57	12.1	
	0.570 - 0.075	1.78	2.10	2.62	18.1	

Note: OD, SSD, and AP are oven-dry, saturated surface-dry, and apparent specific gravity, respectively.

Table 3.4: Sieve analysis of the natural fine aggregate.

Sieve Size (mm)	Individual mass retained (g)	Cumulative mass retained (g)	Cumulative percent mass retained (g)	Percentage passing (%)
4.750	0.4	0.4	0.1	100
2.360	53.5	53.9	18.0	82
1.180	49.6	103.5	34.5	66
0.600	45.2	148.7	49.6	50
0.300	108.1	256.8	85.6	14
0.150	39.5	296.3	98.8	1
0.075	3.3	299.6	99.9	0.1
PAN	0.1	299.7	–	–

Table 3.5: Sieve analysis of the recycled fine aggregate.

Sieve Size (mm)	Individual mass retained (g)	Cumulative mass retained (g)	Cumulative percent mass retained (g)	Percentage passing (%)
4.750	1.1	1.1	0.4	100
2.360	56.8	57.9	18.9	81
1.180	50.8	108.7	35.6	64
0.600	42.4	151.1	49.4	51
0.300	78.7	229.8	75.2	25
0.150	50.0	279.8	91.5	9
0.075	22.1	301.9	98.8	1.2
PAN	3.5	305.4	–	–

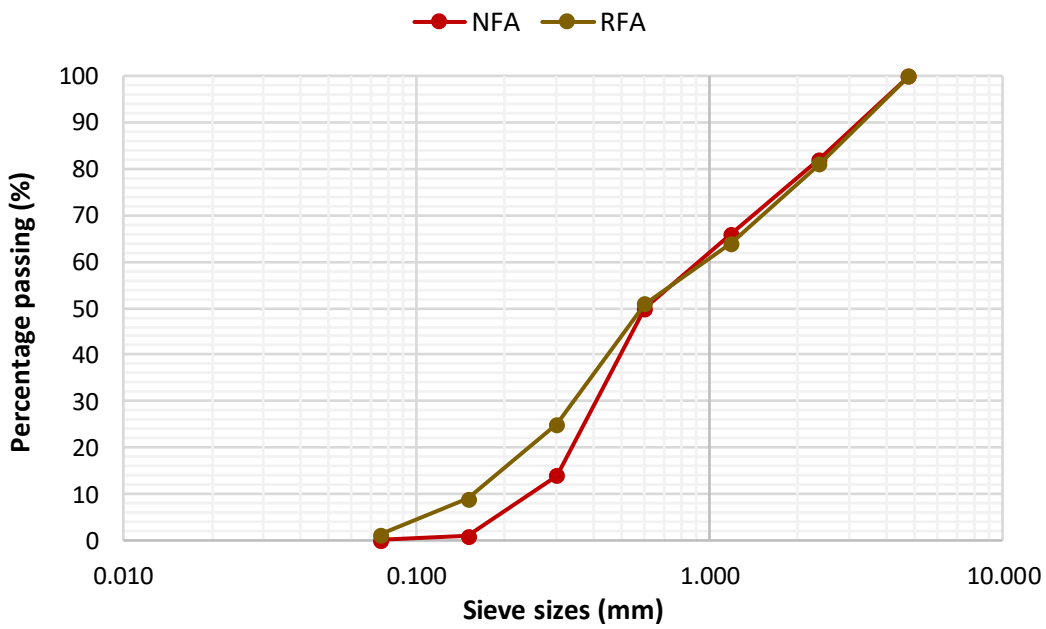

Figure 3.6: Particles size distribution of natural and recycled fine aggregates.

3.2.3.3 Coarse Aggregates

Aggregates that passed through 14mm sieve and retained on 4.75mm sieve were considered as the coarse aggregates for both NA and RA as shown in Figure 3.7 and Figure 3.8, respectively. The aggregates were graded into two in the size ranges: 4.75–10.00mm and 10.00–14mm and integrated in ratio 7:3 to produce concrete. The properties of the natural coarse aggregate (NCA) and recycled coarse aggregate (RCA) used in this investigation are given in Table 3.6. Their sieve analyses are presented in

Table 3.7 and Table 3.8 respectively, while Figure 3.9 shows their particles size distributions.

Figure 3.7: Natural coarse aggregates of grades: (g) 4.75–10mm and (h) 10–4mm.

Figure 3.8: Recycled coarse aggregates of grades: (i) 4.75–10mm and (j) 10–14mm.

Table 3.6: Properties of the natural and recycled coarse aggregates.

Aggregate type	Size fraction (mm)	Specific gravity			Absorption (%)	Void (%)	Loose bulk density (kg/m³)	Dry-rodded density (kg/m³)	Residual mortar content (%)
		OD	SSD	AP					
NCA	4.75 - 10.00	2.60	2.63	2.67	0.9	41	1450	1543	-
	10.00 - 14.00	2.62	2.64	2.66	0.6	39	1479	1586	-
RCA	4.75 - 10.00	2.30	2.42	2.62	5.4	43	1207	1300	51.49
	10.00 - 14.00	2.30	2.42	2.61	5.1	44	1171	1293	51.97

Note: OD, SSD, and AP are oven-dry, saturated surface-dry, and apparent specific gravity, respectively.

Table 3.7: Sieve analysis of the natural coarse aggregate.

Sieve Size (mm)	Individual mass retained (g)	Cumulative mass retained (g)	Cumulative percent mass retained (g)	Percentage passing (%)
13.20	13.6	13.6	0.5	99
10.00	643.5	657.1	24.3	76
9.50	290.3	947.4	35.1	65
8.00	800.8	1748.2	64.7	35
6.30	628.5	2376.7	88.0	12
5.00	231.3	2608.0	96.6	3
4.75	52.2	2660.2	98.5	1.0
PAN	32.2	2692.4	–	–

Table 3.8: Sieve analysis of the recycled coarse aggregate.

Sieve Size (mm)	Individual mass retained (g)	Cumulative mass retained (g)	Cumulative percent mass retained (g)	Percentage passing (%)
13.20	55.3	55.3	2.1	98
10.00	533.3	588.6	22.8	77
9.50	145.9	734.5	28.4	72
8.00	467.5	1202.0	46.5	54
6.30	631.7	1833.7	70.9	29
5.00	465.0	2298.7	88.9	11
4.75	141.7	2440.4	94.4	6.0
PAN	145.7	2586.1	–	–

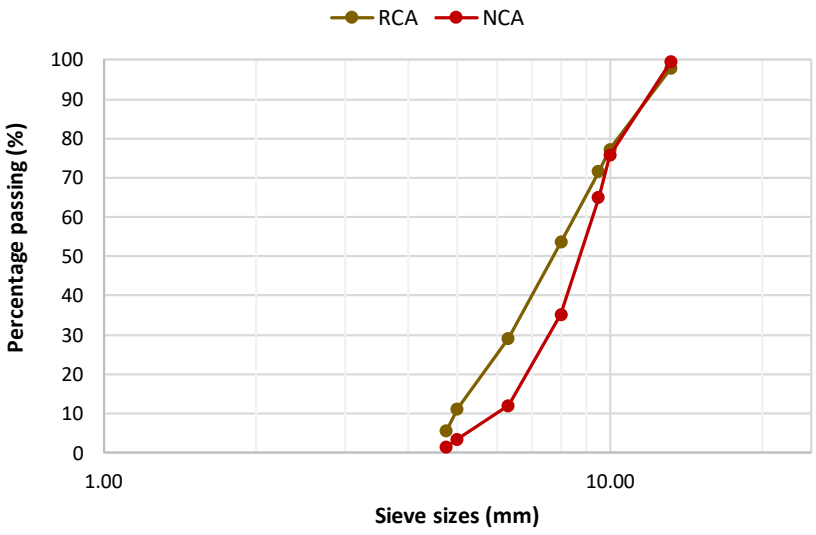

Figure 3.9: Particles size distribution of natural and recycled coarse aggregates.

3.2.3.4 Determination of Mortar Content in RCA

It has been established that the major difference between NA and RA is the presence of the residual mortar in the latter (Fathifazl et al. 2009a, Abbas et al. 2007, BRE Digest 433 1998). This is evident in Figure 3.10(a) and (b) which separately represent RA before and after treatment for the determination of mortar content. The residual mortar content of the RCA used in this study was determined using a similar procedure to that adopted by Abbas et al. (2009) as follows:

- Using the quartering method, the representative samples were obtained and oven-dried at a temperature of 105^{o}C for 24 hours.
- The oven-dry samples were then completely immersed in a 26% (by weight) Sodium Sulphate solution for another 24 hours.
- Then, the RCA was subjected to freezing and thawing, while still immersed in the solution, for five daily cycles at -17^{0}C (for 16 hours) and 80^{o}C (for 8 hours) respectively. This process is similar to the method described in ASTM C672/C672M–12 (2012) for scaling test.
- The solution was drained at the end of the last freezing and thawing cycle, and the samples washed with tap water over a 4.75mm sieve.
- The wet samples were then oven-dried at a temperature of 105^{o}C for 24 hours.
- Finally, the masses (before and after treatment) required were substituted in the expression in Equation 3.1 to obtain the residual mortar content thus:

$$RMC(\%) = \frac{M_b - M_a}{M_b} \qquad \textit{Equation 3.1}$$

Where RMC, M_b and M_a are respectively the residual mortar content (%), mass of RCA before treatment (kg) and mass of RCA after treatment (kg).

The mortar contents for the two size fractions of the coarse aggregate used in this research, determined according to the above method, are given in Table 3.6.

Figure 3.10: RCA before and after treatment for the removal of attached mortar.

3.2.4 Steel Fibre

There are three common shapes of SF that have been used in the past for concrete production. The shapes, shown in Figure 3.11, were all investigated in this research. While all the SF differ only in shape, they have the same dimensions, tensile strength, material and chemical compositions as presented in Table 3.9 and Table 3.10. The steel fibres were supplied by Dalian HARVEST Metal Fibres Co. Ltd. located in Zhongshan District, China.

Table 3.9: Steel fibre types and their properties.

Shape	Length (mm)	Diameter (mm)	Aspect ratio	Cross section	Tensile strength (MPa)
Straight	60	1.0	60	Circular	1900
Hooked-ended	60	1.0	60	Circular	1900
Undulated	60	1.0	60	Circular	1900

Table 3.10: Material and chemical composition of the steel fibre.

Material	Chemical composition (%)								
	C	Si	Mn	P	S	Cr	Ni	Cu	Fe
Carbon steel	0.7	0.22	0.55	0.015	0.006	0.02	0.01	0.03	Balance

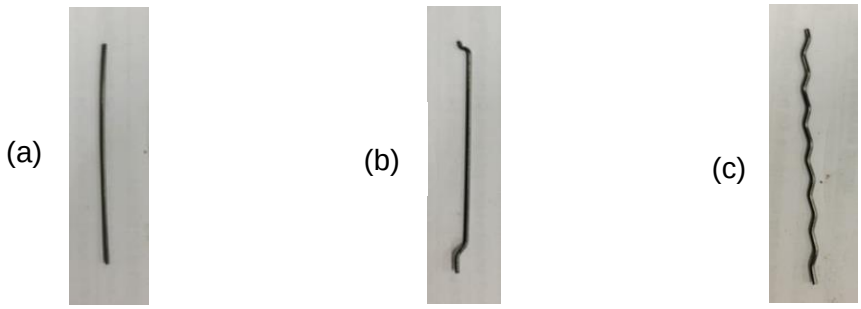

Figure 3.11: 60mm steel fibres: (a) Straight (b) Hooked-ended (c) Undulated.

3.2.5 Superplasticizer

An accelerating high range water reducer liquid admixture, known as Sika ViscoCrete 335, was used in the production of all concretes for this research. The product conforms to the specification by BS EN 934–2 (2012) and its technical data are as shown in Table 3.11.

Table 3.11: Technical data of the superplasticizer.

Chemical base	Modified polycarboxylate
Density	1.08kg/l (at +20°C)
pH value	4.5+/−0.5
Freezing point	+1°C
Total chloride ion content	<0.10% w/w (chloride free)
Air entrainment	Negligible, normally a minimal increase
Effect on setting	Slight extension to normal setting at 0.2% dose, normal setting up to 0.4% dose and accelerated setting at higher dosages due to its chemical nature
Effect of overdosing	Increased workability and segregation
Alkali content	0.25% maximum

3.3 Method

The realization of the aim of this research required a painstaking approach, consequently, the number of mixes needed to actualize the stated objectives was first decided, in which five different mixes were deemed appropriate as follows:

(a) Natural aggregate concrete (NAC) mix: This was the reference mix made entirely of natural aggregates and designed using the conventional method.

(b) Recycled aggregate concrete (RAC) mix: All aggregates in this mix were recycled and the mix was designed with the conventional method.
(c) Steel fibre-reinforced recycled aggregate concrete (SFRRAC) mix: This constituted the mix in (b) with the addition of optimum SF content appropriate to the conventional mix design method.
(d) Blended aggregate concrete (BAC) mix: This mix comprised of both natural and recycled aggregates and was prepared using the EMV technique. The substitution ratio of NA was dependent on the mortar content of the RCA as described in Section 3.3.1.2.
(e) Steel fibre-reinforced blended aggregate concrete (SFRBAC) mix: The mix was achieved as in (d) but also incorporated optimum SF volume fraction appropriate to the EMV mix proportioning method.

3.3.1 Experimental Design

The target strength of concrete for this research, for all mixes, was 40N/mm^2 at 28-day. Generally, two mix design methods were required in line with Section 3.3. That is, the conventional method for NAC, RAC, and SFRRAC mixes and the EMV method for BAC and SFRBAC mixes. However, two standards for conventional mix design method were examined experimentally for RAC mixes, using the compressive strength of 100mm cubes at 7 days. The rationale for this was to determine the approach that would manage resources better without compromising strength at the same time.

3.3.1.1 Conventional Method

Initially, the absolute volume method described in the American Concrete Institute (ACI) standard (ACI Committee 211 2009) and the Department of Environment (DoE) method according to the British Standard (Teychenné, Franklin, and Erntroy 1997) were both investigated experimentally. Then, trial mixes were conducted for mixes described in Section 3.3(a)–(c). This was appropriate to obtain a workable mix proportions (with similar slump values) that would be used in the main experiment. This was followed by optimization of SF in which a series of SF volume fractions from 0.125% to 1.50% was considered in RAC mixes. Afterwards, with the optimum fibre content, the best performing SF type was determined. The design of the concrete mix, using the suitable conventional method adopted for this study is shown in Appendix A.

3.3.1.2 Trial Mixes

The use of RA comes with a workability issues and the inclusion of RFA and steel fibre (SF) takes this challenge further. The motive for the trial mixes was to achieve the first

and second objectives of this research. That is, to optimize the water-to-cement ratio of all mixes, ensuring a slump in the range of 90–170mm for which most structural concrete complies to consistence class S3 according to BS 8500–1:2015+A2 (2019) and National Structural Concrete Specification (2010), and to optimize SF content. Furthermore, some scholars have argued that SF does not have any effects on the compressive strength of concrete while some others say it does. This argument was investigated at this stage of the present research. To this end, ten concrete mixes were designed and proportioned using both conventional and equivalent mortar volume (EMV) methods as shown in Table 3.12.

Table 3.12: Preliminary studies for the determination of workability and optimum SF content for the various mix design methods.

Mix ID	Design method	Mix Proportions (kg/m^3)								w/c	Slump (mm)	ACS§ (MPa)
		Water	Cement	NCA	RCA	NFA	RFA	SP$^{\beta}$	SF$^{\mu}$			
Mix 1	DoE	195	500	0	750	0	890	3.50	0.000	0.39	150	40.4
Mix 2	DoE	205	525	0	750	0	890	3.70	0.125	0.39	155	39.3
Mix 3	DoE	205	525	0	750	0	890	3.70	0.250	0.39	165	40.8
Mix 4	DoE	215	550	0	750	0	890	3.85	0.500	0.39	155	40.4
Mix 5	DoE	225	575	0	750	0	890	4.03	1.000	0.39	120	44.0
Mix 6	DoE	225	575	0	750	0	890	4.03	1.500	0.39	65	45.8
Mix 7	EMV	153	364	203	754	493	305	2.00	0.000	0.42	170	46.0
Mix 8	EMV	153	364	203	754	493	305	2.50	0.250	0.42	150	39.9
Mix 9	EMV	153	364	203	754	493	305	3.00	0.500	0.42	165	47.9
Mix 10	EMV	153	364	493	754	203	305	3.20	0.750	0.42	170	44.8

Note: W/C = water-to-cement ratio; $^{\beta}$superplasticizers added as percentage of cement content; $^{\mu}$steel fibres added as a percentage of concrete volume; §average compressive strength for 6 cubes.

The hooked-ended SF was used for the preliminary studies and the water-to-cement ratios of 0.39 and 0.42 were kept constant for the mixes prepared with conventional and EMV methods, respectively. From the results shown in Table 3.12, 1% SF volume ratio was selected as the candidate for the SFRRAC mix in the next stage of the experiments. The decision was reached from the perspective of cost, concrete strength, and workability (measured in terms of slump value). It should be noted that increase in strength became clear at 1% fibre content with approximately 44.0N/mm^2 compared to 40.4N/mm^2 produced by the control mix with no SF. Although, a further increase to 1.5% in SF content showed a corresponding increase in concrete strength but based on economy and workability issues (reduced slump), 1% volume ratio was deemed suitable. Moreover, the plot in Figure 3.12 shows that if the SF volume keeps increasing, the slope of the graph would continue to drop. In a similar investigation by Afroughsabet, Biolzi,

and Ozbakkaloglu (2017) using a double hooked-ended SF of aspect ratio of 65, the optimum SF volume fraction chosen was 1%.

But for the mix proportioned with the EMV method, 0.5% SF volume ratio was selected and used for the SFRBAC mix, in the next stage of the experiments. It then follows that the optimum SF volume ratio was influenced by the mix design method. Overall, it can be deduced that the addition of SF to recycled aggregate concrete (RAC) either increases or decreases the compressive strength of the resulting concrete, subject to volume fraction of the SF used.

Having used the hooked-ended type to obtain the optimum SF content appropriate to normal mix design method, the same mix was replicated using straight and undulated SF. The results obtained for the three SF types were presented and compared in Table 3.13. Evidently, the undulated type gave the best result, hence was adopted for this research. Additionally, as mentioned in Section 3.3.1.1, the result of the two conventional concrete mix design methods investigated for RAC is presented in

and it shows that the ACI standard offers a higher strength than the DoE standard. Although the variance in the strength produced by the two standards was insignificant, the difference in cement content was quite substantial. Consequently, the ACI standard was adopted as the conventional method for RAC mixes in the main experiment.

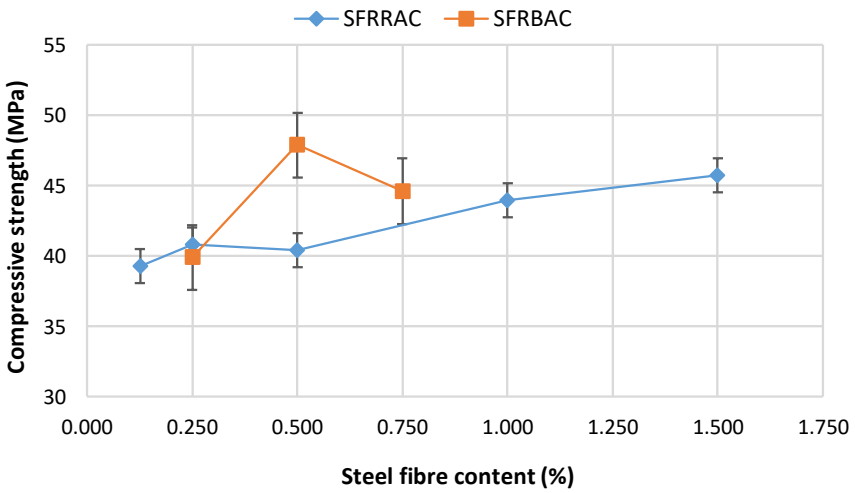

Figure 3.12: The effect of steel fibre volume ratio on the compressive strength of RAC.

Table 3.13: Comparison of the performance of different steel fibres.

Type of SF	Crushing load (kN)	Standard deviation (kN)	Average compressive strength (MPa)	Slump (mm)
Straight	429.37 436.06 420.56 421.81 418.56	7.29	42.5	117
Undulated	442.31 451.87 453.12 463.81 449.56	7.75	45.2	125
Hooked-ended	435.81 438.19 437.19 446.56 437.94	4.25	43.9	120

Table 3.14: Comparison between ACI and DoE standards.

Design method	Mix proportion (kg/m³)					W/C ratio	CS^{μ} (MPa)	ACS (MPa)
	Water	Cement	RFA	RCA	SP			
ACI	213	507	594	786	1.01	0.42	39.95 40.59 41.86 41.06 42.54 41.61	41.3
BS	240	570	576	769	1.14	0.42	40.21 39.99 39.81 38.89 39.29 40.46	39.8

Note: SP = superplasticizer, W/C = water-to-cement ratio, CS^{μ} = compressive strength for each cube, ACS = average compressive strength.

3.3.1.3 Equivalent Mortar Volume Method

The details of this mix design approach can be found in Fathifazl et al. (2009a). The method involves a series of mathematical equations and the percentage replacement of NCA with RCA lies on the residual mortar content of the RCA. According to the EMV mix design provisions, the relationship for determining the maximum theoretical residual (adhered or attached) mortar content of the RCA is given as:

$$RMC_{max}\% = \left(1 - V_{DR-NCA}^{NAC} \times \frac{SG_b^{NCA}}{SG_b^{RCA}}\right) \times 100 \qquad \textit{Equation 3.2}$$

Where V_{DR-NCA}^{NAC} is the dry-rodded volume of natural coarse aggregate in NAC, SG_b^{NCA} and SG_b^{RCA} are respectively bulk specific gravity of NCA and RCA.

If the maximum theoretical RMC obtained from Equation 3.2 is greater than the actual RMC of the RCA, then total substitution of the NCA is feasible, otherwise, not viable. For the current research, the maximum theoretical RMC is 37.6%. Comparing this value with the real (experimental) RMC given in Table 3.6, it is therefore not practicable (in this study) to completely replace the NCA with RCA. Hence, the mixes described in Section 3.3(d)–(e) were designed using the EMV method as detailed in Appendix B. It should be noted, that an additional step to ones given by Fathifazl et al. (2009a) was required to incorporate RFA in the present research.

Hence, the overall mix developed for all the outlined mixes in Section 3.3 is presented in Table 3.15. The mix proportions are based on oven-dry condition of the aggregates.

Table 3.15: Mix proportions of all concrete mixes in kg/m^3.

Mix ID	Water	Cement	RFA	NFA	RCA	NCA	Super-plasticizers	Steel fibres	Slump (mm)
NAC	213	507	0	707	0	856	1.27	0.00	110
RAC	213	507	534	0	754	0	1.52	0.00	135
SFRRAC	213	507	534	0	754	0	3.80	78.50	135
BAC	153	364	305	203	754	493	7.28	0.00	170
SFRBAC	153	364	305	203	754	493	12.0	39.25	170

3.3.2 Production of Concrete

Constituent materials were batched and properly mixed until a consistent mixture was obtained. The mixture was then transferred immediately into an oiled mould where it was

left to harden. After about 24 hours, the specimens were demoulded and transferred into a curing tank until the day of testing. All but beam specimens were cured by immersion in water. The following subsections are given to explain the sequence of activities for the concrete manufacture.

3.3.2.1 Batching

Concrete ingredients were batched according to the volume required and batching was done by weight using a weighing balance of 60kg capacity.

3.3.2.2 Mixing

Mixing was done in a 70-Litre capacity Mixer (Figure 3.13). Similar procedure to that of two-stage mixing approach (TSMA) was adopted for all concrete containing RA. The mixing processes for all the mixes are as illustrated in Figure 3.14–3.18. As soon as a homogeneous and consistent mix was attained, the concrete was transferred to a wheelbarrow, tested for slump (when required) and then poured into suitable moulds for onward processing.

Figure 3.13: 70- Litre capacity mixer.

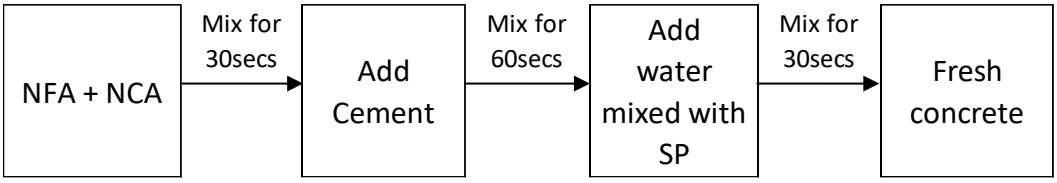

Figure 3.14: Mixing procedure for NAC.

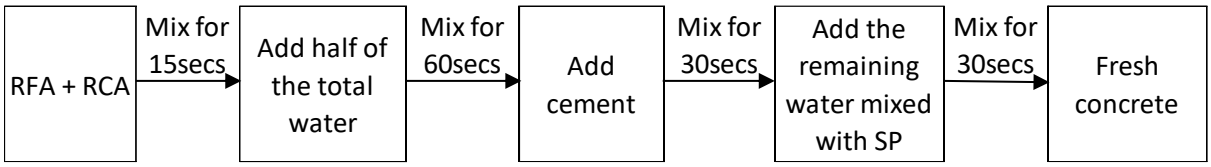

Figure 3.15: Mixing procedure for RAC.

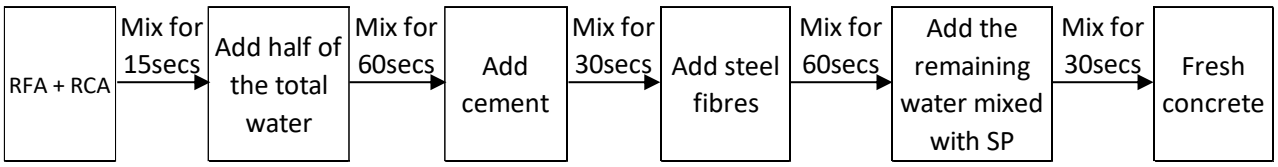

Figure 3.16: Mixing procedure for SFRRAC.

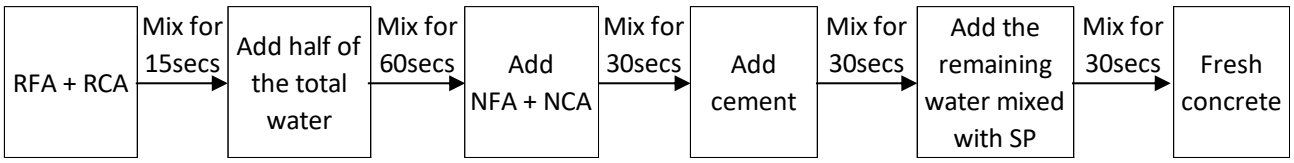

Figure 3.17: Mixing procedure for BAC.

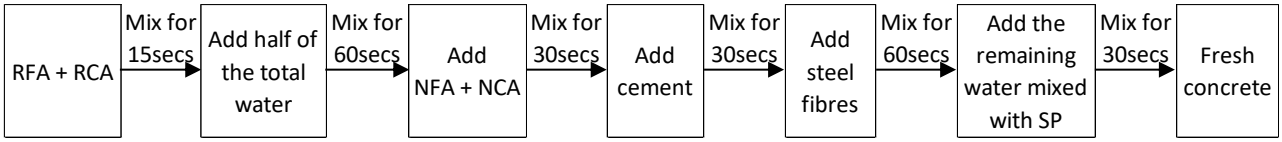

Figure 3.18: Mixing procedure for SFRBAC.

3.3.2.3 Mould

Plastic moulds of dimension 100 × 100 × 100mm and 150 × 300mm (as well as 100 × 200mm) were used for the cubical and cylindrical specimens, respectively. For the

prisms and the reinforced concrete beams, 150 × 150 × 500mm wooden and 80 × 180 × 1500mm steel moulds were used, respectively.

3.3.2.4 Compaction

Plain concretes of 100mm cubes and 100 × 200mm cylinders were compacted in two layers to achieve full compaction using a vibrating table, whereas the 150 × 300mm cylindrical specimens were compacted in three layers. On the other hand, for the steel fibre-reinforced concretes, both the cubes and the small cylinders were compacted in three layers and the big cylinders in five layers, to attain full compaction. The fibre-reinforced concrete prisms were compacted in a single layer and the unreinforced ones in two layers. A needle vibrator was used for the compaction of the reinforced concrete beam specimens. In all, attention was paid during compaction to stop the vibration as soon as air in the composite had been eliminated. This was in accordance with the standard practice to avoid segregation of concrete ingredient induced by excessive vibration.

3.3.2.5 Curing

The curing of specimens was done according to BS EN 12390–2 (2009: 7) standard. The specimens were demoulded after 24 hours and transferred into a curing tank where they were cured by immersion in water for 7, 28, or 56 days as required. The beam specimens were cured in air.

3.3.3 Testing

After curing as stated in Section 3.3.2.5, the mechanical properties of concrete (plain and reinforced) were investigated as described in the following subsections.

3.3.3.1 Density

The density of 100 × 100 × 100mm cube specimens was tested at 7, 28, and 56 days ages according to the BS EN 12390-7 (2009) code of practice. The specimen was removed from the curing tank on the day of testing and surplus water on the surface was allowed to dry (drying was facilitated by wiping with dry towel). Volume of specimen was obtained using water displacement method. Thus, the saturated surface-dry mass was first obtained in air and immediately, the specimen was submerged in water-tank using the equipment set-up in Figure 3.19 and the apparent mass was obtained, and all values recorded. The volume of the specimen was calculated using the formula in Equation 3.3 given as:

$$V = \frac{m_a - m_w}{\rho_w}$$ *Equation 3.3*

Where V, m_a, m_w and ρ_w are the volume of specimen (m^3), mass of specimen in air (kg), apparent mass of the immersed specimen (kg), and the density of water at 20°C, taken as 998kg/m^3, respectively.

Then, the density of all specimens was calculated using Equation 3.4 as follows:

$$D = \frac{m}{V}$$ *Equation 3.4*

Where D, m and V represent the density, mass, and volume of specimen, respectively.

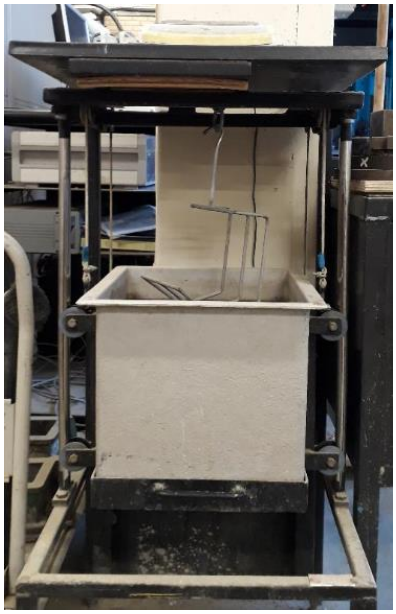

Figure 3.19: Equipment set-up for the determination of apparent weight of samples.

3.3.3.2 Compressive Strength

The compressive strength of 100 × 100 × 100mm cube specimens was tested in accordance with BS EN 12390:3 (2009) using an automated 2000kN bearing capacity Avery-Denison compression testing machine. The machine, shown in Figure 3.20, was designed to register both the load and vertical displacement in the spreadsheet of the computer system. Before placing the specimens in the machine, their surfaces were freed from moisture and any loose material. The top and bottom platens of the machine were also cleaned to remove possible grit from previous test. The specimen was then positioned centrally (with respect to the bottom platen) in the compression machine in a manner that the applied load was perpendicular to the direction of casting. Load

application was done at a constant loading rate of 8kN/s until failure occurred. The maximum load sustained by each specimen was recorded and imputed in the formulae shown in Equation 3.5 to obtain the compressive strength of concrete. This procedure was followed to determine the 7-, 28-, and 56-day compressive strength of the concrete, in which five (5) specimens were produced for each mix and for each age. The compressive strength was obtained using the following expression:

$$f_c = \frac{P}{A_c} \qquad \textit{Equation 3.5}$$

Where f_c is the cube compressive strength (N/mm^2), P is the maximum load at failure (N) and A_c is the cross-sectional area of the specimen being tested (mm^2).

Figure 3.20: Avery-Denison compression testing machine.

3.3.3.3 Tensile Splitting Strength

Tensile splitting strength was studied using 150mm diameter × 300mm high cylindrical specimens in accordance with BS EN 12390–6 (2009) standard after 28 days of curing. The same Avery-Denison testing machine used for compression test was utilized for this testing. First, the bearing surfaces of the jig, packing stripes, loading pieces, and platens were thoroughly wiped. Then excess moisture from the surface of the specimen was wiped, and loose grit or other inappropriate material was cleaned and removed from the surface of the specimen before placing them in the testing machine. The test specimen was positioned centrally in the testing machine, ensuring that the packing stripes and loading pieces were placed along the top and bottom of the plane of loading. It was also ensured that both upper and lower platens were parallel during the application of load at

a constant rate of stress within the range 0.04–0.06N/mm^2·s, in the manner stated in the code. The load was applied until failure occurred and the maximum load value that the specimen could sustain was recorded. The set-up of the whole system for the testing is as in Figure 3.21.

The tensile splitting strength of the specimen was obtained using the formula in Equation 3.6. That is,

$$f_{ct} = \frac{2 \times F}{\pi \times L \times d} \qquad \textit{Equation 3.6}$$

Where f_{ct}, F, L and d represent the tensile splitting strength (N/mm^2), maximum load (N), length of the line of contact of the specimen (mm), and diameter of the specimen (mm) respectively. π is a constant with assigned value of 3.142.

Figure 3.21: Set-up for tensile splitting strength test.

3.3.3.4 Flexural Strength of Plain Concrete

The flexural strength was carried out according to ASTMC78/C78M 12390–5 (2018) standard using third-point loading on 150 × 150 × 500mm specimens, after 28 days of curing. The testing machine bearing surfaces were wiped clean and any loose grit or other extraneous material from the surfaces of the specimen was removed. Excess moisture from the surface of the specimen was wiped before placing it in the testing machine. The test specimen was turned on its side with regard to its position as moulded, so that the direction of casting was at an angle of 90^o to the application of load as shown in Figure 3.22. Ensuring that the specimen was centred on the support blocks, the loading block was brought in contact with the surface of the specimen at the third point

and a force of between 3% and 6% of the estimated ultimate force was applied. The specimen was loaded continuously (without shock) at a constant rate of 125N/s until failure occurred. The loading rate was obtained using the relationship given in Equation 3.7 thus,

$$r = \frac{\mu b d^2}{L} \qquad \textit{Equation 3.7}$$

where r is the loading rate (N/s), μ is the rate of increase in maximum stress on the tension face (taken as 1.0MPa/s), b is the average width of the specimen as oriented for testing (mm), d is the average depth of the specimen as oriented for testing (mm), and L is the span length (mm). At the end of the testing, with the specimen still as positioned, the width and depth measurements were taken at one of the fractured faces. One measurement was taken at each edge and one at the centre of the cross section, for each dimension. The average of the three measurements for each direction, to the nearest 1mm, was used to determine the modulus of rupture of the specimen as given in Equation 3.8. That is,

$$f_f = \frac{PL}{bd^2} \qquad \textit{Equation 3.8}$$

Where f_f is the flexural strength (N/mm^2), P is the maximum applied load (in N), L is the span length (mm), b is the average width of the specimen at the fracture (mm), and d is the average depth of the specimen at the fracture, as oriented for testing (mm). Two specimens were produced for each mix for this test and the average value was taken.

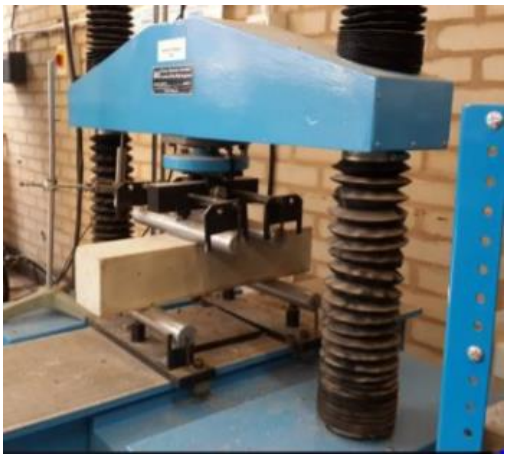

Figure 3.22: Set-up for flexural strength test.

3.3.3.5 Flexural Strength of Steel Fibre-Reinforced Concrete

Moulded specimens of dimension 150 × 150 × 500mm were tested in flexure according to ASTM C1609/C1609M (2012) standard, after 28 days of curing. The specimen was placed on its side on the support system, such that the direction of casting was perpendicular to the application of load as shown in Figure 3.22. The specimen and the loading system were arranged so that the specimen was loaded at the third-point, complying with Test Method C78 (ASTM C78/C78M − 18 2018), ensuring a span length of 450mm. The testing machine was operated to achieve an increasing net deflection of the specimen at a constant rate of 0.002mm/s up to a net deflection of 0.5mm. Thereafter, the rate of increase of net deflection was increased by 0.001mm/s for every 5minutes up to the end-point deflection. The test was terminated at a net deflection of $^1/_{150}$ of the span (i.e., 3mm). Two measurements of the depth and width of the specimen adjacent to the fracture (one on each face of the specimen) were taken to determine the average depth and width. Fracture position was determined by measuring the distance along the middle of the tension face from the fracture to the nearest point of support. The first-peak load was determined as the value of load corresponding to the first point on the load-deflection curve where the slope was zero. Similarly, the peak load was determined as the value of load corresponding to the point on the load-deflection curve that corresponds to the greatest value of load obtained prior to reaching the end-point deflection. Their corresponding deflection values were also determined from the curve. Then, the moduli of rupture for both first-peak and peak loads were calculated using the following formula:

$$f_f = \frac{PL}{bd^2} \qquad \textit{Equation 3.9}$$

Where f_f is the flexural strength (N/mm^2), P is the maximum applied load (N), L is the span length (mm), b is the average width of the specimen at the fracture, as oriented for testing (mm), and d is the average depth of the specimen at the fracture, as oriented for testing (mm).

The residual load values, P^D_{600} and P^D_{150} were determined as appropriate for the specimen depth, corresponding to net deflection values of $^1/_{600}$ and $^1/_{150}$ of the span length. Their corresponding residual strengths, f^D_{f600} and f^D_{f150} were calculated using the residual loads, the average specimen dimensions, and Equation 3.9. Also, the toughness, T^D_{150} as appropriate for the specimen depth was determined by calculating the entire area under the load-deflection curve, up to a net deflection of $^1/_{150}$ of the span length. Finally,

the equivalent flexural strength ratio, $R^D_{T,150}$ as appropriate for the specimen depth, was calculated by inserting the determined first-peak strength and the toughness in the following formula:

$$R^D_{T,150} = \frac{150 \times T^D_{150}}{f_1 \times b \times d^2} \times 100\% \qquad \textit{Equation 3.10}$$

Two specimens were produced for each mix for this test and the average value was determined.

3.3.3.6 Flexural Behaviour of Reinforced Concrete Beams

Reinforced concrete beams of dimension 80 × 180 × 1500mm produced from four mixes described in Section 3.3(a)–(d) were subjected to a four-point load-deflection test to determine their flexural performance such as crack patterns, width, and length, stresses and strains, mid-span deflection, and failure mode. Two specimens were produced from each mix for this investigation. The reinforcements and stirrups used to fabricate the specimens were rebars of sizes 10mm and 8mm diameters, respectively. For each beam, two 10mm reinforcements and ten two-legged stirrups (five at each end spaced at 20mm centre-to-centre), were used. Six rubber spacers, placed alternately at the bottom of the two reinforcements, were employed to achieve a 20mm concrete cover to the reinforcements. The configuration of the reinforcements, stirrups, and spacers is as illustrated in Figure 3.23(a). The whole assembly was then placed in the oiled mould and the fresh concrete was poured in the mould and compacted adequately using a needle vibrator.

The test was carried out after the specimens were cured in air at room temperature, for 28 days. Before the day of testing, one side of each beam was first cleaned of any grits, painted with white paint to reveal crack initiation and propagation during the testing. Also, at the centre of the beam, a vertical line was drawn (dividing the beam into two equal halves) on the painted side. Then, five DEMEC buttons were fixed on either side of the centre line, to measure surface strains. An approximate horizontal distance of 200mm separated consecutive DEMEC buttons, while an approximate vertical distance of 40mm was maintained between successive DEMEC buttons. The horizontal separation aligned with the length of the DEMEC gauge used to measure the strains. The accuracy of placement of the DEMEC buttons was achieved using a setting bar. Glue formed by mixing an Araldite rapid hardener and resin together was used to place the buttons in their positions, at least 24 hours prior to testing. This was appropriate to prevent the buttons from falling off during load application.

Each specimen was then positioned in the testing equipment as shown in Figure 3.23(b). The clear distance between the two supports was 1200mm, whereas the distance between the two-point loads was 400mm (that is, each point load was applied at an approximate distance of 200mm on either side of the centre of the beam). The initial DEMEC readings with no load were recorded, and the mid-span deflection at this stage was automatically zero. The subsequent DEMEC readings at an incremental load of 5kN, applied at the rate of 200N/s, were taken, and recorded. Each reading was multiplied by a gauge factor of 0.403×10^{-2}, afterward, the difference between the initial and the load-step strain gauge readings was calculated as the concrete strain. The corresponding mid-span deflection at each load increment was also read from the computer screen with data logger, through the help of an electronic linear variable displacement transducer (LVDT).

The load at which the first cracks occurred was noted. The cracks were magnified with a marker and the longest crack for each load-step was traced using a thread and measured with a ruler. The propagation of cracks upon additional load was magnified with different colour of marker and measured. The corresponding load producing each crack was also labelled beside the cracks. The load was applied up to failure and the ultimate flexural load and failure mode were recorded as well as crack width estimated.

(a)

(b)

Figure 3.23: Arrangement of reinforcements and the test configuration.

3.3.3.7 Water Absorption

This test was carried out in accordance with BS 1881–122 (2011). Three cylindrical specimens, each of dimension 100mm diameter by 200mm height, were produced for each mix and cured as stated in Section 3.3.4.5. Immediately after demoulding, the surface of specimen was rinsed with clean water, brushed with a weak detergent solution, and rinsed again, to remove possible residual release agent. The specimens were transferred to the tank containing water at a temperature of 20^{o}C ± 2^{0}C for curing until required for testing.

Specimen drying began at the age of 24 days to 28 days. The specimens were placed in the oven at a temperature of 105^{o}C ± 5^{o}C, maintaining a clear distance of not less than 25mm from the heating surface and from each other. It was ensured that no further specimens were placed in the oven as soon as the drying process began. The specimens were removed from the oven after 72 hours and allowed to cool down in a dry airtight vessel (see Figure 3.24(a)) for 24 hours. Immediately after cooling, each specimen was weighed, and the mass obtained was recorded. Then, the specimens were completely immersed in the container shown in Figure 3.24(b) with its longitudinal axis placed horizontally and allowing water level above the top of the specimens at approximately 25mm. After 30 minutes, the specimens were removed from the tank, shook, and wiped with dry towel to remove all of surface water. Each specimen was then weighed, and the mass obtained was recorded.

The rate of water absorption was also obtained using the cumulative immersion periods of 10, 30, 60 and 120 minutes with the same specimens. The increase in mass resulting from immersion, expressed as a percentage of the mass of the dry specimen, was used to calculate the measured absorption of each specimen. A correction factor, obtained as in Equation 3.12, was applied by multiplying its outcome with the measured absorption to obtain the *corrected absorption* as expressed in Equation 3.13. That is,

$$Correction\ factor = \frac{volume\ (mm^3)}{surface\ area\ (mm^3) \times 12.5} \qquad \textit{Equation 3.12}$$

$$Corrected\ absorption = correction\ factor\ \times measured\ absorption \qquad \textit{Equation 3.13}$$

(a) 

(b) 

Figure 3.24: Set-up for water absorption test: (a) airtight vessel (b) specimens immersed in water.

3.4 Numerical Program

In this study, numerical study was carried out on commercial ANSYS Mechanical APDL 2019 R1 software. This finite element analysis (FEA) package was deemed adequate due to its ability to carry out both linear and non-linear analyses as well as high accuracy in predicting most engineering structures. These attributes are possible because structural elements are meshed, and each component possesses varied stress-strain characteristics. FEA is a faster and cost-effective method in predicting the behaviour of structural materials under structural loading compared to experimental and other methods. The purpose of numerical study here was basically to compare the results obtained from the FEA with those of the experimental investigation on the flexural behaviour of reinforced concrete beams.

In the present research, reinforced concrete beam of length 1500mm and cross-sectional area 80 × 180mm was simulated using ANSYS. However, by reason of symmetry, conservation of energy, and speed of analysis, a half of the full length (that is, 750mm) of the beam was modelled and analysed. In summary, the whole process involved in modelling and analysing a reinforced concrete beam on ANSYS Mechanical APDL is given as follows, in the sequence adopted in this study.

- Define and select the element types from ANSYS element library, for the concrete and reinforcements used for the model.
- Define the unique properties (referred to as Real Constants) of the element types.
- Assign the linear, multi-linear, and bilinear properties of the materials used for the model.
- Model the concrete as a volume and the reinforcements (steel rod and stirrup) as lines.

- Mesh and assign the element types and material properties to the modelled beam.
- Apply load and boundary conditions to the model and
- Set the analysis commands and initiate solution.

3.4.1 Definition and Selection of Element Types with Real Constants

Concrete modelling comes with a challenge associated with its brittleness and distinct behaviour in tension and compression. In this research, Solid65 element which is three-dimensional and comprising of eight nodes with three degrees of freedom at each node, was utilized to model concrete behaviour. According to Bâetu and Ciongradi (2011), the Solid65 element is capable of deforming plastically, cracking in three orthogonal directions, and crushing. Additionally, the nodes of the element can translate in the $x-$, $y-$, and $z-$directions. To adequately create the concrete model, both linear isotropic and multi-linear isotropic properties of the element are required. Hence, the linear isotropic properties of the concrete for the different mixes studied are given in Table 3.16, while their multi-linear isotropic properties are given in Table 3.17. It should be noted that the elastic modulus values were estimated analytically, using the relationship between the cylindrical compressive strength and elastic modulus for concrete according to ACI 318R (2014) provisions.

Table 3.16: Linear isotropic properties of the concrete for different mixes.

Mix ID	Elastic modulus, E_c (MPa)	Poisson's ratio, v	Density, ρ (kg/m^3)
NAC	34300	0.2	2370
RAC	30900	0.2	2180
SFRRAC	32600	0.2	2240
BAC	33000	0.2	2340

On the other hand, Link180 element which has two nodes with three degrees of freedom at each node was used to model the reinforcements and stirrups. This element also possesses the ability to translate in the $x-$, $y-$, and $z-$directions. It was assumed that the bond between concrete and reinforcements was perfect. The information provided for the reinforcements and stirrups for the laboratory experiments (see Section 3.3.3.6) were used in the model. Hence, the values of cross-sectional area inputted in the model for the steel reinforcement of size 10mm diameter and stirrup of size 8mm diameter were 78.5mm^2 and 50.3mm^2, respectively. The linear and bilinear isotropic properties and their associated values used for the Link180 element are given in

. The yield strength of steel was assumed and 5% of the elastic modulus for steel was used as the tangent modulus.

Table 3.17: Multilinear isotropic properties of the concrete for different mixes.

NAC		RAC		SFRRAC		BAC	
Strain	**Stress (MPa)**	**Strain**	**Stress (MPa)**	**Strain**	**Stress (MPa)**	**Strain**	**Stress (MPa)**
0.00010	3.43	0.00010	3.09	0.00010	3.26	0.00010	3.30
0.00027	6.60	0.00025	6.94	0.00026	7.08	0.00023	7.11
0.00031	7.21	0.00051	10.42	0.00057	14.15	0.00052	14.21
0.00062	10.81	0.00138	24.30	0.00093	21.23	0.00087	21.32
0.00104	18.01	0.00210	31.25	0.00120	24.77	0.00117	24.88
0.00131	21.62	0.00272	34.72	0.00255	35.38	0.00147	28.43
0.00204	25.22	0.00468	38.19	0.00364	42.46	0.00181	31.98
0.00254	28.82	–	–	0.00527	48.86	0.00214	35.54
0.00331	36.03	–	–	–	–	0.00272	39.09
0.00379	39.63	–	–	–	–	0.00328	42.64
0.00602	43.23	–	–	–	–	–	–

Table 3.18: Linear and bilinear isotropic properties of the steel reinforcements.

Properties	**Values**
Elastic modulus, E_s (MPa)	210000
Poisson's ratio, v	0.3
Density, ρ (kg/m^3)	7850
Yield Strength, f_y (MPa)	500
Tangent modulus, E_s' (MPa)	10500

It is worth mentioning that the elastic modulus and Poisson's ratio for both concrete and steel reinforcements are represented by *EX* and *PRXY* in ANSYS, respectively. The identities assigned to the individual elements in the ANSYS model are given in Table 3.19. Other material properties required for the model are presented in Table 3.20. Although the simulation of the plastic behaviour of concrete is supported by SOLID65 element, it differs from that of metals (e.g., steel) because of cracking and crushing. At crack formation, the stress-strain relationship is modified in the element using shear transfer. The open and closed shear transfer coefficients range from 0 to 1 (ANSYS 2019). For Solid65, these coefficients had a significant influence on the results obtained from FEA (Luo 2008). The author found that the open and closed shear transfer

coefficients within the ranges of 0.35–0.40 and 0.9–1.0 respectively, gave a good correlation between the FEA and experimental results. However, the presence of steel fibre substantially contributes to shear transfer across the cracks (Aziz and Ghailan 2007, Padmarajaiah and Ramaswamy 2002), hence the shear crack coefficients for the SFRRAC mix were slightly higher as shown in Table 3.20. The uniaxial cracking stress and uniaxial crushing stress values used were the experimental flexural and compressive strengths, respectively.

Table 3.19: Identities assigned to the elements of the model.

Elements	Material type	Element type	Bar size (mm)	Real constant	Section ID
Solid65	1	1	-	1	-
Link180	2	2	10	2	1
Link180	2	2	8	3	2

Table 3.20: Relevant material properties for the model.

Mix ID	Open shear transfer coefficient	Closed shear transfer coefficient	Uniaxial cracking stress (MPa)	Uniaxial crushing stress (MPa)
NAC	0.35	0.90	5.04	66.6
RAC	0.35	0.90	4.89	54.0
SFRRAC	0.40	0.95	5.27	60.2
BAC	0.35	0.90	4.73	61.7

The element types were defined in ANSYS by toggling through the ***Preprocessor*** (found at the middle left-hand side on ANSYS window); ***Element Type; Add/Edit/Delete***. The "*Element Type"* window appeared and the ***Add*** button was used to access the "*Library of Element Type"* window where the required element type was selected, and the ***Apply*** then ***OK*** buttons were clicked in succession.

This sequence of commands was carried out, in turn, for the Solid65 and the Link180 elements. However, it should be noted that before exiting the "*Element Type"* window, the Solid65 element has two important features that must be activated. Therefore, the Solid65 was highlighted (by a single click) and the ***Options*** button was clicked and "*Solid65 element type options"* window appeared. On the window, the K3 (Crushed, unreinforced) and K7 (Stress relax after cracking) options were set to "No mass or loads" and "Include" respectively, then ***OK***. The K3 "No mass or loads" option sets the mass of

crushed element to zero, thus transferring stresses to the nearby 'uncrushed' elements and enabling the convergence of solution. On the other hand, the K7 "Include" option relaxes the stresses on the cracked element and transfers them to the nearby element.

The Section ID of the steel reinforcement and stirrup were defined by toggling through the following:

- ***Preprocessor***; ***Sections***; ***Links***; ***Add*** (*"Add Link Section"* window appeared, and the ID was entered); ***OK*** (*"All or Edit Link Section"* window appeared); ***Section Name*** and ***Link area*** (78.5mm^2 for reinforcement bar and 50.3mm^2 for stirrup) were entered; ***OK***.

3.4.2 Assignment of the Material Properties

The material properties of the concrete were assigned by toggling through:

Preprocessor; ***Material Props***; ***Material Models*** (*"Define Material Model Behaviour"* window appeared). The following commands were then used to assign the linear isotropic, nonlinear isotropic, density, and non-metal plasticity properties:

Linear Isotropic—under the *Material Models Available* box: ***Structural***; ***Linear***; ***Elastic***; ***Isotropic*** (*"Linear Isotropic Properties for Material Number 1"* window appeared); ***EX*** (the elastic modulus of concrete given in Table 3.16 was entered); ***PRXY*** (the Poisson's ratio of the concrete given in Table 3.16 was entered); ***OK***.

Nonlinear Isotropic—under the *Material Models Available* box: ***Structural***; ***Nonlinear***; ***Inelastic***; ***Rate Independent***; ***Isotropic Hardening Plasticity***; ***Mises Plasticity***; ***Multilinear*** (*"Multilinear Isotropic Hardening for Material Number 1"* window appeared); ***Strain and Stress values*** (the strain and stress values given in Table 3.17 were entered as required for each mix. Note that the ***Add Point*** button was used to add cells); ***OK***.

Density—under the *Material Models Available* box: ***Structural***; ***Density*** (*"Density for Material Number 1"* window appeared); ***DENS*** (the density value given in Table 3.16 was entered); ***OK***.

Non-metal Plasticity—under the *Material Models Available* box: ***Structural***; ***Nonlinear***; ***Inelastic***; ***Non-metal Plasticity***; ***Concrete*** (*"Concrete for Material Number 1"* window appeared. The values given in Table 3.20 were entered); ***OK***.

The *Material* tab (located at the top left-hand corner of the *"Define Material Model Behaviour"* window) was used to add *Material Number 2* (that is, steel reinforcement) as follows:

- ***Material*** (dropdown list appeared); ***New Model*** (*"Define Material ID"* window appeared); ***Material ID*** (2 entered); ***OK***.

Then, the material properties of the steel reinforcement were assigned to the model using similar commands as those of the concrete explained above. However, instead of the ***Multilinear*** command used for the concrete, ***Bilinear*** was used in assigning the nonlinear isotropic properties for the reinforcement. Hence, the yield stress and tangential modulus for steel required to define the bilinear properties were inputted as given in

, including other properties of steel used for the model.

To exit the *"Define Material Model Behaviour"* window, the following commands were used:

- ***Material*** tab (located at the top left-hand corner of the *"Define Material Model Behaviour"* window) and a dropdown list appeared, ***Exit***.

3.4.3 Modelling of the Reinforced Concrete Beam

In this research, the concrete was modelled as a volume and the steel reinforcement and stirrup as lines. The volume was created by going through the ***Preprocessor***; ***Modeling***; ***Create***; ***Volumes***; ***Block***; ***By Dimensions*** commands. The *"Create Block by Dimensions"* window appeared and (0, 750), (0, 180), and (0, 80) were inputted as the (x_1, x_2), (y_1, y_2), and (z_1, z_2) coordinates, respectively. While the lines were created by going through ***Preprocessor***; ***Modeling***; ***Create***; ***Keypoints***; ***In active CS*** commands. The *"Create Keypoints in Active Coordinate System"* window appeared and the x, y, z *Location in active CS* values were inputted to create the points that defined the reinforcement. The first point created was (750, 20, 20), followed by (20, 20, 20), (20, 160, 20), and (470, 160, 20). The ***Apply*** button was clicked after supplying the coordinates, before inputting the next set of coordinates. These points were joined as appropriate using the following commands: ***Preprocessor***; ***Modeling***; ***Create***; ***Keypoints***; ***Lines***; ***Straight Lines*** (the points were clicked in succession to join). The reinforcement was duplicated into two using the *Copy* command as follows: ***Preprocessor***; ***Modeling***; ***Copy***; ***Lines*** (*"Copy Lines"* window appeared); ***Pick Lines***; ***Apply***; ***OK***. Similarly, the stirrup was formed by creating the following points: (100, 20,

20), (100, 20, 60), (100, 160, 60), and (100, 160, 20). The points were joined as for the reinforcement and the *Copy* command was also used to duplicate (offset) the stirrup into five.

3.4.4 Meshing of the Modelled Reinforced Concrete Beam

The choice of mesh size was governed by the cover to the reinforcements. Therefore, 10mm mesh size was adapted for the model since 20mm cover to reinforcements was used as stated in Section 3.3.3.6. Additionally, this mesh size was chosen for the ease of execution of the complex equations in FEA, and the convergence result from ANSYS validated its adequacy.

Before carrying out the meshing operation, selection and grouping of entities of the model into reinforcement and concrete was done. These were achieved using the following commands:

(i) Selection of entities (Reinforcements) through the following toggles.
- ***Select*** (from the top menu bar); ***Entities*** (*"Select Entities"* window appeared); clicked on the *arrow* of the first button on the box and selected ***Lines*** from the dropdown list; checked ***From Full***; ***OK*** (*"Select Lines"* window appeared on the left-hand side of the screen); checked ***Box*** and selected all the reinforcements; then clicked ***OK***.
- Then, only the line elements were made visible using the following commands: ***Select***; ***Everything Below***; ***Selected Lines***; and
- ***Plot*** (from the top menu bar); ***Lines*** and the line elements (reinforcement and stirrups) appeared on the ANSYS workspace.

(ii) Grouping of entities (Reinforcements) was done by toggling through.
- ***Select***; ***Component Manager*** (*"Component Manager"* window appeared); from the array of commands at the top, clicked on ***Create Component*** (*"Create Component"* box appeared); checked ***Lines***; changed ***CM_1*** to *Reinforcement*; ***OK*** (*"Select Lines"* window appeared); checked ***Pick All*** and clicked ***OK***; then finally closed the ***Component Manager***.

The above steps were repeated for the selection and grouping of the concrete element. Essentially, all the ***Lines*** commands were replaced by ***Volumes***. The modelled reinforced concrete beam was then meshed through the following toggles:

(i) Meshing of the concrete.

- ***Preprocessor***; ***Meshing***; ***Mesh Tool*** (*"MeshTool"* box appeared); under the *Element Attributes*, ***Volumes*** was selected from the dropdown arrow list; ***Set*** button was clicked (*"Volume Attributes*" window appeared); typed in ***1*** and clicked ***OK*** (another *"Volume Attributes"* window appeared); then the material number and the associated element type number were selected from the list as appropriate; ***OK***.

(ii) Meshing of the reinforcements.

- ***Preprocessor***; ***Meshing***; ***Mesh Tool*** (*"MeshTool"* window appeared); under the *Element Attributes*, ***Lines*** was selected from the dropdown arrow list; under the *Size Control*, the ***Set*** command button aligning with ***Lines*** was clicked (*"Element Sizes on Picked Lines"* window appeared); ***Pick All*** (another *"Element Sizes on Picked Lines"* window appeared); type in *10* in the *SIZE Element edge length* option; ***OK***; on the "*MeshTool"* window, ***Hex*** and ***Sweep*** options were checked; then ***Sweep*** (*"Volume Sweeping"* window appeared); and finally ***Pick All***.

The result of the meshing operation for the present study is as shown in Figure 3.25. The ***Merge Item*** command was used to tie the nodes of the concrete material and steel reinforcement together to ensure that two coinciding nodes were represented with a single node.

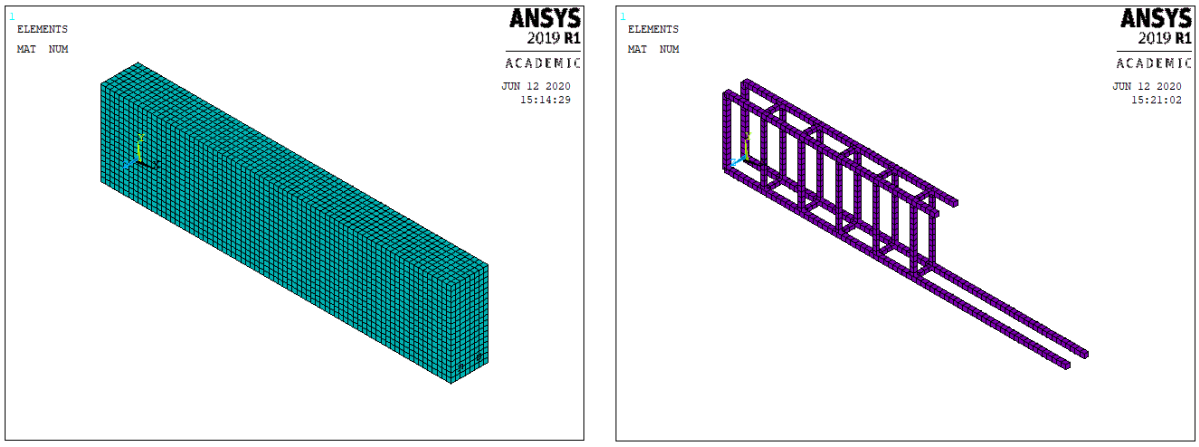

Figure 3.25: Concrete and steel reinforcement meshing.

3.4.5 Application of Loads and Boundary Conditions

Using the ***Coupling/Ceqn*** command, it was found that the support reaction and the point load were to be applied on node number 2642 and 2571 respectively, while the displacement was to be applied on node number 3299. The ***Loads*** command was used to apply the loads at the nodes and set the displacement at the support and the point

load positions to zero (0) and –8mm (downwards), respectively. It should be noted that, to avoid a non-convergent solution prior to the ultimate load, which may not allow for the post-yield region of the analysis to be reached, the displacement control loading was used.

3.4.6 Setting the Analysis and Solution Commands

The analysis commands were set through the following toggles:

Solutions; ***Analysis Type***; ***Sol'n Controls*** (*"Solution Controls"* window appeared). By toggling through ***Basic***; ***Sol'n Options***; ***Nonlinear***; ***Advanced NL*** tabs in the *"Solution Controls"* window, the following commands were set with the chosen options in the brackets:

Basic—(1) *Analysis Options* (Larger Displacement Static); (2) *Time Control*: (i) Time at end of load step (8), (ii) Automatic time stepping (On), (iii) Number of substeps (200), (iv) Maximum number of substeps (500), (v) Minimum number of substeps (180); (3) *Write Items to Results File*: (i) All Solution Items (Checked), (ii) Frequency (Write every substep). It is important to note that the selection of the *Larger Displacement Static* of the *Analysis Options* was because the load–displacement linear relationship was not expected to be constant throughout the analysis. The alternative *Small displacement Static* may not be sensitive to deformations beyond the yield point of the material.

Sol'n Options—(1) *Equation Solvers*: Program chosen solver (Checked); (2) *Restart Control*: (i) Number of restart file to write (0), (ii) Frequency (Write every Nth substep).

Nonlinear—The default settings in this tab were maintained. However, the *Set Convergence Criteria* option was used to set the force and displacement convergence criteria. On the *"Default Nonlinear Convergence Criteria"* window that appeared, the settings were carried out with the aid of the following toggles: ***Replace*** ("*Nonlinear Convergence Criteria"* window appeared); then the following setting was done on the new window: (i) *Lab Convergence is based on* (Displacement U), (ii) *TOLER Tolerance VALUE* (0.05); ***OK*** (the new window exited). Similarly, the force convergence criteria were set in the *"Lab Convergence is based on"* option using the ***Add*** tab on the *"Default Nonlinear Convergence Criteria"* window. But the force convergence criteria set (visible on the *"Default Nonlinear Convergence Criteria"*), were highlighted (by a single click) and deleted (by clicking ***Delete*** button). This was essential because, the analysis was governed by the displacement criteria, on the basis that the force criteria offer a non-convergent solution after the material has yielded.

Advanced NL—Only the *Termination Criteria* option was set as follows: Program behaviour upon nonconvergence (Terminate but Do Not Exit); ***OK*** (*"Solution Controls"* window exited).

Then, the finite element analysis solution solving was initiated by toggling through:

Solution; ***Solve***; ***Current LS*** (two windows: *"STATUS Command"* and *"Solve Current Load Step"* appeared, the former which was hidden behind the latter was closed); ***OK***; ***Proceed***.

The NAC beam was first modelled and the FEA carried out as above. Thereafter, the material properties of the RAC, SFRRAC, and BAC beams were inputted in the model, in turn, to replace those of the NAC beam. The following toggles were used for this purpose:

Preprocessor; ***Material Props***; ***Material Models*** (*"Define Material Model Behaviour"* window appeared). Then, the *Material Model Number 1 and 2* (under the *"Material Model Defined"* box) were opened in succession, to update the material properties of the new beam (of either RAC, SFRRAC, or BAC mix) to be analysed. The *Material Model Number 1* include: *Density, Linear Isotropic* (Table 3.16 values)*, Concrete* (Table 3.20 values)*,* and *Multilinear Isotropic* (Table 3.17 values). On the other hand, the material properties for *Material Model Number 2* (that is, the steel reinforcement) were constant for all the mixes. Finally, the *"Define Material Model Behaviour"* was exited as already described in Section 3.4.2 and the analysis and solution commands were set as above.

Chapter 4

4 RESULTS, ANALYSIS, AND DISCUSSION OF EXPERIMENTAL INVESTIGATION

4.1 Introduction

The research method adopted in this study has been discussed in detail in the previous chapter. This chapter presents the results obtained from the experimental investigation of this research. The results of each examination carried out are presented, analysed, and discussed concurrently with some of those available in the literature. Some results have already been presented in Chapter 3 in attempt to give an in-depth characterization of the aggregates used. However, such results shall be referred to in this chapter when deemed appropriate and discuss in more details. This is necessary because of the negative effects of the remnants of mortar on the properties of recycled aggregate (RA). Thus, this chapter is divided into two sections to reveal the results from aggregate characterization and the main laboratory experiments.

4.2 Aggregate Characterization

From the literature, RA is deemed inferior compared to its parallel natural aggregate (NA) due to the clinging mortar. The results of this research (see Table 3.3 and Table 3.6) showed that the properties measured for RA were lower (except for water absorption capacity and percentage voids) compared to those of NA. The oven-dry, saturated surface-dry, and apparent specific gravity obtained for the three size fractions of recycled fine aggregate (RFA) employed in this study were 1.96, 2.21, and 2.62 on the average, respectively. While those of the comparable natural fine aggregate (NFA) were respectively 2.56, 2.58, and 2.62. It can also be deduced from Table 3.3 that specific gravity of the NFA increased as the particles size decreased, whereas the specific gravity of RFA increased with increasing particles size. Similarly, the average specific gravity (oven-dry, saturated surface-dry, and apparent) of the recycled coarse aggregate (RCA) used were 2.30, 2.42, and 2.62 while those of their corresponding natural coarse aggregate (NCA) were 2.61, 2.64, and 2.67, respectively. These results show that there are 23% and 14.3% differences in the oven-dry and saturated surface-dry specific gravity respectively between RFA and NFA, in favour of the latter. These variations are reduced to 12% and 8% respectively for the coarse aggregate, in favour of NCA. This may be the reason why some authors have discouraged the use of RFA and the oven-dry form of RA for the manufacture of concrete.

The average absorptions of RFA and NFA were 13.0% and 1.0%, while those of RCA and NCA were 5.3% and 0.8%, respectively. From Table 3.3, the absorption capacity of

RFA increased as particles size reduced, whereas that of NFA decreased with particles size. This can be attributed to high degree of tiny particles of mortar in RFA produced during the crushing process. Conversely, according to results given in Table 3.6, the absorptions of both NCA and RCA decreased with increasing particles size. Thus, the results obtained justify the assertion that the greatest setback of RA is its high water affinity (Boulekbache et al. 2016, Kang et al. 2014) and that this effect is worse when RFA is used.

The average voids in NCA and RCA were 40% and 43.5% and their average dry-rodded density were 1565kg/m^3 and 1297kg/m^3, respectively. The average mortar content of the RCA was 52%.

4.3 The Main Experimental Results

4.3.1 Workability

This fresh property of concrete determines the ease with which concrete is placed. In practice, superplasticizers are used to improve the workability of concrete mixes. For this research, slump value was used to measure the workability of the concretes produced. The results showed that the workability of concrete mixes was affected by the presence of both RA and SF, as well as mix design method. According to Chakradhara Rao et al. (2011), the attached mortar, rough surface texture and more angularity in shape of the RA compared to NA, is the reason why concretes containing RA requires more water than the conventional concrete. This is because the contact area for aggregates with angular surface is greater than their rounded counterpart, leading to a higher absorption tendency (Matias et al. 2013). When SF was added to RAC mixes, workability was further reduced resulting in a dry (harsh) mix.

To maintain a similar slump values with the other mixes, the mixes incorporating SF required more superplasticizer (refer to Table 3.15). This is similar to the findings of previous researchers (Afroughsabet, Biolzi, and Ozbakkaloglu 2017, Gao, Zhang, and Nokken 2017b, 2017a). Comparatively, the volume of superplasticizer required in one kilogramme per cubic metre of RAC mix was 1.2 times that required for natural aggregate concrete (NAC) mix to match their workability. On the other hand, the inclusion of SF required 2.5 times the volume of superplasticizer employed for RAC mix, while the use of an alternative to normal mix design approach (as in blended aggregate concrete (BAC)) needed around 4.8 times the volume used for RAC mix. This inordinate increase can be attributed to a higher aggregate content and reduced quantity of water in the mix developed with the EMV guide. Furthermore, the combined effect of SF addition and the

EMV mix proportioning technique on flowability of the formed concrete (SFRBAC) increased by 89%, 87%, 68% and 39% compared to NAC, RAC, SFRRAC, and BAC, respectively.

4.3.2 Hardened Density

The result of the density of hardened concrete obtained in this study is presented in Figure 4.1, Figure 4.2 and Table 4.1. Figure 4.1 compares the implication of design methods on the density of the hardened RAC. This includes the results obtained from the preliminary study carried out to examine the two conventional mix design methods for RAC and the EMV approach for BAC mix. The density of NAC was included as the reference for the other mixes. In the Figure 4.1, the recycled concrete mix designed with the ACI guide was represented by RAC(ACI) while that formulated using the DoE method was designated by RAC(DoE). In all, concrete made of NA gave the highest density relative to the mixes consisting of either partial or full replacement with RA, irrespective of the mix design method. Nevertheless, when RAC(ACI) and RAC(DoE) were compared, the latter produced about 4% higher density than the former. The slightly greater mass of the combined constituents for the mix resulting from the DoE method (see Table 3.14) was responsible for this variation.

On the other hand, the BAC whose mix was designed using the EMV technique showed a marginal reduction when its density was compared with that of NAC and a notable increase compared with those of RAC(ACI) and RAC(DoE). Similar result between normal concrete and the concrete prepared using the EMV guidelines was reported by Fathifazl et al. (2009a). This is primarily because the overall mass of concrete ingredients resulting from the BAC mix is lesser than that of the NAC and greater than those of the RAC(ACI) and RAC(DoE) mixes. Technically, however, the decrease in the density of the concretes incorporating RA relative to their parallel reference concrete, was due to the mortar adhering to the RA. Essentially, the mortar is a porous and lightweight material and causes the reduction in the overall density of the concrete.

Table 4.1 shows the density of hardened concrete obtained from the main experiment at 7, 28 and 56 days and the average density is presented in Figure 4.2. It was deemed appropriate to determine the density of concrete at different ages because the compressive strength was required at these periods. Since density does not change with age, the average density of each mix plotted (in) Figure 4.2 was derived from 15 specimens. It can be seen from Figure 4.2 that the addition of SF increased the density of hardened concrete in spite of mix design approach. Also, it can be deduced that the

presence of SF increased the density of SFRRAC and SFRBAC when compared to those of RAC and BAC, respectively.

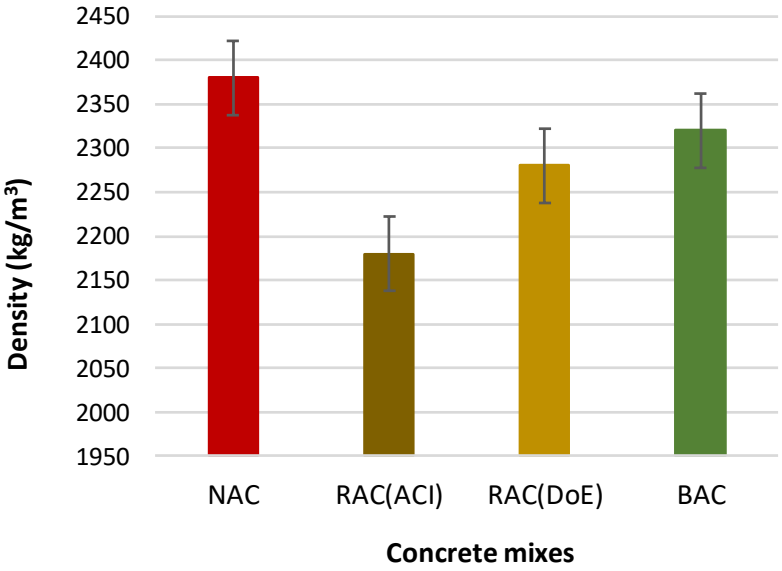

Figure 4.1: Effect of mix design methods on density of hardened concrete measured at 7 days.

In general, from the current study, the density of concrete made of 100% RA and proportioned using the conventional method was reduced by 8% in comparison with the NAC. This gap was reduced to 6% when SF was added to the recycled concrete mix. But the use of the EMV mix design mechanism resulted in just 1% less dense concrete (BAC) than the normal concrete (NAC). With the addition of SF to the BAC mix this difference was reduced to 0.8%. Finally, between RAC and BAC, there was up to 7% variance in density in favour of BAC.

Table 4.1: Density of hardened concrete tested at different ages.

Age (days)	Average density (kg/m³)				
	NAC	RAC	SFRRAC	BAC	SFRBAC
7	2380	2180	2230	2320	2340
28	2360	2180	2240	2360	2370
56	2370	2190	2240	2330	2360

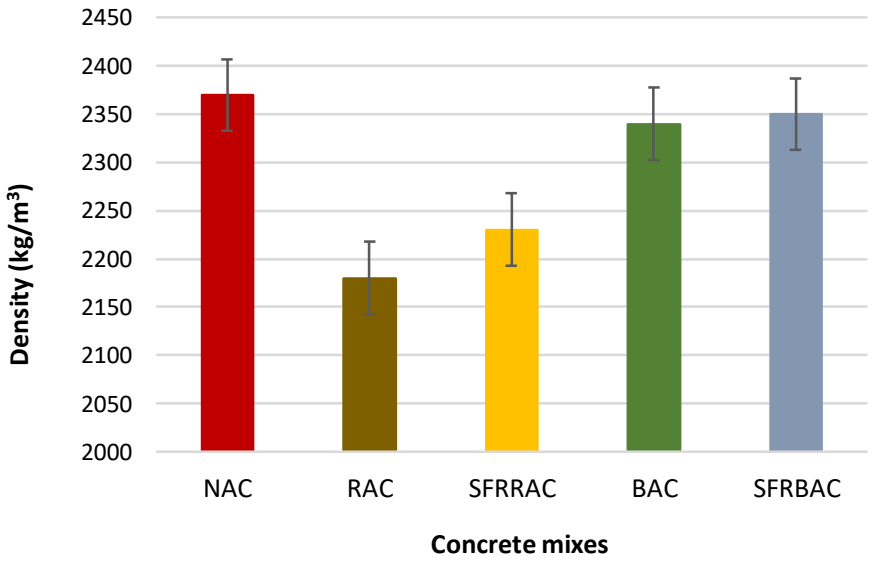

Figure 4.2: Average density of hardened concrete of different mixes at 7, 28 and 56 days.

4.3.3 Compressive Strength

The results of the compressive strength of the five concrete mixes investigated are presented in Figure 4.3 and Figure 4.4 while the full data are shown in Appendix C. The target strength of 40MPa set for this research was achieved by all the mixes, however, age, aggregate type, SF, RA content, and mix proportioning method influenced the compressive strength of the concrete. Expectedly, this property of concrete increased with curing age irrespective of the mix design approach and type of aggregate used as given in Figure 4.3. This was due to cement action in the concrete known as hydration process. The reference mix prepared with NA had a higher compressive strength than its corresponding recycled concretes, notwithstanding the replacement level with RA or the presence of SF as shown in Figure 4.3. The percentage differences in 7 days compressive strength of RAC, SFRRAC, BAC, and SFRBAC mixes were 23.5, 10.8, 7, and 12.9 compared to NAC mix, respectively. These inequalities were significantly decreased at 28 days except for the BAC mix which maintained a 7% difference. This is in agreement with the proposition that the rate of strength development is higher in recycled concrete than in conventional concrete (Evangelista and de Brito 2007, Poon et al. 2004) due to further hydration reaction engendered by the residual mortar (Kurad et al. 2017). In terms of replacement ratio of NA with RA, the BAC mix consisting of 60% RCA and RFA showed a higher compressive strength at 7, 28, and 56 days in excess of 17.8%, 12.5%, and 12.5% compared to the RAC mix made of 100% RA, respectively. This shows that as the RA content increases, the compressive strength of concrete

decreases and this agrees with the findings of previous researchers (Kou, Poon, and Chan 2007, Xiao, Li, and Zhang 2005).

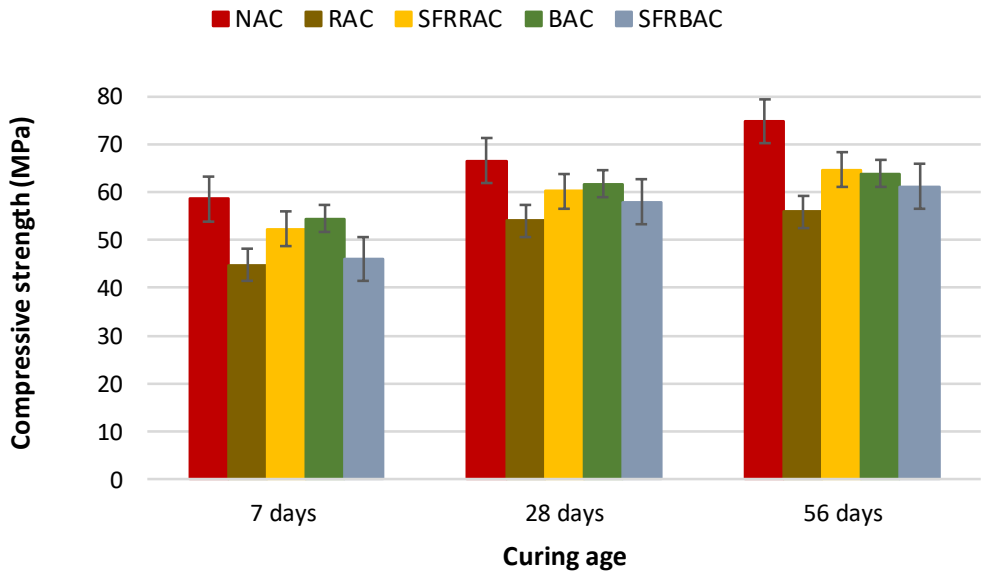

Figure 4.3: Effect of curing age on the compressive strength of concrete for different mixes.

Notice therefore that the adoption of alternative to normal mix design method led to a remarkable result for the concrete incorporating RA. Even though the NAC mix used a substantially higher amount of cement relative to the BAC mix, just 7% more strength than the BAC was noticed. As already mentioned, the BAC showed up to 13% higher compressive strength than RAC produced with the conventional method. Improved particle packing and a higher dosage of superplasticizer were the two phenomena responsible for this impressive result. This is according to Moosberg-Bustnes, Lagerblad, and Forssberg (2004), who maintain that the presence of superplasticizer in the concrete matrix engenders a loose but more homogeneous particles packing. From Table 3.15, it can be observed that the BAC mix required up to 80% more superplasticizer than the RAC mix. Also, from the granular skeleton optimization carried out by Wardeh et al. (2015), the packing density of RA was found lower than that of the NA due to the residual mortar. Therefore, the BAC mix with a lower RA content is expected to have a higher packing density than RAC made of 100% RA (Anike et al. 2020a), thus performance is improved since concrete properties are improved by packing density (Pradhan, Kumar, and Barai 2017).

The present results were compared to those obtained by the early researchers who also adopted the EMV method in their investigation. A higher compressive strength was

published by Gupta and Bhatia (2013), for the concrete prepared with RCA using the EMV guide compared to the normal concrete made entirely of NA. In a similar investigation, Fathifazl et al. (2009a) observed up to 13% greater strength for the recycled concrete proportioned with the EMV procedure than the conventional concrete. Unlike these studies, the current study did not achieve a higher compressive strength for the BAC (proportioned using the EMV technique) than the NAC (normal concrete). This can be ascribed to the addition of RFA in the present research. More so, the quality of the RCA used in those studies differ from that of the present study, as reflected in the reported mortar contents.

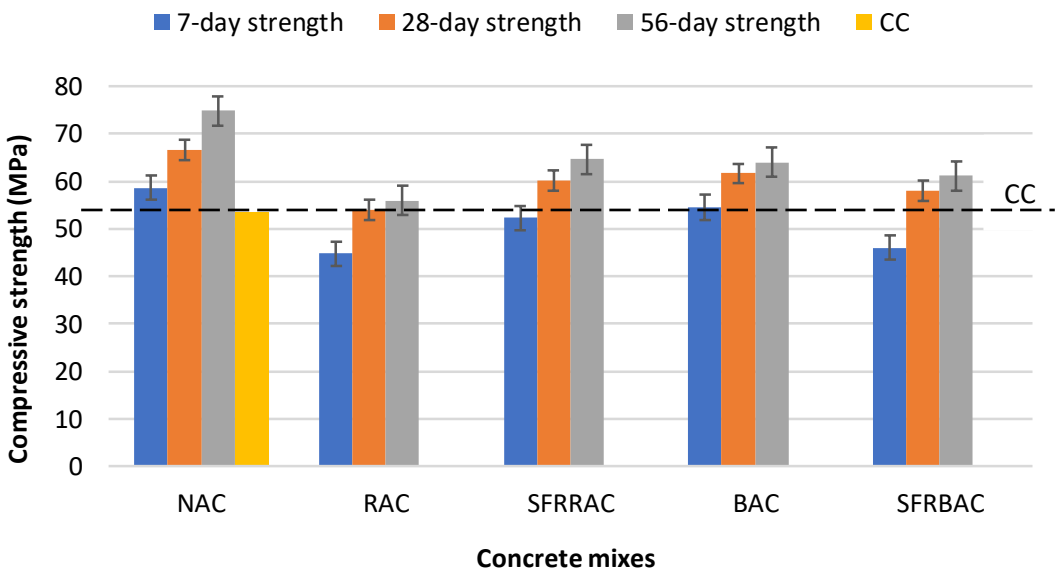

Figure 4.4: Compressive strength of concrete for different mixes tested at different ages.

According to Figure 4.4, it is evident that the presence of SF improved the compressive strength of RAC. This result agrees with the findings of previous researchers who maintain that the addition of SF improves the compressive strength of concrete (Younis et al. 2014, Graeff 2011, Pilakoutas, Neocleous, and Tlemat 2004, Tlemat 2004, Lim and Oh 1999). The improvement was possible through the bridging effect of SF which prevented micro-crack propagation. Gao et al. (2017a) also upheld that SF promotes hydration reaction of the paste and that the reaction is more complete in concrete incorporating SF. In the present study, the SFRRAC prepared with the conventional method showed a 14.3% improvement relative to comparable RAC at 7 days. This value was slightly reduced to 10.3% and 13.6% at maturity ages of 28 and 56 days, respectively. Similarly, the SFRBAC proportioned with the EMV method showed an improvement of 2.6% at the early age compared with RAC. This percentage difference increased to 6.9% and 8.7% respectively at 28 and 56 days. It can therefore be

concluded that the contribution of the EMV method to strength when SF was used (as in SFRBAC) was lower compared to the conventional method. This can be attributed to a higher SF content and better quality of paste associated with the latter method than the former. However, the SFRRAC showed only 3.7% higher strength than the SFRBAC at 28 days. It is pertinent to recall that for the current research, the EMV approach used a lower cement content than its comparable conventional method.

Notice the *golden* bar labelled CC (control concrete) in Figure 4.4. That is the result of a normal concrete mix consisting of an equivalent cement content (364kg/m^3) there is in the BAC mix. This was deemed necessary to validate the result obtained for the recycled concrete prepared using the EMV mix proportioning guidelines. The CC mix had exactly the same water-to-cement ratio with that of the BAC mix and was tested at 28 days after curing in water. Obviously, the BAC mix showed a greater compressive strength of over 13% compared to the CC mix. Also, the SFRBAC mix (containing 0.5% steel fibre content by volume of concrete) proportioned with the EMV technique had up to 8% higher strength than the CC mix.

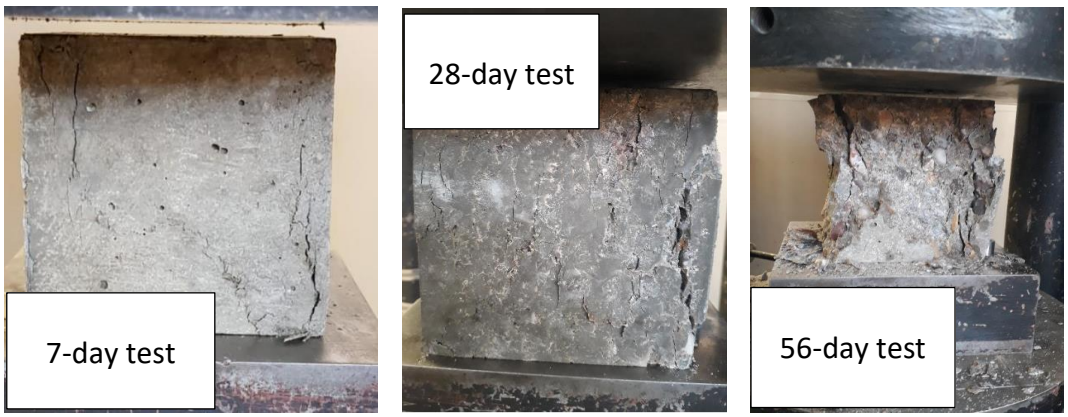

Figure 4.5: Failure pattern of tested cubes in compression at 7, 28, and 56 days, respectively.

Finally, all the tested cubes failed in compression and exhibited a similar failure pattern, but the crushing of the specimens at 56 days was more severe than at 7 and 28 days as revealed in *Figure 4.5*.

4.3.4 Tensile Splitting Strength

The tensile splitting strength results of all the five mixes investigated in this study are presented in Figure 4.6. It is clear from the Figure 4.6 that the type of aggregate, mix design method, and presence of SF, all influenced this property of concrete. All mixes containing RA showed a higher tensile splitting strength than the mix prepared with

comparable NA, whether with partial or full replacement of NA with RA. While the RAC mix consisting of 100% RA gave a tensile splitting strength of 4.05MPa, its equivalent NAC made of 100% NA gave 3.80MPa. These values showed an appreciable difference of 6% between the two mixes in favour of recycled concrete. Similar results have been reported by previous researchers (Afroughsabet, Biolzi, and Ozbakkaloglu 2017, Andreu and Miren 2014, Malešev, Radonjanin, and Marinković 2010, Etxeberria et al. 2007).

Some researchers maintain that the tensile splitting strength of RAC does not depend mainly on the quantity of RA used, but rather on the quality (Soares et al. 2014, Malešev, Radonjanin, and Marinković 2010, Tabsh and Abdelfatah 2009). However, it is important to note that different replacement ratios with RA have different impact on the tensile splitting strength of concrete. In the present study, the use of the EMV mix proportioning technique resulted in 60% replacement for both NCA and NFA. Consequently, the BAC mix exhibited up to 6% higher strength than the RAC mix (comprising of 100% RA) proportioned with the conventional method. In other words, this shows the implication of mix design method on the tensile strength of RAC. With reference to the NAC, the BAC showed up to 12% higher strength. A similar result of 11% difference was obtained by Fathifazl et al. (2009b), in favour of the mix proportioned with the EMV method compared to the normal concrete.

In this research, the SFRRAC mix showed the greatest tensile splitting strength with an average value of 6.15MPa. This value shows a tremendous increase when compared to other mixes without SF. This was expected due to the ability of SF to intercept cracks, thus sustaining load for a while before failure was initiated. In spite of the mix design approach, SFRRAC and SFRBAC showed up to 38% and 10% higher strength relative to the normal concrete, respectively. This was even with about 28% reduction in cement content of the SFRBAC mix compared to the NAC mix. Primarily, SF is effective in bridging cracking propagation, thereby improving post-cracking resistance and toughness of the concrete (Akinkurolere 2010). Notice also that there was approximately 32% variation in the tensile strength shown by SFRRAC and SFRBAC, in favour of the former. This was anticipated since the SF volume ratio in the SFRRAC mix was twice that of the SFRBAC mix (refer to Table 3.15). Again, this was a direct consequence of the different mix design approach.

Nevertheless, the use of SF engendered a ductile failure mode of the concrete specimens. Clearly, from Figure 4.7, it can be seen that, while the tested specimens of the mixes with no SF failed catastrophically by splitting into two, those incorporating SF (that is, SFRRAC and SFRBAC) resisted splitting. During the testing in the laboratory, it

was difficult to visually detect cracks on the steel fibre-reinforced concrete (SFRC) specimens after failure occurred.

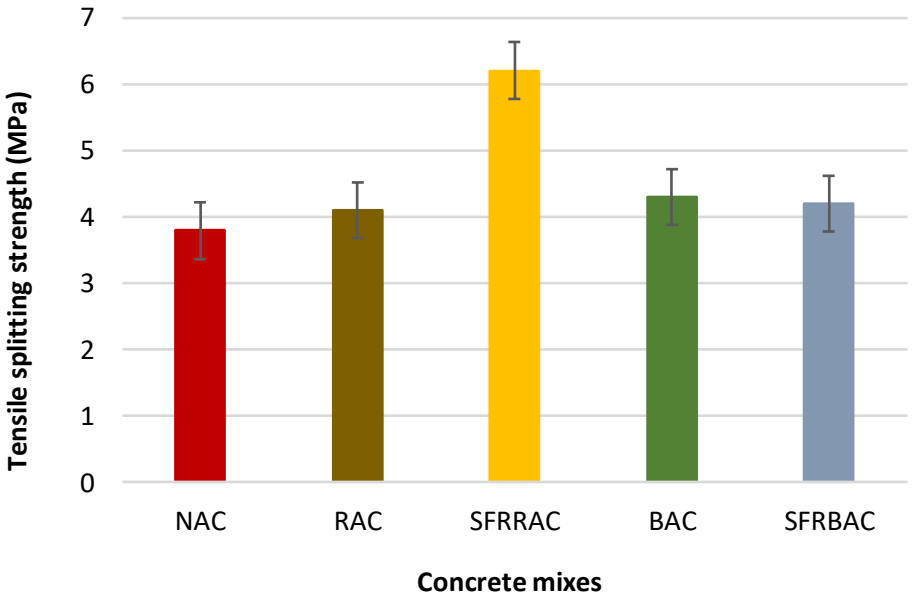

Figure 4.6: Tensile splitting strength of concrete for different mixes at 28 days.

Figure 4.7: Failure mode of concrete cylinders of different mixes tested in tension.

Furthermore, it is worth noting that the presence of superplasticizer offsets the requirement for more water which is usually the case for recycled concrete mix. Although water-to-cement ratio reduces with the addition of superplasticizer, workability of concrete improves at the same time (Barbudo et al. 2013). Soares et al. (2014) who reported 39% improvement in tensile strength when superplasticizer was added to concrete mix, maintained that the use of superplasticizer led to an excellent performance

using a RA obtained from a precast reject. Overall, from the results of the current study (which also used RA obtained from a precast waste), it can be stated that RA can completely replace NA without any detrimental effects, in terms of tensile strength.

Table 4.2 presents relationship between compressive and tensile splitting strengths of the five principal mixes investigated in this research. It can be deduced that the tensile strength of the concretes ranged from 7–13% of the compressive strength. It should be noted that the cylindrical compressive strength of the concretes was used for this calculation. The necessary conversion was made according to BS EN 206:2013+A1 (2016). Evidently, the presence of RA did not show a negative effect on the ratio of tensile strength to compressive strength. It can also be seen that the SFRRAC mix (made of 1% steel fibre volume ratio) gave the highest ratio compared to the other mixes.

Table 4.2: Relationship between compressive and tensile splitting strengths of different concrete mixes.

Mix ID	Compressive strength†, f_c (MPa)	Standard deviation (MPa)	Tensile splitting strength, f_{ct} (MPa)	Standard deviation (MPa)	f_{ct}/f_c
NAC	53.3	2.25	3.80	1.55	0.07
RAC	43.2	2.36	4.10	2.65	0.09
SFRRAC	48.2	0.82	6.15	3.94	0.13
BAC	49.4	2.28	4.30	3.05	0.09
SFRBAC	46.4	1.60	4.20	2.26	0.09

†*Cylindrical compressive strength.*

4.3.5 Flexural Strength

The results of the flexural strength of all the mixes studied are presented in Figure 4.8 and it can be deduced that this property of concrete is affected by a number of factors at different degrees. The influencing factors recognised from the results of the present research include the presence of RA, mix design method adopted for the concrete produced with RA, and the inclusion of SF. Generally, the normal concrete showed a slightly superior flexural strength than the concretes produced with either partial or full replacement of NA with RA. The flexural strength of the RAC mix made of 100% RA was reduced by just 3% compared to the NAC mix made entirely of virgin aggregate. This is in agreement with the results published by some authors who maintained that the flexural strength of concrete containing RA was the same or marginally lower than that of the

conventional concrete (Ignjatović et al. 2013, Choi, Yun, and Kim 2012, Fathifazl et al. 2009b). Malešev et al. (2010) upheld that this concrete property depends mainly on the quality of RA used rather than its quantity.

With regard to mix design method, flexural strength of the RAC mix prepared using the orthodox technique showed approximately 3% deficiency while the BAC mix proportioned with the EMV approach showed up to 6% decrease relative to the NAC. Although the conventional method gave 3% better performance than the EMV approach, but the latter resulted in a more eco-friendly and economical approach.

The flexural strength of the concrete produced from SFRRAC mix prepared with the conventional method was found higher, with up to 4% margin than the reference mix made of NA. This difference increased to 7.2% when the SFRRAC mix was compared to that of RAC. It should be noted that both RAC and SFRRAC mixes were exactly the same except for the absence of SF in the former. Hence, the gap in their flexural strength was due to the presence of SF. Conversely, the use of the EMV mix design method caused a reduction of approximately 11% in the flexural strength of SFRBAC relative to its corresponding BAC prepared with the same method. Unlike the tensile splitting strength, the unconventional method induced up to 17% decrease in the modulus of rupture of SFRBAC compared to the NAC. Additionally, about 20% difference was recorded in the flexural strength between SFRRAC and SFRBAC, in favour of SFRRAC. This variance is significant and can be accredited to a greater optimum SF content of 1% engendered by the conventional method as against 0.5% by the EMV guidelines.

Nevertheless, irrespective of the mix design approach, all SFRC exhibited a ductile failure mode while the unreinforced specimens failed in a brittle manner as shown in Figure 4.9. Typically, the presence of SF was responsible for the ductile mode of failure (Biolzi and Cattaneo 2017, Erdem, Dawson, and Thom 2011). From the load versus displacement diagram of the fibre-reinforced concretes given in Figure 4.10, it can be noticed that the specimens did not fail suddenly having attained their ultimate loads. This was unlike their plain (unreinforced) counterparts which failed as soon they reached their peak load. Furthermore, the Figure 4.10 depicts that the higher the SF volume ratio, the greater the peak load. In the same vein, the cracks generated in the case of SFRRAC with a higher volume of SF were fewer than those in SFRBAC (see Figure 4.9(b) and (c)). These findings are in agreement with the results reported in the work by Gao et al. (2017a).

Detailed analysis of the load–displacement plot given in Figure 4.10 has been provided in Table 4.3. It can be observed from the plot that, for all the specimens, the first-peak load and the corresponding net deflection are the same with the peak load and net deflection at peak load, respectively. The results showed that the SFRBAC had an average toughness of 45 Joules while its comparable SFRRAC was approximately 43 Joules. Consequently, the equivalent flexural strength ratio for SFRBAC and SFRRAC were obtained as 0.05% and 0.04% respectively. The slightly higher toughness of the SFRBAC can be attributed to its higher aggregate content compared to SFRRAC. It should be stated that the unusual pattern seen at the beginning of the load-displacement plot in Figure 4.10 is due to the stiffness of the test machine.

The relationship between compressive and flexural strengths of the mixes studied in this research was evaluated and presented in Table 4.4. The results showed that, for all the mixes, the flexural strength of concrete ranged from 7–9% of the cube compressive strength. It can be noticed from Table 4.4 that RA did not affect the ratio of flexural strength to compressive strength. In fact, recycled concrete prepared with the EMV technique gave the same ratio as normal concrete.

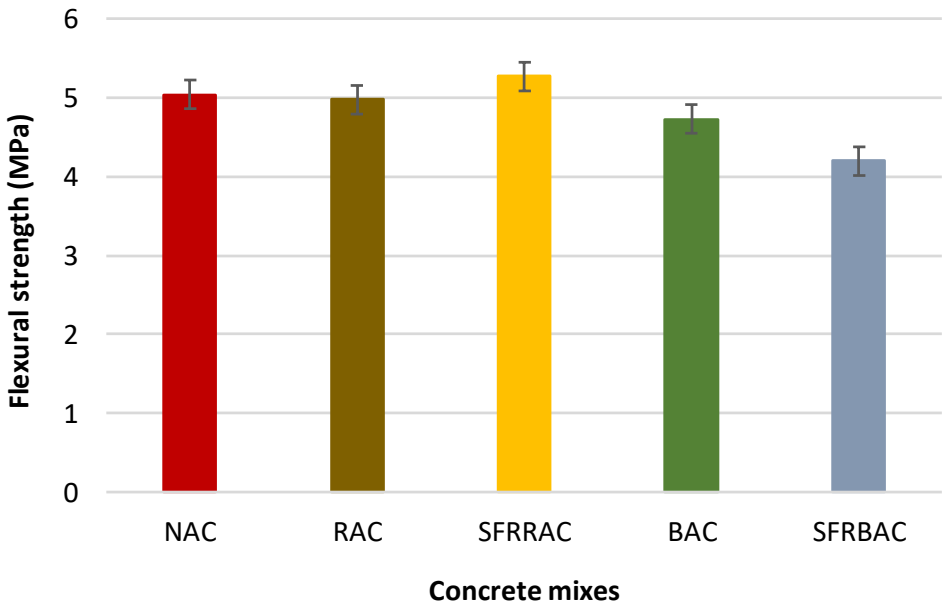

Figure 4.8: Flexural strength of concrete for different mixes at 28 days.

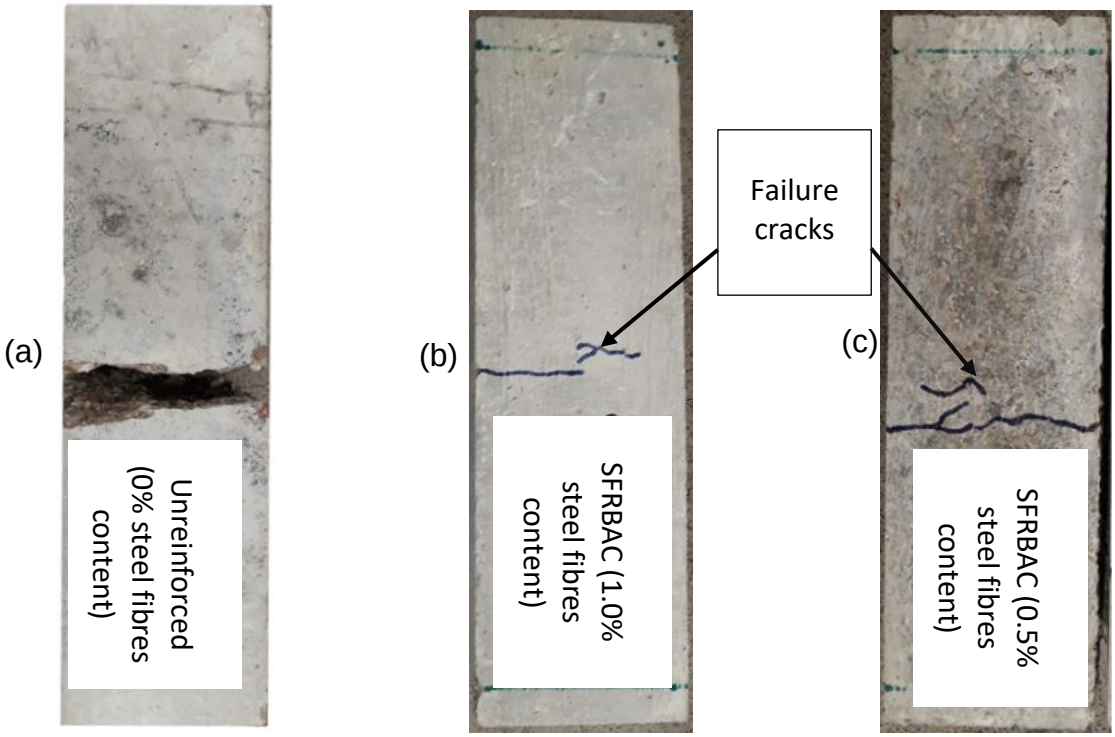

Figure 4.9: Flexural failure mode of unreinforced and steel fibre-reinforced recycled concretes.

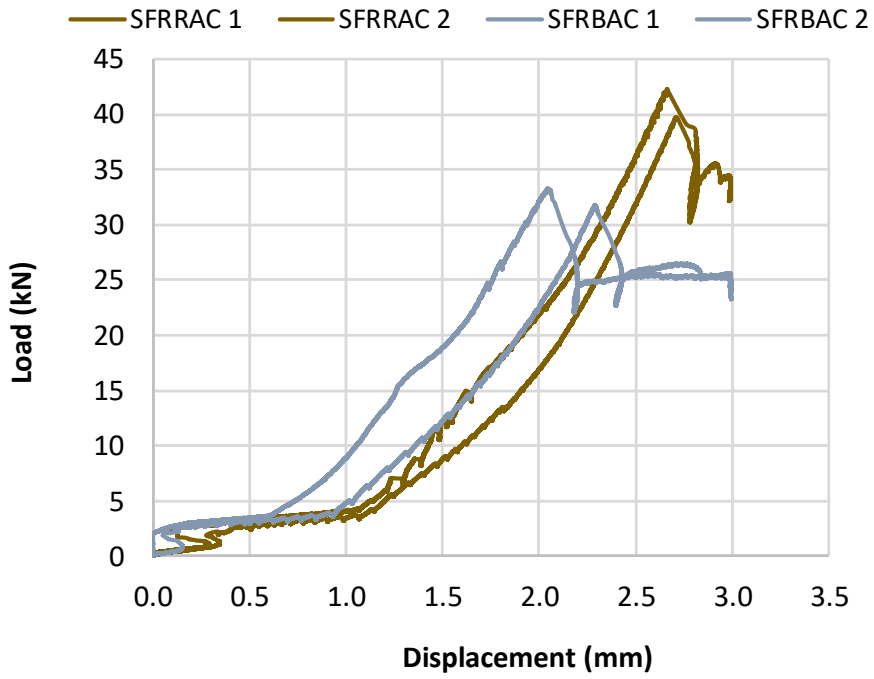

Figure 4.10: Load-displacement plot of steel fibre-reinforced recycled concrete prepared using different mix design method.

Table 4.3: Properties of steel fibre-reinforced recycled concretes proportioned using different mix design approach.

Mix ID	P_1 (kN)	f_{f1}† (MPa)	δ_1 (mm)	P_p (kN)	f_{fp}† (MPa)	δ_p (mm)	P^D_{600} (kN)	f^D_{f600}† (MPa)	P^D_{150} (kN)	f^D_{f150}† (MPa)	T^D_{150} (J)
SFRRAC 1	41.23	5.35	2.664	41.23	5.35	2.664	3.64	0.45	35.12	4.55	46
SFRRAC 2	39.73	5.15	2.710	39.73	5.15	2.710	3.19	0.40	34.29	4.45	40
Average	40.48	5.25	2.687	40.48	5.25	2.687	3.42	0.40	34.71	4.50	43
SFRBAC 1	33.29	4.25	2.043	33.29	4.25	2.043	5.15	0.65	25.16	3.20	49
SFRBAC 2	31.77	4.20	2.292	31.77	4.20	2.292	3.58	0.45	25.55	3.35	41
Average	32.53	4.20	2.168	32.53	4.20	2.168	4.37	0.55	25.36	3.25	45

†*Rounded to the nearest 0.05MPa*

$P_p = P_1$ *= Peak load = first-peak load*

$\delta_p = \delta_1$*= Net deflection at peak and first-peak loads*

$f_{fp} = f_{f1}$ *= Peak strength and first-peak strength*

P^D_{600} *= Residual load at net deflection of L/600*

f^D_{f600} *= Residual strength at net deflection of L/600*

P^D_{150} *= Residual load at net deflection of L/150*

f^D_{f150} *= Residual strength at net deflection of L/150*

T^D_{150} *= Toughness = Area under the load vs net deflection curve 0 to L/150*

Table 4.4: Relationship between compressive and flexural strengths of different concrete mixes.

Mix ID	Compressive strength, f_c (MPa)	Standard deviation (MPa)	Flexural strength, f_f (MPa)	Standard deviation (MPa)	f_f / f_c
NAC	66.6	2.25	5.04	4.72	0.08
RAC	54.0	2.36	4.89	2.91	0.09
SFRRAC	60.2	0.82	5.27	1.06	0.09
BAC	61.7	2.28	4.73	1.15	0.08
SFRBAC	58.0	1.60	4.20	1.07	0.07

4.3.6 Flexural Behaviour of Reinforced Concrete Beam

The schematic of the experimental set-up for the flexural behaviour test on the concrete beams of dimension 80 × 180 × 1500mm using a four-point loading arrangement is as

shown in Figure 4.11(a). The central cross section of the reinforced concrete beam is shown in Figure 4.11(b).

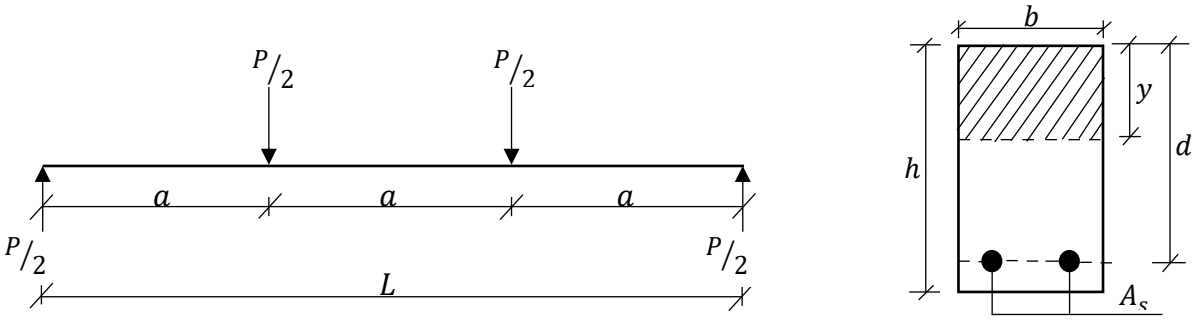

(a) (b)

Figure 4.11: Idealised equipment set-up for the four-point loaded beam and the central cross section of the reinforced beam.

Where a is the shear span (400mm), L is the span of the beam (1200mm), and P is the applied load (kN), b is the width (mm) of the beam, y is the neutral axis depth (mm), A_s is the cross-sectional area (mm^2) of the steel reinforcement, d is the effective depth (mm) of the beam, and h is the overall depth of the beam.

The theoretical values for the load-deflection plots for the loading in Figure 4.11 were obtained using the following mathematical expression (Ogbologugo 2018):

$$\delta = -\frac{23Pa^3}{48E_cI} \qquad \textit{Equation 4.1}$$

Where δ, E_c, and I are deflection, elastic modulus for concrete, and second moment of area about the neutral axis (mm^4), respectively.

According to Megson (2014), I for a transformed section is given as:

$$I = \frac{by^3}{3} + nA_s(d-y)^2 \qquad \textit{Equation 4.2}$$

Where n is the ratio of the elastic modulus of steel to that of concrete known as the modular ratio.

Also,

$$y = \frac{nA_s}{b}\left(\sqrt{1 + \frac{2bd}{nA_s}} - 1\right) \qquad \textit{Equation 4.3}$$

For concrete beam of a rectangular section, Megson (2014) gave the moment of resistance, M_R as:

$$M_R = \frac{f_c}{2} by \left(d - \frac{y}{3}\right) \qquad \textit{Equation 4.4}$$

Where f_c is the compressive strength (MPa) of the concrete.

From Figure 4.11, the ultimate theoretical moment will occur under the point loads from either supports of the beam. This is expressed mathematically as:

$$M_{ult} = \frac{Pa}{2} \qquad \textit{Equation 4.5}$$

Where M_{ult} is the ultimate moment.

It should be noted, that the load value at which the induced moment (using Equation 4.5) equals the beam moment of resistance (using Equation 4.4) is the theoretical failure load (Punmia, Jain, and Jain 1992). Therefore, the ultimate theoretical load, P_{ult} can be expressed as:

$$P_{ult} = \frac{2M_R}{a} \qquad \textit{Equation 4.6}$$

Putting the dimensional values of the transformed beam section and the modular ratio into Equations 4.2–4.6, the theoretical values of I, y, M_{ult}, and P_{ult} were obtained for all the mixes studied and presented in Table 4.5. The details of the computation are given in Appendix D.

Table 4.5: Parameters defining the idealised reinforced concrete beams for all the mixes.

Mix ID	Modular ratio, n	Neutral axis, y (mm)	Second Moment of area, I ($\times 10^6$ mm^4)	Ultimate load, P_{ult} (kN)	Ultimate moment, M_{ult} (kNm)
NAC	6.12	50.19	13.93	74.00	14.80
RAC	6.80	52.36	15.08	62.25	12.45
SFRRAC	6.44	51.23	14.48	68.10	13.62
BAC	6.36	50.97	14.34	69.50	13.90

From the experimental study, the behaviour of the reinforced concrete beams produced from NAC, RAC, SFRRAC, and BAC mixes were investigated. These included the mid-span deflection, failure load, mode of failure, cracking initiation and development,

stresses and strains development, and estimation of crack width at failure. In this study, the RAC beam showed the least load capacity, and this was due to the presence of RA. The RAC beam had up to 6.3% lower load bearing capacity than its corresponding NAC beam. This follows that RAC mix containing 100% RA and proportioned with the conventional method, requires a strengthening material to compensate for strength loss. According to the results presented in Table 4.6, SFRRAC beam had the highest load bearing capacity relative to beams of other mixes. In comparison with the NAC beam made completely of normal aggregates, the SFRRAC beam consisting of 100% RA sustained more load up to a degree of about 8%. Between RAC and SFRRAC mixes, the effect of SF on the load capacity of the recycled concrete beams was over 13% increase.

However, the use of alternative mix proportioning technique for concrete containing RA gave similar load capacity with the conventional concrete. It is noteworthy that the BAC mix, which was designed with the EMV method, consisted of 60% by volume each of fine and coarse aggregates. From Table 4.6, approximately 6% difference exists between the failure load of RAC and BAC, in favour of the latter. This was upon the fact that the cement content for each of RAC, SFRRAC, and NAC mixes was in excess of 143kg per m^3 of concrete compared to the BAC mix. Furthermore, it can be deduced from Table 4.6 that the maximum experimental load for the NAC, RAC, SFRRAC, and BAC beams are respectively 86%, 96%, 101%, and 91% that of their corresponding theoretical values. The difference in the actual and the predicted load capacity was mainly because the elastic modulus of concrete was estimated according to Equation 2.3 (that is, $E_c = 4700\sqrt{f_c}$).

Similarly, with respect to ultimate moment, the SFRRAC beam had the greatest value than its comparable RAC, BAC, and NAC beams. Moment being a function of the applied load, exactly the same increase or decrease effect in the load capacity were recorded for the ultimate moment as given in Table 4.6. According to Ignjatovic´ et al. (2013), cracking moment depends majorly on the tensile strength of the concrete. This justifies why the SFRRAC mix with the highest tensile splitting strength produced the beam with the highest experimental ultimate moment.

In terms of crack initiation, all but RAC beam had their first cracks occur at a load of 20kN. The RAC beam showed its first cracks at a load of 15kN. The longest of the first cracks measured for the NAC, RAC, BAC, and SFRRAC beams were separately 70mm, 97mm, 60mm, and 56mm. The corresponding average number of cracks observed (at the first cracks) were 10, 9, 3, and 4, respectively. However, the nature of the cracks was

hair-like for all the samples and emanated from the tensile zone (bottom) of the beam. Again, the cracks were all flexural, staggering upwards from the bottom and mostly concentrated toward the middle-third of the span of the beams as can be observed in Figure 4.12(a)–(d). As the load intensity increased, the cracks developed further, spread within the span of the beams, and shear cracks initiated and migrated mainly from near the supports toward the nearest point load. The shear cracks were all inclined (diagonal) in nature.

Table 4.6: Results of the experimental and theoretical properties of the beams produced from the different mixes.

Mix ID	Ultimate load, P (kN)			Ultimate moment, M (kNm)			Mid-span deflection¶, δ (mm)	Estimated crack width†, α (mm)
	E_P	T_P	E_P/T_P	E_M	T_M	E_M/T_M		
NAC	63.72	74.00	0.86	12.74	14.80	0.86	8.47	4.0
RAC	59.71	62.25	0.96	11.94	12.45	0.96	7.60	3.5
SFRRAC	69.04	68.10	1.01	13.81	13.62	1.01	11.75	3.0
BAC	63.43	69.50	0.91	12.69	13.90	0.91	9.64	1.0

Note: E and T mean experimental and theoretical respectively; ¶Deflection at the load step before failure occurred; †Experimental crack width at failure.

According to Gu et al. (2016), concretes in the vicinity of crack cannot withstand tensile forces and therefore the stresses are passed to the nearby unbroken concrete. Consequently, crushing of concrete occurred in the compression zone (top) of the beams as the load intensity was sustained and failure was induced. Typically, as the applied load was increased and cracks developed, the neutral axis depth reduced, leading to a corresponding reduction of the compression zone. The failure mode of the tested samples can best be described as a ductile mode of failure in which the steel reinforcements yielded first, then followed by a localized crushing of the concrete (under the point load) in the compression zone.

It is important to note that the nature of cracking propagation was similar for the NAC, RAC, and BAC specimens (containing no steel fibres) as evident in Figure 4.12(a)–(c). Nevertheless, the BAC beam had fewer cracks and lesser severity of critical cracks (before and at failure) than the comparable beams including the SFRRAC beam. This can be attributed to a higher amount of total coarse aggregates in its mix compared to those of the others. This statement had been validated in the findings of Kumar et al. (2007) who showed that when a concrete beam was subjected to a flexural testing, cracking propagation was impeded by coarse aggregates and the cracks found a path

of lowest resistance round the aggregates. Additionally, the greater volume of superplasticizer (in the BAC mix) which improves particles packing density in concrete, played a significant role in the behaviour observed. Overall, the SFRRAC beams had the highest number of cracks on average, but the cracks were less severe compared to those exhibited by the beams of other mixes. It can also be noticed from Figure 4.12(a)–(c) that the crack patterns of the samples with no SF (NAC, RAC, and BAC), were such that, the subsequent cracks due to incremental load continued from where the initial cracks stopped. On the other hand, the crack pattern of the SFRRAC sample was characterised by a few disjointed cracks. The SF was responsible for the bridging effect known as "kinking" and can be further explained as illustrated in Figure 4.12(e)–(f). Eventually, this phenomenon engendered a more ductile mode of failure of the samples produced with SF.

Table 4.6 shows that BAC beam had the least estimated crack width. Experimentally therefore, from serviceability perspective, the BAC mix designed using the EMV method performed better than all the other concrete mixes prepared with the conventional method. Likewise, from cost point of view, the BAC mix would be relatively cheaper than SFRRAC mix due to the addition of steel fibres and a higher cement content.

(a)

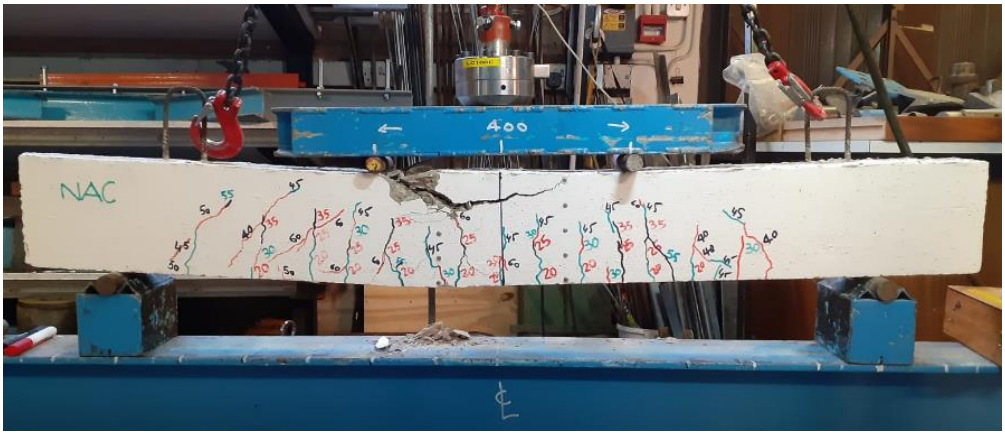

(b)

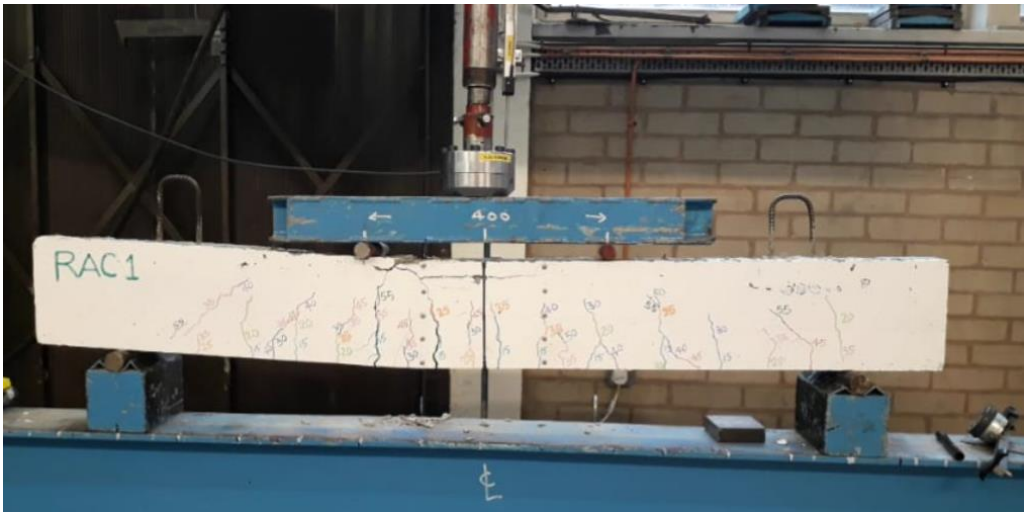

(c)

(d)

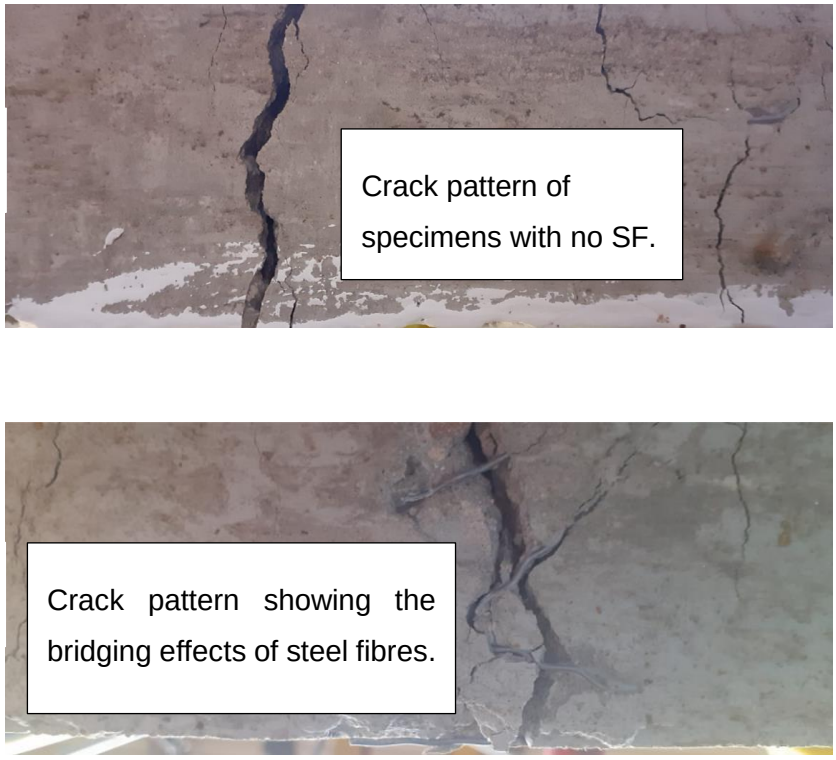

Figure 4.12: Crack patterns of reinforced concrete beams for different mixes.

The value of load at each load step was plotted against the corresponding mid-span deflection values derived from Equation 4.1 and the experiments for all the mixes as shown in Figure 4.13(a)–(d). The NAC, RAC, and SFRRAC beams which mixes were proportioned with the conventional method exhibited similar experimental load-deflection behaviour. Thus, the general theory of bending suitable for conventional concrete can be applied to the RAC. However, the impact of SF can be seen at the beginning and the end of graph shown in Figure 4.13(c). Clearly, the BAC mix designed using the EMV technique showed a load-deflection response at variant with those of other mixes prepared in a traditional way. This is also be ascribed to a higher amount of total coarse aggregates in the BAC mix. Additionally, comparing the gap between the observed and predicted load-deflection behaviour for all the mixes, the BAC mix showed a narrower difference compared to the other mixes. However, it should be stated that both mix proportions and elastic modulus of aggregate affect the elastic modulus for concrete, and the expected difference between the experimental and theoretical (calculated) values of elastic modulus for concrete range from 80–120% (ACI 318R 2014). Hence, the significant variation noticed between the observed and predicted deflections was because the elastic modulus for concrete used was estimated according to ACI 318R (2014). Additionally, the possible overestimation of the theoretical deflections due to the exclusion of tension stiffening effect in the calculation, is worth noting.

(a)

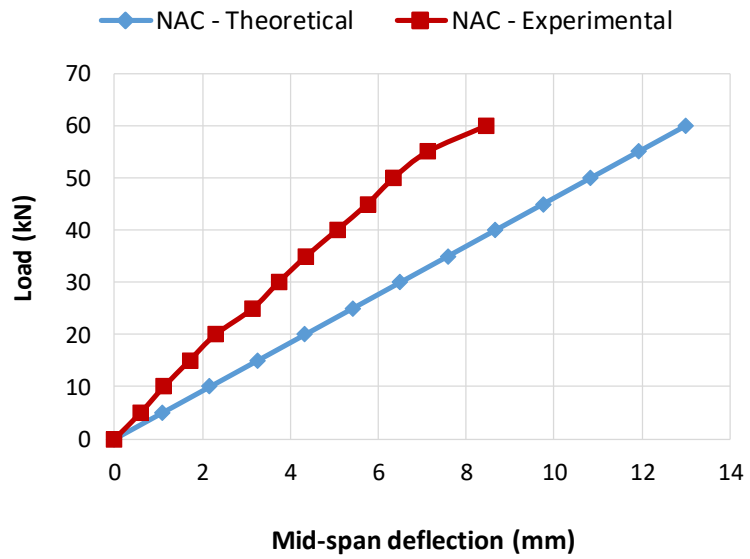
NAC - Theoretical
NAC - Experimental
Load (kN)
0
10
20
30
40
50
60
70
0
2
4
6
8
10
12
14
Mid-span deflection (mm)

(b)

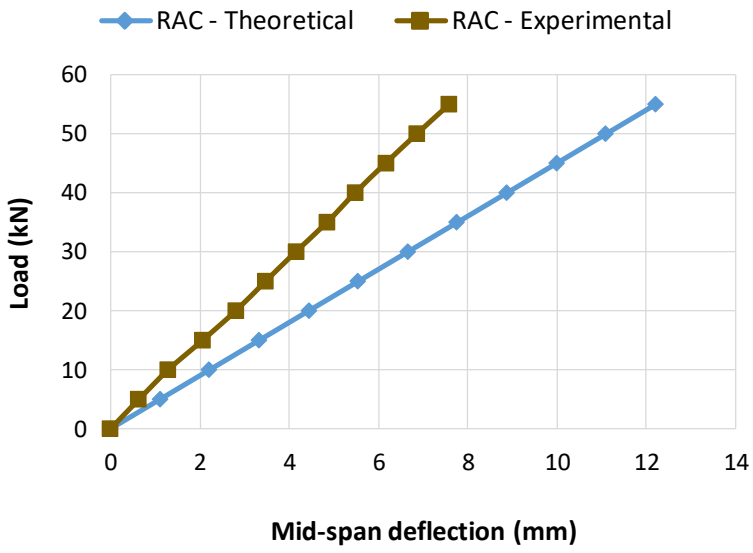
RAC - Theoretical
RAC - Experimental
Load (kN)
0
10
20
30
40
50
60
0
2
4
6
8
10
12
14
Mid-span deflection (mm)

(c)

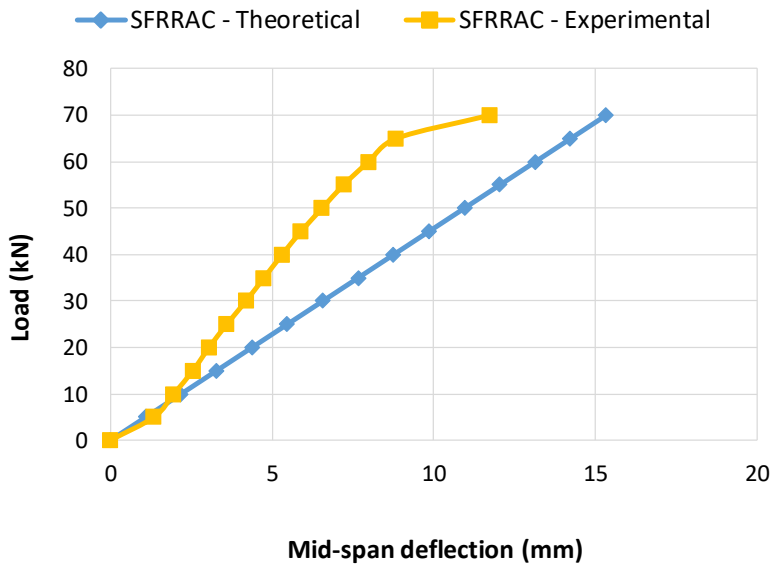
SFRRAC - Theoretical
SFRRAC - Experimental
Load (kN)
0
10
20
30
40
50
60
70
80
0
5
10
15
20
Mid-span deflection (mm)

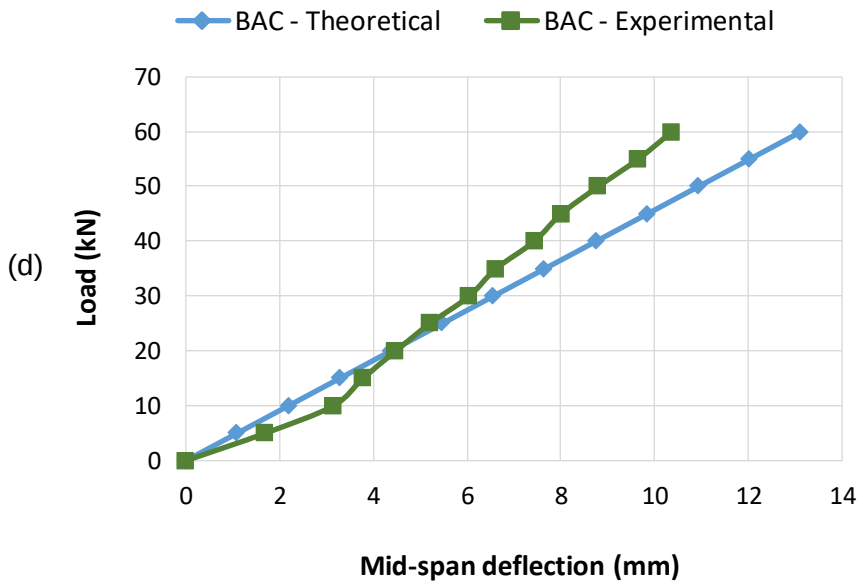

Figure 4.13: Theoretical and experimental mid-span deflection.

Finally, the strains developed in the beams as the load was applied were measured as explained in Section 3.3.3.6 and plotted in Figure 4.14(a)–(d). Apparently, all the beams showed a linear distribution of strain across their depths. However, the beams produced from the mixes containing no SF showed a similar pattern of strain distribution regardless of aggregate type. On the other hand, the beam incorporating SF showed a different distribution pattern. Furthermore, both BAC and SFRRAC beams had the same maximum strain 0.0044 prior to failure. This value is higher compared to those of NAC and RAC beams and was expected due to the ability of SF to intercept cracks and the more content of coarse aggregate (which also restrain cracks) in the BAC mix. Within the elastic limit, the points on the plots at which the lines of best fit (through the measured strains across beam depth) intersect the vertical axis give the neutral axis depth. Noticeably, the neutral axis position was shifting as the applied load was increasing and it almost stabilized at a higher loading. Hence, the estimated experimental values of neutral axis for the NAC, RAC, SFRRAC, and BAC beams range from 56–70mm, 54–70mm, 50–110mm, and 52–68mm respectively, from the top of the beams. Their corresponding values from the analytical method were 50.19mm, 52.36mm, 51.23mm, and 50.97mm (see Table 4.5) respectively. Therefore, there is a good correlation between the experimental and analytical results. Based on the maximum compressive strain results of the current study, the flexural behaviour of concrete beams containing RA does not vary significantly from that of the conventional concrete beam.

Notwithstanding, it is important to mention that the accuracy of the strain values depends on the ability to place the DEMEC buttons at the right positions. This is a difficult task

and most times; 100% accuracy cannot be attained for all the ten DEMEC buttons (as in the present study). Another factor that may have influenced the results is the fact that the actual (from the experiments) elastic modulus of the concretes was not used in the analytical method, which ultimately would affect the modular ratio of the composite beam used in calculating the neutral axis position. Also, from practical point of view, the positions of the rebars may change following a shift of the spacers during casting operation (vibration of concrete), resulting in alteration of the neutral axis position.

(a)

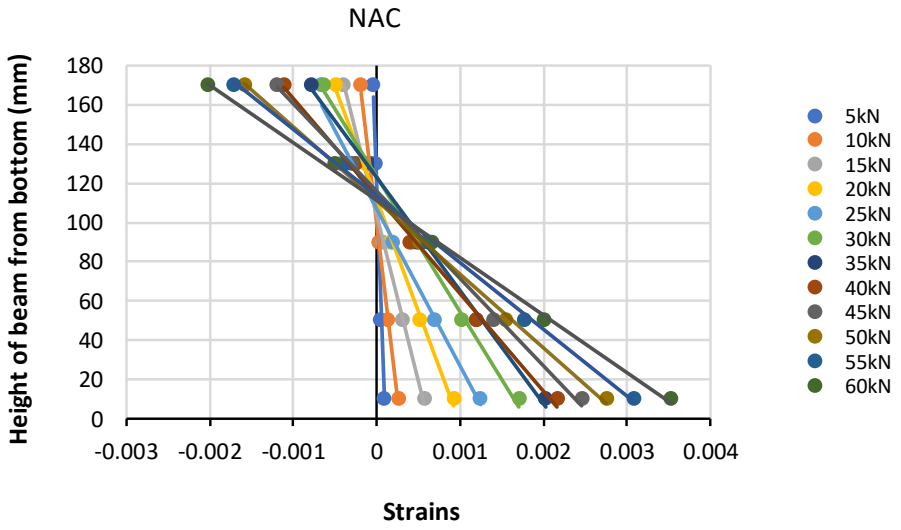

(b)

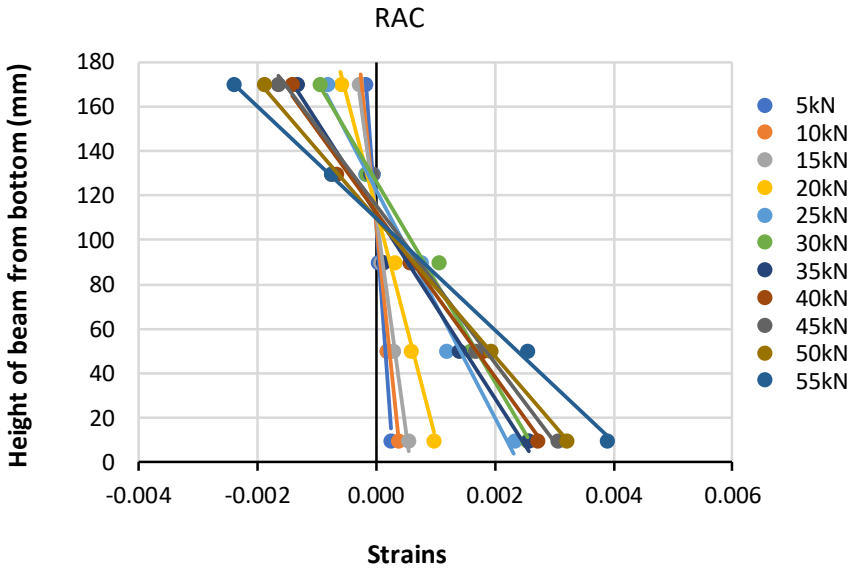

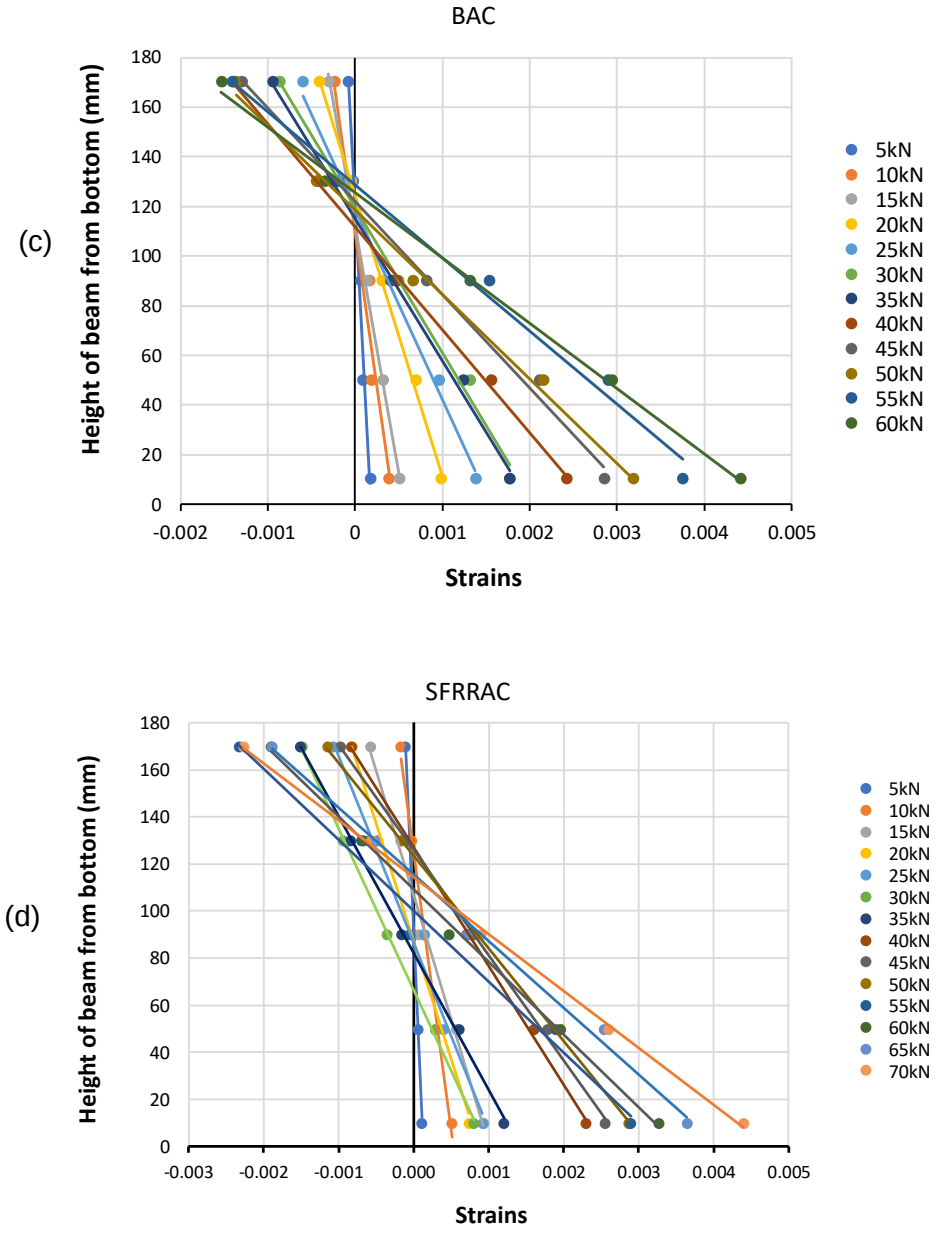

Figure 4.14: Strain plot across the height of the beams from different mixes.

4.3.7 Water Absorption

The water absorption capacity of the specimens produced from the concrete mixes investigated was determined at 28 days and presented in Table 4.7. Notably, the specimens produced from concrete mixes consisting of RA showed a higher absorption capacity than those of their comparable NAC mix made entirely of NA. This was anticipated due to the porous nature of RA and water not only travelled through the paste of the RAC but also through the RA. Again, the presence of RFA (which has already been established to have a greater water absorption capacity than its equivalent NFA) in the recycled concrete mixes contributed further to the results obtained. According to

Table 4.7, it can be deduced that concretes containing RA had a more water absorption capacity than the NAC.

However, the recycled concretes showed varied degrees of absorption at different replacement ratios with RA. Relatively, RAC mix comprising of 100% RA had approximately 39% higher absorption tendency than the BAC mix consisting of 60% for each of RCA and RFA. This implies that water absorption increases as the replacement ratio with RA increases and this is in agreement with the findings of previous authors (Fan et al. 2016, Malešev, Radonjanin, and Marinković 2010).

It can be observed from the results presented in Table 4.7, that the use of the EMV mix design approach improved this durability property of concrete. This may be attributed to a denser packing associated with this method, which offers a more quality paste thereby limiting passage of water. Again, as already pointed out, the EMV method resulted in concrete mix of a higher superplasticizer demand than the traditional method. The work of superplasticizer was to prevent the formation of and break down agglomerates in the cement matrix, thereby releasing water trapped between the agglomerates and dispersing the fine particles into the pores, thus reducing water demand (Van Der Putten et al. 2017, Moosberg-Bustnes, Lagerblad, and Forssberg 2004). This phenomenon is expected to be more effective in concrete consisting of RA, whereby, the dry mortar present in the RA is readily dissolved upon mixing. Also, due to the decrease in both water-to-cement ratio and void index by the use of superplasticizer, there was a drop in water absorption capacity of concrete (Soares et al. 2014). Hence, the BAC mix having a higher superplasticizer content than its RAC counterpart showed a substantially lower water absorption capacity.

Furthermore, the impact of mix design method on the water absorption capacity reflected on the result observed for recycled concretes incorporating SF. The different optimum SF volume ratios obtained for SFRRAC and SFRBAC mixes was because of the design approach. From Table 4.7, the SFRRAC (designed with the normal method) and SFRBAC (proportioned with the EMV method) showed a higher absorption tendency in excess of 49% and 9% respectively, relative to the NAC. Obviously, the high absorption capacity shown by the SFRRAC was as a result of 100% replacement of NA. Also, according to Heeralal et al. (2009), the addition of SF increases pore density of the concrete. Apparently, the SFRRAC constituting of 1% optimum SF volume ratio was expected to have more pores than SFRBAC of 0.5% SF volume fraction, resulting in a higher water absorption tendency. Additionally, the presence of SF slightly increased the water absorption capacity of the recycled concrete proportioned with the conventional

method compared with similar mix with no SF. Conversely, there was no effects in the absorption tendency for the recycled concrete incorporating SF and prepared with the EMV technique, relative to similar mix without SF. Even though the presence of SF in the SFRBAC was expected to slightly raise its absorption capacity above that of the analogous BAC, the effect was offset by more superplasticizer required by the SFRBAC.

Table 4.7: Water absorption capacity of different concrete mixes measured at 28 days.

Mix ID	Specimen No.	Absorption (%)	Corrected absorption (%)	standard deviation (%)	Average corrected absorption (%)
NAC	1	1.9	3.1	0.00	3.1
	2	1.9	3.1		
	3	1.9	3.1		
RAC	1	3.5	5.6	0.15	5.6
	2	3.5	5.7		
	3	3.3	5.4		
SFRRAC	1	3.7	6.0	0.13	6.1
	2	3.9	6.2		
	3	3.7	6.0		
BAC	1	2.2	3.5	0.07	3.4
	2	2.1	3.4		
	3	2.1	3.4		
SFRBAC	1	2.1	3.3	0.15	3.4
	2	2.0	3.3		
	3	2.2	3.5		

This study further investigated the rate of water absorption of the specimens, considering some cumulative immersion periods up to 2 hours. The results revealed that, at all periods studied, the RAC showed a higher absorption rate than the parallel NAC (see Figure 4.15). However, the slopes of each plot at consecutive periods of observation proved that the rate of water absorption decreased with time. According to Figure 4.15, while the absorption rate of NAC has almost stabled (with no significant increase between the 1- and 2-hours observations), the RAC continued to show an appreciable increase of around 11%. Furthermore, both SFRRAC and SFRBAC showed an identical rate of absorption, even though the former had a higher water absorption capacity. This is because both mixes contain the same amount of RCA.

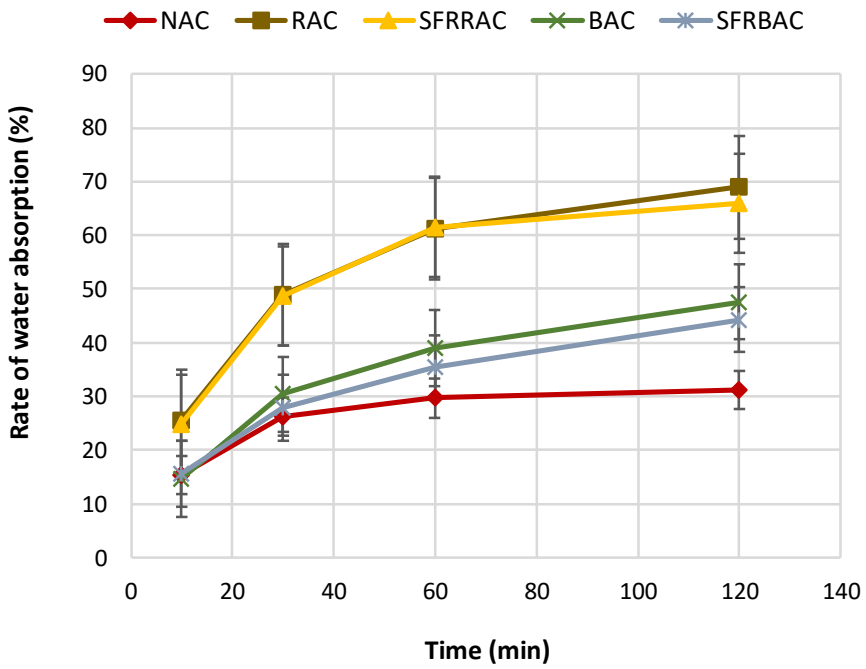

Figure 4.15: Rate of water absorption measured at some cumulative immersion period.

Chapter 5

5 RESULTS, ANALYSIS, AND DISCUSSION OF NUMERICAL INVESTIGATION

5.1 Introduction

This chapter presents the results of the numerical study carried out using commercial ANSYS Mechanical APDL 2019 R1. The properties of the concrete derived from the experimental investigation were used to model the flexural behaviour of the beams. The results from the finite element analysis (FEA) were compared with those obtained from the laboratory experiments. In this study, the parameters of interest, to properly investigate the flexural behaviour of the concrete beams included: stress development, ultimate load bearing capacity, mid-span deflection, strains and cracks development, and mode of failure. In addition, a parametric study was carried out on the FE model to investigate the effects of shear transfer coefficients, tangent modulus of steel, and to predict the load capacity of the reinforced beams for early and matured ages.

5.2 Stress Development and Failure Mode

The FEA contour plots showing the maximum principal stresses developed in the concrete beams, for all the mixes, are shown in Figure 5.1. The maximum compressive stresses resulting from the ANSYS model are 52.1MPa, 50.2MPa, 54.7MPa, and 55.5MPa for NAC, RAC, SFRRAC, and BAC mixes, respectively. Their comparable experimental values are 45.9MPa, 41.5MPa, 48.9MPa, and 45.1MPa, respectively. The variation between the numerical and experimental results was because the elastic modulus for concrete (which has direct relationship with compressive strength) used in this study was derived analytically. Also, the actual yield strength of the steel reinforcement used for the laboratory experiments was not known. Hence, the 500MPa strength assumed for the steel reinforcement in the ANSYS model may have affected the outcomes of the numerical study. According to the stress distribution diagram in Figure 5.1, the FEA results showed that the BAC and RAC beams had the highest and lowest tensile stresses respectively compared to the other beams. This can be ascribed to greater amount of coarse aggregates (capable of restricting cracking propagation (Kumar et al. 2007)) in the BAC mix relative to the other mixes. Nevertheless, the compressive and tensile stress values by the ANSYS model for all the beams are approximately the same. This confirms that the use of recycled aggregate, of similar quality with the one used in the present study, has no detrimental effects on the flexural behaviour of the reinforced concrete beam.

Figure 5.1 and Figure 5.2 show that the experimental compressive stresses were reached and that strain hardening of the reinforced concrete beams was attained before failure was induced in the FE model. These suggest therefore that failure of the modelled beams was due to the yielding of the steel reinforcements at the tension zone and the local crushing of the concrete under the point load at the compression zone. This is typical of a simply supported concrete beam under the influence of a two-point load and this pattern of failure aligns with that obtained from the experimental investigation.

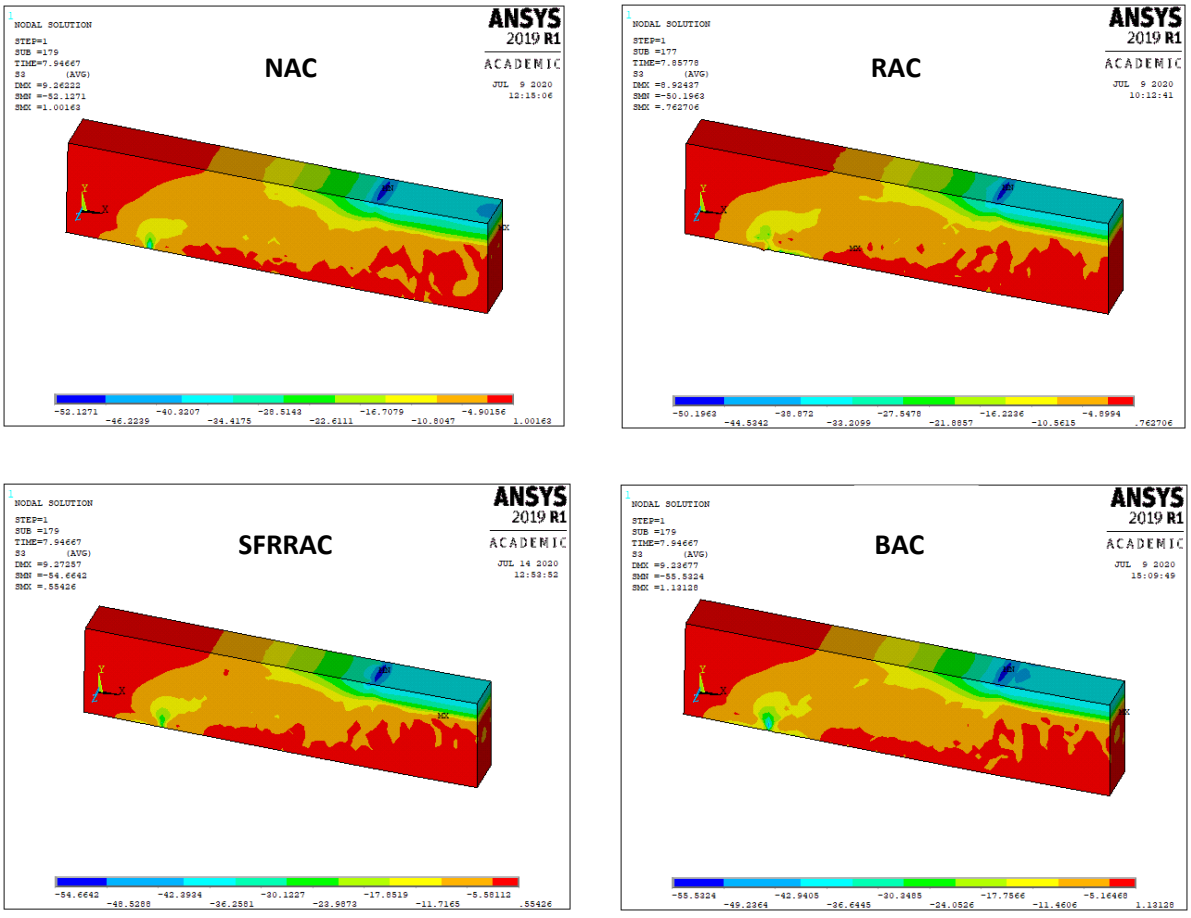

Figure 5.1: Compressive stress distribution in concrete for the FEA model for different mixes.

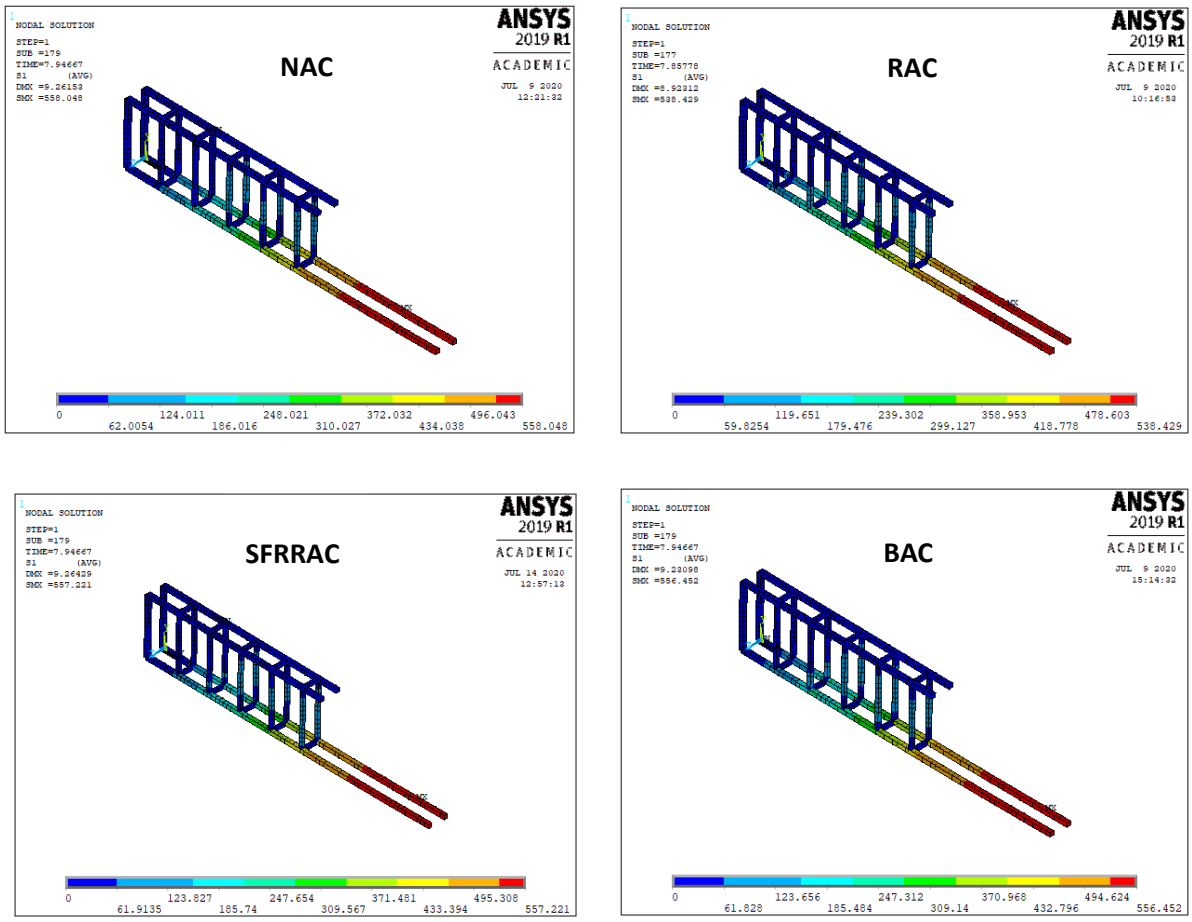

Figure 5.2: Stress distribution in steel reinforcements for the FEA model for different mixes.

5.3 Ultimate Load Capacity and Mid-span Deflection

The experimental and FEA ultimate load capacity of the concrete beams manufactured from the four mixes investigated are presented in Table 5.1. The result shows that the load capacity predicted by the FE model is approximately 98%, 100%, 91%, and 100% the value obtained from the experimental investigation of the NAC, RAC, SFRRAC, and BAC beam, respectively. According to Figure 5.3, the mixes with or without RA showed similar trend of load-deflection plot. It is important to note that deflections up to the convergent point were plotted, as no convergence can be attained beyond this point. Comparing the mid-span deflection values in Table 5.1, it can be deduced that the ANSYS model prediction does not vary widely from that of the experiment. It should be stated, however, that the experimental values given in Table 5.1 were the mid-span deflection recorded at the penultimate load-step prior to failure.

Table 5.1: Experimental and FEA predicted ultimate load and mid-span deflection for different mixes.

Mix ID	Ultimate Load, P (kN)			Mid-span deflection, δ (mm)	
	Expt., E_P	Num., N_P	N_P/E_P	Expt., E_δ	Num., N_δ
NAC	63.72	62.64	0.98	8.47	9.26
RAC	59.71	60.08	1.01	7.60	8.90
SFRRAC	69.04	63.17	0.91	11.75	9.16
BAC	63.43	63.15	1.00	9.64	9.23

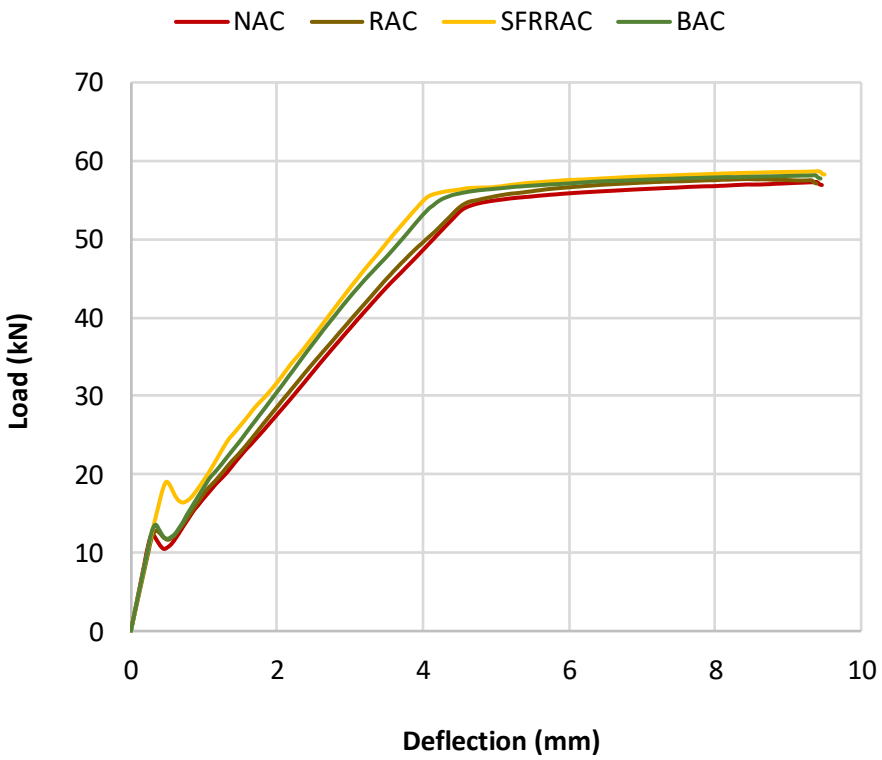

Figure 5.3: Load-deflection relationship for the FEA model for different mixes.

5.4 Strains and Cracks Development

Normally, when a beam is subjected to an increasing load (within the span), bending is bound to occur in the beam with time. Due to the sustained increasing load, strains will be induced and subsequently, cracks would set in when the strain capacity of the beam has been exceeded. From the maximum principal strain contour plots shown in Figure 5.4, the two critical regions are the support and the section at the tension zone between the position of the applied load and the centre of the beam. Also, Figure 5.5 presented the crack patterns resulting from the experimental and numerical studies. Although the

ANSYS plot for the cracks generated showed the probable cracking regions predicted by the software (Vasudevan, Kothandaraman, and Azhagarsamy 2013), the results of the current study showed similar cracking propagation between the ANSYS model prediction and the laboratory experiments. The Figure 5.5 showed that all cracks initiated at the bottom (tension zone) of the beams and propagated upwards towards the region of the applied load. Again, it can be observed from the experimental and numerical results, that the cracks at the support region are inclined while those within the region of the applied load have very little or no inclination.

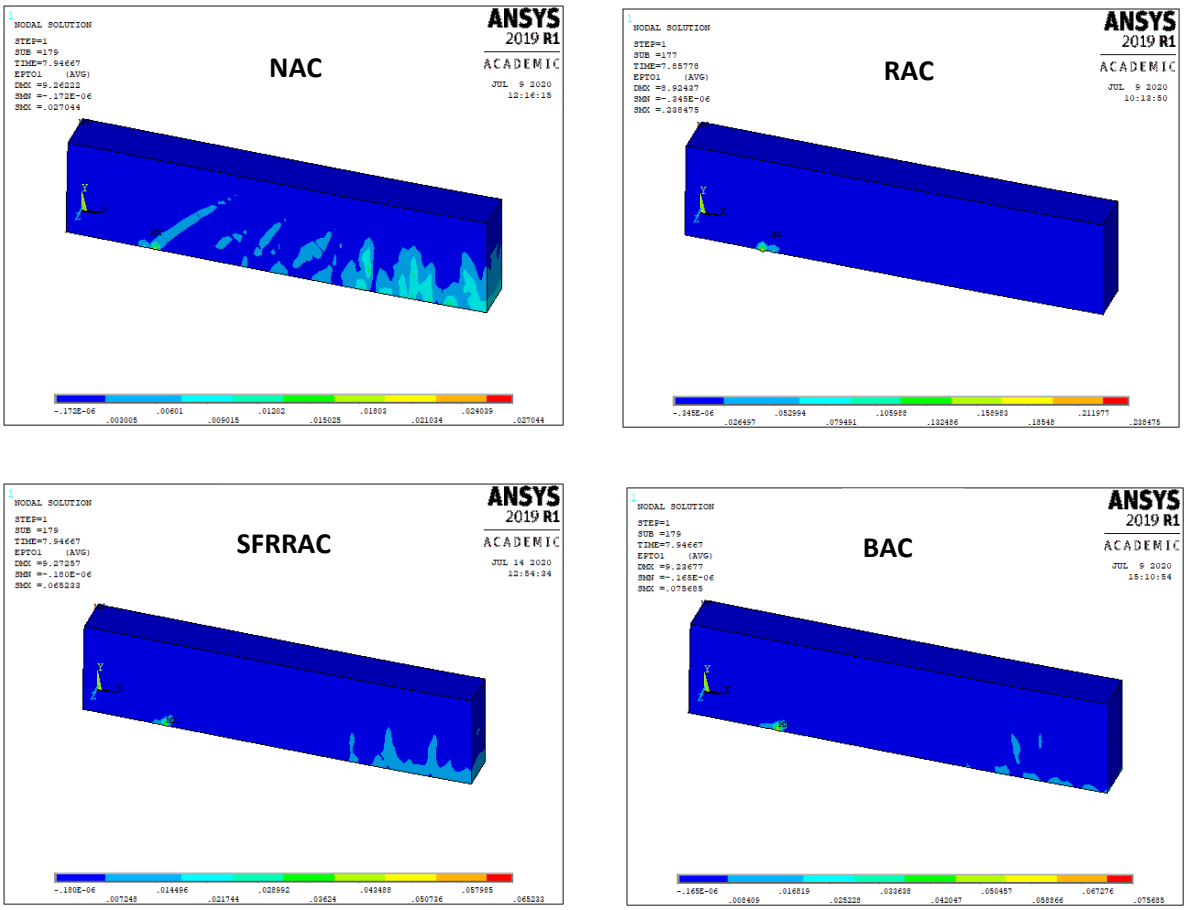

Figure 5.4: Strain distribution in concrete for the FEA model for different mixes.

Figure 5.5: Cracks in the ANSYS model versus experiment.

5.5 Parametric Study on the FE Model

5.5.1 Tangent Modulus of Steel

According to ANSYS (2019), "The tangent modulus cannot be less than zero or greater than the elastic modulus." Consequently, this study investigated the effect of this material property in the FE model. Firstly, a tangent modulus of 20MPa (approximately 0.0095% of the elastic modulus for steel) was considered for steel in the bilinear isotropic properties section in ANSYS. The result showed that 91%, 97%, 85%, and 92% of the experimental load capacities of the NAC, RAC, SFRRAC, and BAC beams respectively were predicted by the FE model. Nevertheless, it was found that failure occurred in the modelled reinforced concrete beams as soon as the tensile stresses in the rebar reached 500MPa (which was the assumed yield strength of steel) as revealed in Figure 5.6. Subsequently, using the NAC beam properties, tangent moduli of 1050MPa, 1995MPa, 10500MPa, and 21000MPa respectively corresponding to 0.5%, 0.95%, 5%, and 10% of the elastic modulus for steel were considered. From the results, there was no substantial difference (except for the 21000MPa tangent modulus) in the load capacity of the beams as shown in Table 5.2. However, the stress value shown by the 10500MPa tangent modulus indicated a better strain hardening stage compared to 1050MPa and 1995MPa tangent moduli whose stress values suggest a premature failure of the reinforced concrete beams. On the other hand, with 21000MPa tangent modulus, the load capacity of the beam was overestimated, and the stresses developed in the rebar at the strain hardening stage were excessively higher than those of the others. Therefore, a balance between the load capacity of the beam and the stresses developed in the reinforcement is required when choosing the tangent modulus value for the FE model.

Table 5.2: Effect of tangent modulus in the FE model.

Tangent modulus (MPa)	Ultimate load (kN)	Stress in reinforcement (MPa)
1050	57.8	506.42
1995	58.2	511.82
10500	61.2	549.76
21000	64.4	585.01

Note: Experimental ultimate load is 63.72kN.

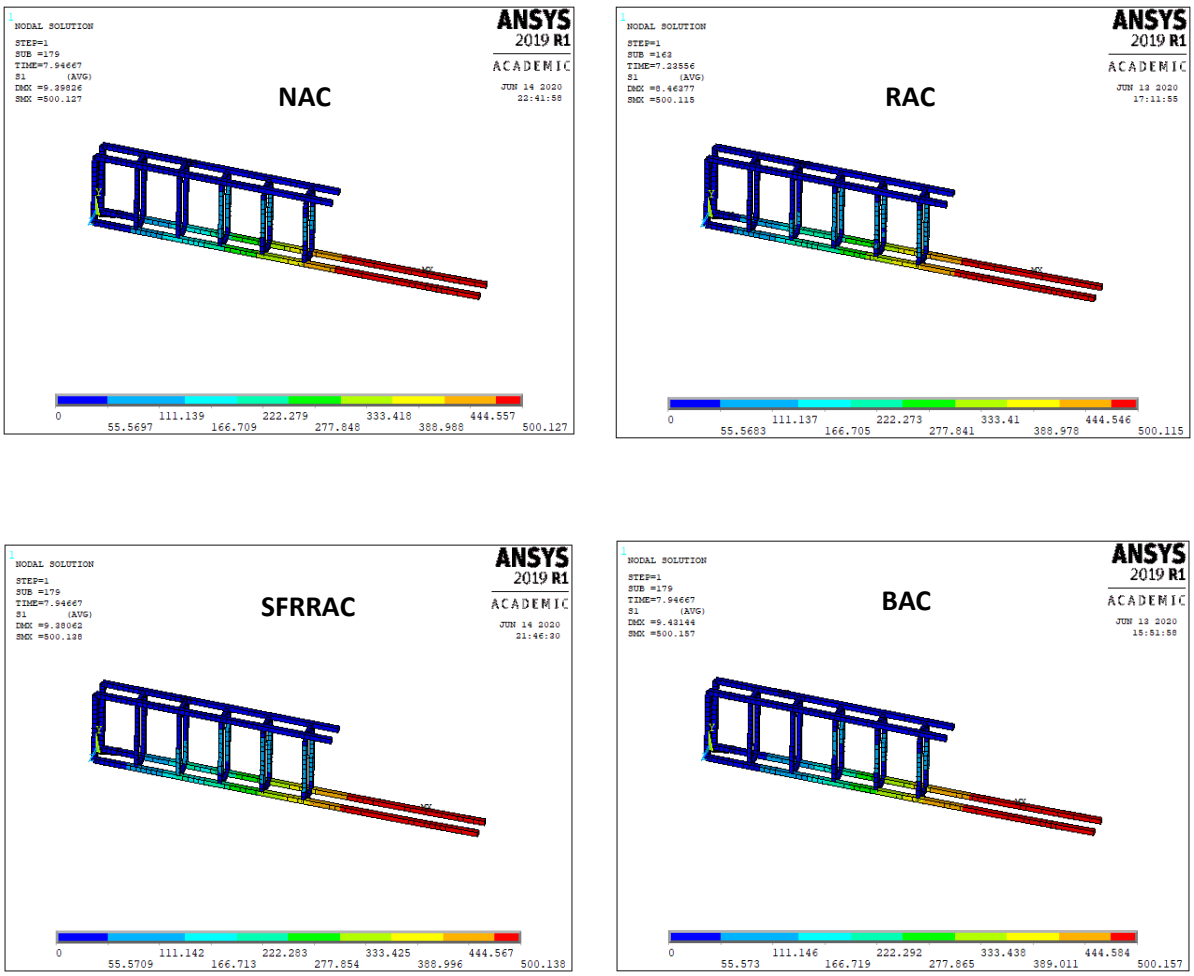

Figure 5.6: Effect of using a tangent modulus of 20MPa on the rebar stresses in the FE model.

5.5.2 Shear Transfer Coefficients

The open shear transfer coefficient and closed shear transfer coefficient affect the results of the FEA carried out on ANSYS. According to ANSYS Mechanical APDL (2019), values range from 0.0 (complete loss of shear transfer) to 1.0 (no loss of shear transfer) can be selected for the shear transfer coefficients. Kachlakev et al. (2001) noticed a convergence problem at a shear transfer coefficient below 0.2. While different shear transfer coefficients have been adopted in different studies (Aziz and Ghailan 2007, Padmarajaiah and Ramaswamy 2002, Kachlakev et al. 2001), open shear transfer coefficient in the range 0.35–0.4 and closed shear transfer coefficient in the range 0.9–1.0 gave a FEA result at agreement with the experimental results (Luo 2008). This follows that the open shear transfer coefficient is lower than its closed counterpart. However, due to the bridging effect of steel fibre (SF), reinforced concrete beam consisting of SF was expected to have higher shear transfer coefficients than those without SF. Thus, the present study examined the effect of open/closed shear transfer

coefficients of 0.35/0.90 and 0.35/0.95 for the NAC, RAC, and BAC beams and 0.40/0.95 and 0.4/1.0 for the SFRRAC beam. The FE model results correlated with those of the experiments for the reinforced concrete beams (without SF) when the open and closed shear transfer coefficient of 0.35 and 0.90 respectively were used (Table 5.3). While shear transfer coefficients of 0.40 and 0.95 performed better for the SFRRAC beam, it was also found that the use of 0.35 and 0.95 coefficients resulted in an incomplete analysis with error message.

Table 5.3: Effect of shear transfer coefficients in the FE model.

Mix ID	β_o	β_c	Ultimate load (kN)		Maximum stress in rebar (MPa)
			FEA	Expt.	
NAC	0.35	0.90	62.64	63.72	558.05
	0.35	0.95	62.54		557.54
RAC	0.35	0.90	60.08	59.71	528.43
	0.35	0.95	57.04		514.13
SFRRAC	0.40	0.95	63.17	69.04	557.22
	0.40	1.00	63.13		556.98
BAC	0.35	0.90	63.15	63.43	556.45
	0.35	0.95	63.07		555.93

Note: β_o and β_c are open and closed shear transfer coefficients respectively.

5.5.3 Prediction of Ultimate Load for Reinforced Concrete Beams of Early and Matured Ages

The load capacity of the reinforced concrete beams for early and matured ages were predicted using the established model for 28 days concrete strength. Essentially, only the uniaxial crushing stress was replaced in the developed model, in turn, with the 7- and 56-days compressive strength. The FE model results presented in Table 5.4 show that the load capacities of the beams are comparable at the three ages investigated. The ultimate load capacity predicted by the ANSYS model using the 56 days compressive strength was the same with that of 28 days strength for all the beams except for the RAC beam which showed about 7% difference.

Table 5.4: FE model prediction of the load capacity of the beams for early and mature ages strength.

Mix ID	β_o	β_c	Compressive strength (MPa)	Ultimate load, P_{ult} (kN)	$\frac{P_{ult,7}}{P_{ult,28}}$	$\frac{P_{ult,56}}{P_{ult,28}}$
NAC	0.35	0.90	58.6[a]	62.64	1.00	
			66.6[b]	62.64		
			74.8[c]	62.52		1.00
RAC	0.35	0.90	44.8[a]	—	—	
			54.0[b]	60.08		
			55.9[c]	56.03		0.93
SFRRAC	0.40	0.95	52.3[a]	61.34	0.97	
			60.2[b]	63.17		
			64.7[c]	63.39		1.00
BAC	0.35	0.90	54.5[a]	—	—	
			61.7[b]	63.15		
			63.9[c]	63.41		1.00

Note: β_o and β_c are open and closed shear transfer coefficient respectively; [a]7 days compressive strength; [b]28 days compressive strength; [c]56days compressive strength.

Chapter 6

6 CONCLUSIONS AND RECOMMENDATIONS

6.1 Conclusions

The main objective of this study was to determine the flexural performance of reinforced concrete beams prepared with recycled aggregate (RA) and steel fibre (SF). Alongside are other specific objectives set to fully actualize the aim of this research. To this end, five basic mixes were formulated and examined experimentally. The list include: (1) Natural aggregate concrete (NAC) mix consisting entirely of natural aggregate (NA) and designed with the conventional method, (2) Recycled aggregate concrete (RAC) mix comprising of 100% RA and proportioned in the conventional way, (3) Steel fibre-reinforced recycled aggregate concrete (SFRRAC) mix made up of RAC mix plus the optimum SF content, (4) Blended aggregate concrete (BAC) mix containing both normal and recycled aggregates and prepared with the Equivalent mortar volume (EMV) design technique, and (5) Steel fibre-reinforced blended aggregate concrete (SFRBAC) mix constituting of mix 4 and the optimum SF content.

The experimental campaign commenced with adequate characterization of the aggregates, followed by preliminary studies involving the experimental review of two conventional mix design methods and the determination of SF volume ratio suitable for SFRRAC and SFRBAC mixes. Then, the mechanical properties of concrete produced from all the mixes were investigated including hardened density, compressive strength, tensile splitting strength, flexural strength (using a third-point loading system on prisms) and the flexural behaviour (using a four-point loading system) of the concrete. Water absorption capacity of concrete was also assessed. At the end, a numerical analysis was carried out on the concrete beams using ANSYS application software with the aid of a finite element model and the results were compared with those obtained from the experimental program. The following are the conclusions drawn from this research:

- ◊ The specific gravity of RA is generally lower than that of the NA. The difference in the average saturated surface-dry specific gravity of RA and NA was found to be over 14% for the fines and 8.3% for the coarse aggregates, in favour of the NA. This gap is ascribed to the mortar adhering to the RA which is characterised as a lightweight material.
- ◊ Both recycled fine and coarse aggregates have a higher average water absorption capacity than their corresponding NA. While the recycled fine aggregate (RFA) showed a greater absorption (in excess of 92%) relative to its

natural counterpart, the recycled coarse aggregate (RCA) showed up to 86% higher absorption than the comparable natural aggregates. This, again, was caused by the high porosity of RA due to the mortar attached.

- ◊ The experimental and theoretical (obtained using the EMV mix design guidelines) residual mortar content of the RCA were 52% and 37.6% respectively. By the EMV standard, a complete replacement of NCA was not feasible since the theoretical residual mortar content was lower than its equivalent experimental value.
- ◊ The RAC mix developed with the EMV mix design method utilized a lower amount of cement (up to 206kg of cement per m^3 of concrete) to produce concrete with a higher performance relative to that prepared using the American Concrete Institute (ACI) method. Remarkably, with reference to the conventional concrete mix (comprising entirely of NA with a higher cement content of up to 143kg/m^3 of concrete), the EMV mix produced a concrete of comparable characteristics. Hence, the EMV technique is an economical and eco-friendly approach as it reduces carbon footprint.
- ◊ To maintain a similar workability for RAC mixes proportioned with the conventional mix design methods, the EMV approach required a higher amount of superplasticizer. But this was advantageous because the presence of the admixture enabled the transmission of fine particles into the voids created between large particles, thereby improving particles packing density which subsequently increased concrete strength.
- ◊ All concretes containing RA showed a lower density than their comparable NAC, with up to 8% difference. In terms of mix design method, the RAC prepared using the orthodox methods presented up to 7% loss in density compared to that prepared using the EMV recommendations. This follows that an increase in the replacement level of NA reduces the density of the concrete, since in this study, the EMV method involved 60% RA and the orthodox method used 100% RA. Relatively, however, the ACI mix design provisions resulted in 4% less dense RAC than its corresponding DoE method. This was as a consequence of higher aggregate content associated with the mix resulting from the latter.
- ◊ In spite of the concrete composition and design method, the cube compressive strength of all the mixes surpassed the design target strength of 40MPa. But, generally, the conventional concrete showed a higher compressive strength than all the concretes constituting RA. Similarly, the RAC mix designed with the EMV technique showed a superior compressive strength than those developed with its

equivalent traditional methods. Analogous to the density of hardened concrete, the RAC resulting from the ACI design guidelines gave a marginally greater compressive strength relative to that of the DoE approach. This is because, unlike density that depends on the overall mass of the combining concrete ingredients, compressive strength depends mainly on the quality of the paste.

- ◊ In terms of compressive strength of the concrete, the undulated SF performed better than its comparable straight and hooked-ended types made of the same material and dimensional properties. Nonetheless, the contribution of SF to compressive strength of the concrete was dependent on the SF volume ratio as well as mix design method adopted. Also, the results showed that the optimum SF content was influenced by mix design method. Whereas the EMV design principles gave an optimum SF content of 0.5% by volume of concrete, the conventional method gave 1%.
- ◊ Impressively, all RAC mixes produced a higher tensile splitting strength than their corresponding NAC mix regardless of the RA content. More angularity of the RA than the NA was mainly responsible for this result. It should also be stated, that the EMV mix proportioning method provided a better performance than the ACI mix design method with regard to tensile splitting strength of the concrete. The tensile splitting strength for all the mixes investigated was in the range of 7–13% of their cylindrical compressive strength with the NAC and SFRRAC mixes at the lower and upper boundaries, respectively.
- ◊ The impact of SF in the concrete properties was greatest in the tensile splitting strength, however, the extent of influence depended on the mix design mechanism used. While SFRRAC showed 38% higher tensile strength, the SFRBAC gave approximately 10% higher value compared to NAC. But the toughness value for SFRBAC was found greater than that of the SFRRAC and this was as a result of higher aggregate content in the former. Nevertheless, it should be stated, that the main work of SF was to restrict cracking propagation thereby engendering a ductile failure mode.
- ◊ The flexural strength of all the mixes examined was in the range of 7–9% of their cube compressive strength with the RAC and SFRRAC mixes at the lower and upper boundaries respectively and the NAC and BAC mixes both having 8%. In this study, this property of concrete was not adversely affected by both RA and RA content.
- ◊ The flexural behaviour of the reinforced concrete beams showed that the SFRRAC had the highest load bearing capacity of 69kN compared to 63.7kN,

59.7kN, and 63.4kN pulled in by NAC, RAC, and BAC beams respectively. Similar trend was also recorded for the moment capacity of the beams and the results showed that both RA content and the EMV mix design technique were influential. While beams manufactured from other mixes had their first cracks at 20kN load, those of the RAC beam appeared at 15kN.

- ◊ Although the NAC, RAC, and BAC beams showed a similar cracking propagation, the BAC beam had a relatively fewer number and less severe cracks attributed to greater amount of coarse aggregates. On the other hand, the SFRRAC beam had the highest number of cracks but were mostly disjointed due to the bridging effect of the SF. At failure, the BAC and NAC beams showed the least and highest estimated crack width of 1mm and 4mm, respectively. Ductile failure mode was observed for all the beams; however, the presence of SF (in SFRRAC) was of added advantage in this regard. Furthermore, the correlation between the experimental and analytical load-deflection plots was closest for the BAC beam and, visually, it showed a higher resistance to deflection at failure compared to the other beams. The range of neutral axis position estimated from the strain distribution diagram showed a good correlation with that obtained using analytical equation.
- ◊ At all substitution levels of NA with RA, the RAC presented a noticeable higher water absorption capacity than its comparable NAC up to a degree of 45% (at full replacement with RA). This was due to the high absorption capacity of the RA caused by the adhering mortar. However, it is pertinent to mention that the unconventional EMV mix design procedure improved this durability property of concrete. Whereas the NAC made entirely of conventional aggregates had an average of 3.1% water absorption capacity, the BAC exhibited 3.4% leading to a difference of 8.8% between the two mixes.
- ◊ Even though the actual absorption of SFRRAC was 44% higher than that of SFRBAC, their rate of water absorption was the same. Similar trend was also observed for the RAC and BAC. Overall, the presence of RA and SF raised the water absorption capacity of the resulting concretes by up to 49% above their comparable normal concrete produced with virgin aggregates.
- ◊ Finally, the finite element model results showed that at matured ages (28 and 56 days), the behaviour of the reinforced concrete beams subjected to a four-point loading system did not vary substantially and they correlated with the results from the experiments. However, it was found that both shear transfer coefficients and the tangent modulus of steel influenced the finite element analysis (FEA) results.

The parametric study carried out in this research showed that the ANSYS model gave a comparable result with those of the experiments when the open and closed shear transfer coefficients were 0.35 and 0.90 respectively, for the reinforced concretes beams with no SF. Conversely, due to the ability of SF to bridge cracking propagation, the shear transfer coefficients of 0.4 and 0.95 were found adequate for the SFRRAC beam. Following the ANSYS Mechanical APDL 2019 R1 guides which stated that the tangent modulus must not be less than zero or higher than elastic modulus, a tangent modulus of 10500MPa (corresponding to 5% of the elastic modulus for steel) was found satisfactory in the present study.

6.2 Recommendations

The following recommendations are made for future works:

- The use of guesswork for the replacement ratio (say 20%, 30%, 50%, etc. by weight or volume) of NA should be abolished. In other words, any design methods that would not use the properties of the employed aggregates to determine the substitution level with RA, should be discouraged. This is important because the properties of RA vary widely depending on the source (or concrete grade for those sourced from concrete), as a result, the raw material would present different characteristics and perform differently in concrete.
- Using the EMV mix design guidelines, further investigations should be carried out on RAC incorporating RFA using RA from other sources. This is a necessity in promoting this technique which has been proven efficient in a number of studies and towards its global endorsement.
- Future works should investigate the sustainability of the EMV method in multi-recycling (that is, recycling recycled concrete manufactured with the EMV principles, say up to the third generation).
- The extended EMV mix proportioning technique (as applied to the present study) should be investigated more for durability properties of the concrete. This is ideal since the use of recycled fines in concrete is said to be associated with durability issues.
- Further study should be carried out on the SFRBAC considering a range of SF volume ratios, to ascertain a suitable SF content for a more consistent and workable concrete mix.
- Since the effect of SF is more in tensile splitting strength of the concrete, future experiments should consider the optimization of SF using this property of the

concrete instead of compressive strength (which either increases or decreases with SF addition).

- There is a need to develop a computer program for the EMV mixture design, such that as soon as the aggregates are characterized, concrete mix proportions can be attained with a lesser effort.

6.3 Limitation of Study

Delay in the procurement of the concrete rubble was the first factor that limited the extent of concrete properties investigated. The next factor was the breaking down of the freezing and thawing apparatus for several months. As such, the mortar content of the recycled coarse aggregates could not be determined on time, and this is key for the application of the EMV mix design method.

There were also some constraints material-wise. Firstly, because the concrete rubble was not supplied in the desired size, there was the need to crush the chunks in the laboratory at some point to meet the quantity required. Due to time restrictions, such variation in the properties of RA due to different crushing methods, was not accounted for. Secondly, there was a switch of cement brand for just one of the concrete properties investigated. It was inevitable as every effort to purchase the same product proved abortive. The supplier had switched to another brand and dealers were not ready to sell the small amount needed. It should be noted, however, that the compressive strength (which relates to all other mechanical properties of concrete) was determined for all the mixes studied, using the “new” cement. The outcome of the “new” compressive strength is presented in Appendix E. Thirdly, due to the length of steel fibre used in this study, the width of the moulds available in the laboratory were not the most convenient for easy compaction of concrete for the beam specimens. As a consequence, the specimens that did not meet the desired finishing were discarded and a fresh one was cast.

Also, equipment constraints could not enable the determination of elastic modulus of concrete experimentally. Because previous works have not recorded significant success in improving this property for RAC, it would have been more appropriate to validate the experimental results with the codes provisions. Although effort was made twice to measure elastic modulus for concrete in this research using the available equipment, but the results in both attempts were not satisfactory.

Finally, there is no known method to evaluate the mortar content of RFA, as such, the potentials of the raw material may have been either underestimated or overestimated.

6.4 Contribution to Knowledge

This research has made the following contributions to knowledge:

- This is the first work carried out on RAC mix consisting of both recycled coarse and fine aggregates and designed with the EMV technique. This mix proportioning method was developed to incorporate only RCA in concrete, but this study has gone a step further to incorporate recycled fines. The findings show that applying the same replacement ratio appropriate to RCA (obtained using the EMV guidelines) to RFA (of the same source as the coarse aggregates) has no detrimental effects on properties of the resulting concrete.
- There has never been any research conducted on steel fibre-reinforced concrete using the EMV mechanism, hence, this work forms the basis for further studies for future researchers.
- To the best of the writer's knowledge, this work is the first of its kind to apply the EMV mix design method to RA obtained from a precast facilities site. Previous studies utilizing the EMV approach were based on RA obtained from other sources (construction and demolition waste, crushed concrete from laboratory experiments and unused in-situ concrete). According to the findings of this research, precast concrete industries can be sure to re-use their concrete waste in new productions, provided quality control is ensured.
- The results obtained from this study have exposed the need to modify the ACI and DoE codes of practice, especially the latter, if they must be employed for the design of RAC mixes.

References

Abbas, A., Fathifazl, G., Isgor, O.B., Razaqpur, A.G., and Fournier, B. (2007) 'Proposed Method for Determining the Residual Mortar'. *Journal of ASTM Internaltional* 5 (1), 1–12

Abbas, A., Fathifazl, G., Isgor, O.B., Razaqpur, A.G., Fournier, B., and Foo, S. (2009) 'Durability of Recycled Aggregate Concrete Designed with Equivalent Mortar Volume Method'. *Cement and Concrete Composites* [online] 31 (8), 555–563. available from <http://dx.doi.org/10.1016/j.cemconcomp.2009.02.012>

ACI 318R (2014) *ACI 318R-14 Building Code Requirements for Structural Concrete*.

ACI Committee 211 (2009) *ACI 211 1-91 Standard Practice for Selecting Proportions for Normal, Heavyweight, and Mass Concrete*.

Afroughsabet, V., Biolzi, L., and Ozbakkaloglu, T. (2017) 'Influence of Double Hooked-End Steel Fibers and Slag on Mechanical and Durability Properties of High Performance Recycled Aggregate Concrete'. *Composite Structures* [online] 181, 273–284. available from <http://dx.doi.org/10.1016/j.compstruct.2017.08.086>

Ajdukiewicz, A. and Kliszczewicz, A. (2002) 'Influence of Recycled Aggregates on Mechanical Properties of HS/HPC'. *Cement and Concrete Composites* 24 (2), 269–279

Akbarnezhad, A., Ong, K.C.G., Zhang, M.H., Tam, C.T., and Foo, T.W.J. (2011) 'Microwave-Assisted Beneficiation of Recycled Concrete Aggregates'. *Construction and Building Materials* [online] 25 (8), 3469–3479. available from <http://dx.doi.org/10.1016/j.conbuildmat.2011.03.038>

Akinkurolere, O.O. (2010) 'Experimental Investigation on the Influence of Steel Fiber on the Compressive and Tensile Strength of Recycled Aggregate Concrete'. in *Journal of Engineering and Applied Sciences* [online] vol. 5 (4). 264–268. available from <http://www.medwelljournals.com/abstract/?doi=jeasci.2010.264.268>

Altun, F., Haktanir, T., and Ari, K. (2007) 'Effects of Steel Fiber Addition on Mechanical Properties of Concrete and RC Beams'. *Construction and Building Materials* 21 (3), 654–661

American Concrete Pavement Association (2009) 'Recycling Concrete Pavements'. *ENGINEERING BULLETIN* [online] 1–79. available from <www.acpa.org/wp-

content/uploads/2019/02/EB043P.pdf>

Andreu, G. and Miren, E. (2014) 'Experimental Analysis of Properties of High Performance Recycled Aggregate Concrete'. *Construction and Building Materials* [online] 52, 227–235. available from <http://dx.doi.org/10.1016/j.conbuildmat.2013.11.054>

Anike, E., Saidani, M., Ganjian, E., Tyrer, M., and Olubanwo, A. (2020a) 'Evaluation of Conventional and Equivalent Mortar Volume Mix Design Methods for Recycled Aggregate Concrete'. *Materials and Structures* [online] 53 (1), 22. available from <http://link.springer.com/10.1617/s11527-020-1457-3>

Anike, E., Saidani, M., Olubanwo, A., Tyrer, M., and Ganjian, E. (2020b) 'Effect of Mix Design Methods on the Mechanical Properties of Steel Fibre-Reinforced Concrete Prepared with Recycled Aggregates from Precast Waste'. *Structures* [online] 27, 664–672. available from <https://linkinghub.elsevier.com/retrieve/pii/S2352012420302502>

Anike, E.E., Saidani, M., Ganjian, E., Tyrer, M., and Olubanwo, A.O. (2019) 'The Potency of Recycled Aggregate in New Concrete: A Review'. *Construction Innovation* 19 (4), 594–613

ANSYS (2019) 'ANSYS Mechanical APDL 2019 R1'. in *ANSYS Inc.* U.S.A

Arezoumandi, M., Drury, J., Volz, J.S., and Khayat, K.H. (2015a) 'Effect of Recycled Concrete Aggregate Replacement Level on Shear Strength of Reinforced Concrete Beams'. *ACI Materials Journal* [online] 112 (4). available from <http://www.concrete.org/Publications/InternationalConcreteAbstractsPortal.aspx?m=details&i=51687766>

Arezoumandi, M., Smith, A., Volz, J.S., and Khayat, K.H. (2015b) 'An Experimental Study on Flexural Strength of Reinforced Concrete Beams with 100% Recycled Concrete Aggregate'. *Engineering Structures* [online] 88, 154–162. available from <http://dx.doi.org/10.1016/j.engstruct.2015.01.043>

Arezoumandi, M., Smith, A., Volz, J.S., and Khayat, K.H. (2014) 'An Experimental Study on Shear Strength of Reinforced Concrete Beams with 100% Recycled Concrete Aggregate'. *Construction and Building Materials* [online] 53, 612–620. available from <http://dx.doi.org/10.1016/j.conbuildmat.2013.12.019>

ASTM C127 − 15 (2015) *Standard Test Method for Relative Density (Specific Gravity) and Absorption of Coarse Aggregate*.

ASTM C128 (2015) *Standard Test Method for Relative Density (Specific Gravity) and Absorption of Fine Aggregate*.

ASTM C136 (2014) *Standard Test Method for Sieve Analysis of Fine and Coarse Aggregates*.

ASTM C1609/C1609M − 12 (2012) *Standard Test Method for Flexural Performance of Fiber-Reinforced Concrete (Using Beam With Third-Point Loading)*.

ASTM C29/C29M-09 (2009) *Standard Test Method for Bulk Density (" Unit Weight ") and Voids in Aggregate*.

ASTM C672/C672M − 12 (2012) *Standard Test Method for Scaling Resistance of Concrete Surfaces Exposed to Deicing Chemicals*.

ASTM C702/C702M − 18 (2018) *Standard Practice for Reducing Samples of Aggregate to Testing Size*. vol. i

ASTM C78/C78M − 18 (2018) *Standard Test Method for Flexural Strength of Concrete (Using Simple Beam with Third-Point Loading)*.

Aziz, A.H. and Ghailan, D.B. (2007) 'Shear Behavior of RC Beams with Full or Partial SFRC Shear Span'. *Journal of Engineering and Development* [online] 11 (2), 30–45. available from <https://www.iasj.net/iasj?func=fulltext&aId=10106>

Băetu, S. and Ciongradi, I.-P. (2011) 'NONLINEAR FINITE ELEMENT ANALYSIS OF REINFORCED CONCRETE SLIT WALLS WITH ANSYS (I)'. *BULETINUL INSTITUTULUI POLITEHNIC DIN IAŞI* LVII (Lxi)

Barbudo, A., de Brito, J., Evangelista, L., Bravo, M., and Agrela, F. (2013) 'Influence of Water-Reducing Admixtures on the Mechanical Performance of Recycled Concrete'. *Journal of Cleaner Production* 59, 93–98

Behera, M., Bhattacharyya, S.K., Minocha, A.K., Deoliya, R., and Maiti, S. (2014) 'Recycled Aggregate from C&D Waste & Its Use in Concrete - A Breakthrough towards Sustainability in Construction Sector: A Review'. *Construction and Building Materials* [online] 68, 501–516. available from <http://dx.doi.org/10.1016/j.conbuildmat.2014.07.003>

Belin, P., Habert, G., Thiery, M., and Roussel, N. (2013) 'Cement Paste Content and Water Absorption of Recycled Concrete Coarse Aggregates'. *Materials and Structures/Materiaux et Constructions* 47 (9), 1451–1465

Beltran, M.G., Barbudo, A., Agrela, F., Galvin, A.P., and Jimenez, J.R. (2014) *Effect of Cement Addition on the Properties of Recycled Concretes to Reach Control Concretes Strengths*. 79, 124–133

Biolzi, L. and Cattaneo, S. (2017) 'Response of Steel Fiber Reinforced High Strength Concrete Beams: Experiments and Code Predictions'. *Cement and Concrete Composites* [online] 77, 1–13. available from <http://dx.doi.org/10.1016/j.cemconcomp.2016.12.002>

Boulekbache, B., Hamrat, M., Chemrouk, M., and Amziane, S. (2016) 'Flexural Behaviour of Steel Fibre-Reinforced Concrete under Cyclic Loading'. *Construction and Building Materials* [online] 126, 253–262. available from <http://dx.doi.org/10.1016/j.conbuildmat.2016.09.035>

Boulekbache, B., Hamrat, M., Chemrouk, M., and Amziane, S. (2012) 'Influence of Yield Stress and Compressive Strength on Direct Shear Behaviour of Steel Fibre-Reinforced Concrete'. *Construction and Building Materials* [online] 27 (1), 6–14. available from <http://dx.doi.org/10.1016/j.conbuildmat.2011.07.015>

Boulekbache, B., Hamrat, M., Chemrouk, M., and Amziane, S. (2010) 'Flowability of Fibre-Reinforced Concrete and Its Effect on the Mechanical Properties of the Material'. *Construction and Building Materials* [online] 24 (9), 1664–1671. available from <http://dx.doi.org/10.1016/j.conbuildmat.2010.02.025>

Bravo, M., De Brito, J., Pontes, J., and Evangelista, L. (2015a) 'Mechanical Performance of Concrete Made with Aggregates from Construction and Demolition Waste Recycling Plants'. *Journal of Cleaner Production* [online] 99, 59–74. available from <http://dx.doi.org/10.1016/j.jclepro.2015.03.012>

Bravo, M., De Brito, J., Pontes, J., and Evangelista, L. (2015b) 'Durability Performance of Concrete with Recycled Aggregates from Construction and Demolition Waste Plants'. *Construction and Building Materials* [online] 77, 357–369. available from <http://dx.doi.org/10.1016/j.conbuildmat.2014.12.103>

BRE Digest 433 (1998) 'Recycled Aggregates'. *BRE Digest 433, CI/SfB p(T6). Watford, UK: Building Research Establishment* (November)

De Brito, J. and Silva, R. V (2016) ‘Current Status on the Use of Recycled Aggregates in Concrete: Where Do We Go from Here?’ *RILEM Technical Letters* 1, 1–5

BS 8500-2 (2006) *Concrete Complementary British Standard to BS EN 206 Part 1 -Part 2: Specification for Constituent Materials and Concrete.*

BS 8500-1:2015+A2 (2019) *Concrete- Complementary British Standard to BS EN 206-1; Part 1:Method of Specifying and Guidance for the Specifier*.

BS EN 12390-2 (2009) *Testing Hardened Concrete- Part 2: Making and Curing Specimens for Strength Tests*. vol. 3

BS EN 12390-3 (2009) *Testing Hardened Concrete- Part3: Compressive Strength of Test Specimens*. 3 (1), 1–19

BS EN 12390-6 (2009) *Testing Hardened Concrete- Part 6: Tensile Splitting Strength of Test Specimens*. vol. 3

BS EN 12390-7 (2009) *Testing Hardened Concrete Part 7: Density of Hardened Concrete*. vol. 53

BS EN 12620:2002+A1 (2008) *Aggregates for Concrete*. vol. 3

BS EN 197-1 (2011) *Part 1: Composition, Specifications and Conformity Criteria for Common Cements*.

BS EN 206:2013+A1 (2016) *Concrete — Specification , Performance , Production and Conformity*.

BS EN 934-2:2009 +A1:2012 (2012) *Admixtures for Concrete , Mortar and Grout: Part 2: Concrete Admixtures — Part 2: Concrete Admixtures — Definitions, Requirements, Conformity, Definitions, Requirements, Conformity, Marking and Labelling Marking*.

BS1881-122 (2011) *BSI Standards Publication Testing Concrete Part 122 : Method for Determination of Water Absorption*.

Buratti, N. and Mazzotti, C. (2012) ‘Effects of Different Types and Dosages of Fibres on the Long Term Behaviour of Fibre-Reinforced Self-Compacting Concrete.’ in *Proceedings of 8th RILEM Inertnational Symposium on Fibre Reinforced Concrete,RILEM PRO88*. held 2012 at Guimarães, Portugal. 715–725

Butler, L., West, J.S., and Tighe, S.L. (2013) 'Effect of Recycled Concrete Coarse Aggregate from Multiple Sources on the Hardened Properties of Concrete with Equivalent Compressive Strength'. *Construction and Building Materials* [online] 47, 1292–1301. available from <http://dx.doi.org/10.1016/j.conbuildmat.2013.05.074>

Chakradhara Rao, M., Bhattacharyya, S.K., and Barai, S. V. (2011) 'Behaviour of Recycled Aggregate Concrete under Drop Weight Impact Load'. *Construction and Building Materials* [online] 25 (1), 69–80. available from <http://dx.doi.org/10.1016/j.conbuildmat.2010.06.055>

Van Chanh, N. (2005) 'Steel Fiber Reinforced Concrete'. *JSCE-VIFCEA Joint Seminar on Concrete Engineering* [online] (1), 108–116. available from <http://www.jsce.or.jp/committee/concrete/e/newsletter/newsletter05/JSCE-VIFCEA Joint Seminar Papers.htm>

Chen, G.M., He, Y.H., Yang, H., Chen, J.F., and Guo, Y.C. (2014) 'Compressive Behavior of Steel Fiber Reinforced Recycled Aggregate Concrete after Exposure to Elevated Temperatures'. *Construction and Building Materials* 71, 1–15

Choi, W.-C. and Yun, H.-D. (2012) 'Compressive Behavior of Reinforced Concrete Columns with Recycled Aggregate under Uniaxial Loading'. *Engineering Structures* [online] 41, 285–293. available from <http://linkinghub.elsevier.com/retrieve/pii/S0141029612001629>

Choi, W.-C., Yun, H.-D., and Kim, S.-W. (2012) 'Flexural Performance of Reinforced Recycled Aggregate Concrete Beams'. *Magazine of Concrete Research* [online] 64 (9), 837–848. available from <http://www.icevirtuallibrary.com/doi/10.1680/macr.11.00018>

Corinaldesi, V. (2011) 'Structural Concrete Prepared with Coarse Recycled Concrete Aggregate: From Investigation to Design'. *Advances in Civil Engineering* 2011, 1–7

Corinaldesi, V. and Moriconi, G. (2009) 'Influence of Mineral Additions on the Performance of 100% Recycled Aggregate Concrete'. *Construction and Building Materials* [online] 23 (8), 2869–2876. available from <http://dx.doi.org/10.1016/j.conbuildmat.2009.02.004>

Correia, J.R., De Brito, J., and Pereira, A.S. (2006) 'Effects on Concrete Durability of Using Recycled Ceramic Aggregates'. *Materials and Structures/Materiaux et Constructions* 39 (2), 169–177

Cucchiara, C., La Mendola, L., and Papia, M. (2004) 'Effectiveness of Stirrups and Steel Fibres as Shear Reinforcement'. *Cement and Concrete Composites* 26 (7), 777–786

Damtoft, J.S., Lukasik, J., Herfort, D., Sorrentino, D., and Gartner, E.M. (2008) 'Sustainable Development and Climate Change Initiatives'. *Cement and Concrete Research* 38 (2), 115–127

Dhir, R.K., Limbachiya, M.C., and Leelawat, T. (1999) 'Suitability of Recycled Concrete Aggregate for Use in BS 5328 Designated Mixes'. in *Proc. Inst. Civ. Eng., Struct. Build.* held 1999. 257–274

DIN 4226-100 (2002) *Aggregate for Mortar and Concrete: Recycled Aggregates.*

Dinh, H.H., Parra-Montesinos, G.J., and Wight, J.K. (2010) 'No Title'. *ACI Structural Journal* 107 (5), 597–606

Domingo-Cabo, A., Lázaro, C., López-Gayarre, F., Serrano-López, M.A., Serna, P., and Castaño-Tabares, J.O. (2009) 'Creep and Shrinkage of Recycled Aggregate Concrete'. *Construction and Building Materials* [online] 23 (7), 2545–2553. available from <http://dx.doi.org/10.1016/j.conbuildmat.2009.02.018>

Duan, Z.H. and Poon, C.S. (2014) 'Properties of Recycled Aggregate Concrete Made with Recycled Aggregates with Different Amounts of Old Adhered Mortars'. *Materials and Design* [online] 58, 19–29. available from <http://dx.doi.org/10.1016/j.matdes.2014.01.044>

Ebrahim Abu El-Maaty Behiry, A. (2013) 'Utilization of Cement Treated Recycled Concrete Aggregates as Base or Subbase Layer in Egypt'. *Ain Shams Engineering Journal* 4 (4), 661–673

EPA (2000) *Office of Solid Waste and Emergency Response. Building Savings: Strategies for Waste Reduction of Construction and Demolition Debris from Buildings. USA: The U.S. Environmental Protection Agency (EPA).*

Erdem, S., Dawson, A.R., and Thom, N.H. (2011) 'Microstructure-Linked Strength Properties and Impact Response of Conventional and Recycled Concrete Reinforced with Steel and Synthetic Macro Fibres'. *Construction and Building Materials* 25 (10), 4025–4036

ETC/SCP (2009) 'EU as a Recycling Society. Present Recycling Levels of Municipal

Waste and Construction & Demolition Waste in the EU'. *European Topic Centre on Resource and Waste Management* [online] (April), 1–73. available from <http://scp.eionet.europa.eu/publications/wp2009_2/wp/WP2009_2>

Etxeberria, M., Marí, A.R., and Vázquez, E. (2007) 'Recycled Aggregate Concrete as Structural Material'. *Materials and Structures* [online] 40 (5), 529–541. available from <http://www.springerlink.com/index/10.1617/s11527-006-9161-5>

Etxeberria, M., Vázquez, E., Marí, A., and Barra, M. (2007) 'Influence of Amount of Recycled Coarse Aggregates and Production Process on Properties of Recycled Aggregate Concrete'. *Cement and Concrete Research* 37 (5), 735–742

Evangelista, L. and de Brito, J. (2007) 'Mechanical Behaviour of Concrete Made with Fine Recycled Concrete Aggregates'. *Cement and Concrete Composites* 29 (5), 397–401

Fan, C.C., Huang, R., Hwang, H., and Chao, S.J. (2016) 'Properties of Concrete Incorporating Fine Recycled Aggregates from Crushed Concrete Wastes'. *Construction and Building Materials* [online] 112, 708–715. available from <http://dx.doi.org/10.1016/j.conbuildmat.2016.02.154>

Fathifazl, G., Abbas, A., Razaqpur, A.G., Isgor, O.B., Fournier, B., and Foo, S. (2009a) 'New Mixture Proportioning Method for Concrete Made with Coarse Recycled Concrete Aggregate'. *Journal of Materials in Civil Engineering* [online] 21 (10), 601–611. available from <http://ascelibrary.org/doi/10.1061/%28ASCE%290899-1561%282009%2921%3A10%28601%29>

Fathifazl, G., Razaqpur, A.G., Isgor, O.B., Abbas, A., Fournier, B., and Foo, S. (2009b) 'Flexural Performance of Steel-Reinforced Recycled Concrete Beams'. *ACI Structural Journal* 106 (6), 858–867

Ferreira, L., de Brito, J., and Barra, M. (2011) 'Influence of the Pre-Saturation of Recycled Coarse Concrete Aggregates on Concrete Properties'. *Magazine of Concrete Research* [online] 63 (8), 617–627. available from <http://www.icevirtuallibrary.com/doi/10.1680/macr.2011.63.8.617>

FHWA (2005) 'Transportation Applications of Recycled Concrete Aggregate-FHWA State of the Practice National Review September 2004'. in *U.S. Department of Transportation*. vol. 39 (5). 27–29

Freedonia (2012) ‘World Construction Aggregates - Industry Study with Forecasts for 2015 & 2020’. *The Freedonia Group* [online] 6. available from <https://www.freedoniagroup.com/brochure/28xx/2838smwe.pdf>

Freedonia (2007) ‘World Construction Aggregates -Industry Study with Forecasts for 2011 and 2016’. *The Freedonia Group, USA* 6

Gagan and Agam (2015) ‘FLEXURAL BEHAVIOR OF REINFORCED RECYCLED CONCRETE BEAMS: A REVIEW’. *International Journal of Research in Engineering and Technology* 04 (1), 1–6

Gameiro, F., De Brito, J., and Correia da Silva, D. (2014) ‘Durability Performance of Structural Concrete Containing Fine Aggregates from Waste Generated by Marble Quarrying Industry’. *Engineering Structures* [online] 59, 654–662. available from <http://dx.doi.org/10.1016/j.engstruct.2013.11.026>

Gao, D., Zhang, L., and Nokken, M. (2017a) ‘Compressive Behavior of Steel Fiber Reinforced Recycled Coarse Aggregate Concrete Designed with Equivalent Cubic Compressive Strength’. *Construction and Building Materials* [online] 141, 235–244. available from <http://dx.doi.org/10.1016/j.conbuildmat.2017.02.136>

Gao, D., Zhang, L., and Nokken, M. (2017b) ‘Mechanical Behavior of Recycled Coarse Aggregate Concrete Reinforced with Steel Fibers under Direct Shear’. *Cement and Concrete Composites* [online] 79, 1–8. available from <http://dx.doi.org/10.1016/j.cemconcomp.2017.01.006>

Gettu, R., Zerbino, R., and Jose, S. (2017) ‘Factors Influencing Creep of Cracked Fibre Reinforced Concrete: What We Think We Know & What We Do Not Know.’ in *Creep Behaviour in Cracked Sections of Fibre Reinforced Concrete*. RILEM Book. ed. by Serna, P., Llano-Torre, A., Cavalaro, S. vol. 14. Dordrecht: Springer

Gokce, A., Nagataki, S., Saeki, T., and Hisada, M. (2004) ‘Freezing and Thawing Resistance of Air-Entrained Concrete Incorporating Recycled Coarse Aggregate: The Role of Air Content in Demolished Concrete’. *Cement and Concrete Research* 34 (5), 799–806

Graeff, Â.G. (2011) *Long-Term Performance of Recycled Steel Fibre Reinforced Concrete for Pavement Applications*. University of Sheffield Sheffield

Gu, X., Jin, X., and Zhou, Y. (2016) *Basic Principles of Concrete Structures*.

Guo, H., Shi, C., Guan, X., Zhu, J., Ding, Y., Ling, T.C., Zhang, H., and Wang, Y. (2018) 'Durability of Recycled Aggregate Concrete – A Review'. *Cement and Concrete Composites* [online] 89, 251–259. available from <https://doi.org/10.1016/j.cemconcomp.2018.03.008>

Gupta, P.K. and Bhatia, R. (2013) 'Study of Engineering Properties of Recycled Concrete Aggregate Concrete'. *I-Manager's Journal on Structural Engineering* 2 (1), 20–27

Hansen, T.C. (1992) *Recycling of Demolished Concrete and Masonry. E & FN Spon, London, UK*.

Hansen, T.C. (1986) 'Recycled Aggregates and Recycled Aggregate Concrete Second State-of-the-Art Report Developments 1945-1985'. *Materials and Structures* 19 (3), 201–246

Hansen, T.C. and Narud, H. (1983) 'Strength of Recycled Concrete Made from Crushed Concrete Coarse Aggregate'. *Concrete International* 79–83

Heeralal, M., Kumar Rathish, P., and Rao, Y. V. (2009) 'Flexural Fatigue Characteristics of Steel Fiber Reinforced Recycled Aggregate Concrete (SFRRAC)'. *Architecture and Civil Engineering* [online] 7 (1), 19–33. available from <http://www.doiserbia.nb.rs/Article.aspx?ID=0354-46050901019H>

Huda, S.B. and Alam, M.S. (2014) 'Mechanical Behavior of Three Generations of 100% Repeated Recycled Coarse Aggregate Concrete'. *Construction and Building Materials* [online] 65, 574–582. available from <http://dx.doi.org/10.1016/j.conbuildmat.2014.05.010>

Hunger, M. and Brouwers, H.J.H. (2009) 'Flow Analysis of Water-Powder Mixtures: Application to Specific Surface Area and Shape Factor'. *Cement and Concrete Composites* [online] 31 (1), 39–59. available from <http://dx.doi.org/10.1016/j.cemconcomp.2008.09.010>

Ibrahim, M. (2016) 'Estimating the Sustainability Returns of Recycling Construction Waste from Building Projects'. *Sustainable Cities and Society* [online] 23, 78–93. available from <http://dx.doi.org/10.1016/j.scs.2016.03.005>

Ignjatović, I.S., Marinković, S.B., Mišković, Z.M., and Savić, A.R. (2013) 'Flexural Behavior of Reinforced Recycled Aggregate Concrete Beams under Short-Term Loading'. *Materials and Structures* [online] 46 (6), 1045–1059. available from

<http://link.springer.com/10.1617/s11527-012-9952-9>

Ismail, S. and Ramli, M. (2013) 'Engineering Properties of Treated Recycled Concrete Aggregate (RCA) for Structural Applications'. *Construction and Building Materials* [online] 44, 464–476. available from <http://dx.doi.org/10.1016/j.conbuildmat.2013.03.014>

de Juan, M.S. and Gutiérrez, P.A. (2009) 'Study on the Influence of Attached Mortar Content on the Properties of Recycled Concrete Aggregate'. *Construction and Building Materials* [online] 23 (2), 872–877. available from <http://dx.doi.org/10.1016/j.conbuildmat.2008.04.012>

Kachlakev, D., Miller, T., Yim, S., Chansawat, K., and Potisuk, T. (2001) *Finite Element Modeling of Reinforced Concrete Structures Strengthened with FRP Lamiantes*. vol. SPR 316

Kang, S.-T., Lee, Y., Park, Y.-D., and Kim, J.-K. (2010) 'Tensile Fracture Properties of an Ultra High Performance Fiber Reinforced Concrete (UHPFRC) with Steel Fiber'. *Composite Structures* [online] 92 (1), 61–71. available from <http://linkinghub.elsevier.com/retrieve/pii/S0263822309002323>

Kang, T.H.-K., Kim, W., Kwak, Y.-K., and Hong, S.-G. (2014) 'Flexural Testing of Reinforced Concrete Beams with Recycled Concrete Aggregates'. *ACI Structural Journal* [online] 111 (3). available from <http://www.concrete.org/Publications/InternationalConcreteAbstractsPortal.aspx?m=details&i=51686622>

Kang, W.-H., Ramesh, R.B., Mirza, O., Senaratne, S., Tam, V., and Wigg, D. (2017) 'Reliability Based Design of RC Beams With Recycled Aggregate and Steel Fibres'. *Structures* [online] 11 (March), 135–145. available from <http://dx.doi.org/10.1016/j.istruc.2017.05.002>

Katz, A. (2004) 'Treatments for the Improvement of Recycled Aggregate'. *Journal of Materials in Civil Engineering* [online] 16 (6), 597–603. available from <http://ascelibrary.org/doi/10.1061/%28ASCE%290899-1561%282004%2916%3A6%28597%29>

Katz, A. (2003) 'Properties of Concrete Made with Recycled Aggregate from Partially Hydrated Old Concrete'. *Cement and Concrete Research* 33 (5), 703–711

Khatib, J.M. (2005) *Properties of Concrete Incorporating Fine Recycled Aggregate*. 35 (June 2004), 763–769

Kisku, N., Joshi, H., Ansari, M., Panda, S.K., Nayak, S., and Dutta, S.C. (2012) 'A Critical Review and Assessment for Usage of Recycled Aggregate as Sustainable Construction Material'. *Construction and Building Materials* [online] 131, 721–740. available from <http://dx.doi.org/10.1016/j.conbuildmat.2016.11.029>

Kou, S.C. and Poon, C.S. (2015) 'Effect of the Quality of Parent Concrete on the Properties of High Performance Recycled Aggregate Concrete'. *Construction and Building Materials* [online] 77, 501–508. available from <http://dx.doi.org/10.1016/j.conbuildmat.2014.12.035>

Kou, S.C. and Poon, C.S. (2012) 'Enhancing the Durability Properties of Concrete Prepared with Coarse Recycled Aggregate'. *Construction and Building Materials* [online] 35, 69–76. available from <http://dx.doi.org/10.1016/j.conbuildmat.2012.02.032>

Kou, S.C., Poon, C.S., and Chan, D. (2007) 'Influence of Fly Ash on the Properties of Recycled Coarse Aggregate Concrete'. *JOURNAL OF MATERIALS IN CIVIL ENGINEERING* 19 (9), 709–717

Kou, S.C., Poon, C.S., and Etxeberria, M. (2014) 'Residue Strength, Water Absorption and Pore Size Distributions of Recycled Aggregate Concrete after Exposure to Elevated Temperatures'. *Cement and Concrete Composites* [online] 53, 73–82. available from <http://dx.doi.org/10.1016/j.cemconcomp.2014.06.001>

Kumar, P.S., Mannan, M.A., Kurian, V.J., and Achuytha, H. (2007) 'Investigation on the Flexural Behaviour of High-Performance Reinforced Concrete Beams Using Sandstone Aggregates'. *Building and Environment* 42, 2622–2629

Kurad, R., Silvestre, J.D., de Brito, J., and Ahmed, H. (2017) 'Effect of Incorporation of High Volume of Recycled Concrete Aggregates and Fly Ash on the Strength and Global Warming Potential of Concrete'. *Journal of Cleaner Production* 166, 485–502

Kurda, R., Brito, J. de, and Silvestre, J.D. (2017) 'Influence of Recycled Aggregates and High Contents of Fly Ash on Concrete Fresh Properties'. *Journal of Cleaner Production* [online] 84, 198–213. available from <http://dx.doi.org/10.1016/j.jclepro.2015.10.109>

Kwan, W.H., Ramli, M., Kam, K.J., and Sulieman, M.Z. (2012) 'Influence of the Amount of Recycled Coarse Aggregate in Concrete Design and Durability Properties'. *Construction and Building Materials* [online] 26 (1), 565–573. available from <http://dx.doi.org/10.1016/j.conbuildmat.2011.06.059>

Lee, M.K. and Barr, B.I.G. (2004) 'An Overview of the Fatigue Behaviour of Plain and Fibre Reinforced Concrete'. *Cement and Concrete Composites* 26 (4), 299–305

Leite, M.B. (2001) *Evaluation of the Mechanical Properties of Concrete Made with Construction and Demolition Waste Recycled Aggregates (in Portuguese). PhD Thesis in Civil Engineering, School of Engineering of the Federal University of Rio Grande Do Sul, Porto Alegre.*

Li, J., Xiao, H., and Zhou, Y. (2009) 'Influence of Coating Recycled Aggregate Surface with Pozzolanic Powder on Properties of Recycled Aggregate Concrete'. *Construction and Building Materials* [online] 23 (3), 1287–1291. available from <http://dx.doi.org/10.1016/j.conbuildmat.2008.07.019>

Liang, Y.C., Ye, Z.M., Vernerey, F., and Xi, Y. (2013) 'Development of Processing Methods to Improve Strength of Concrete with 100% Recycled Coarse Aggregate.' *J. Mater. Civil Eng.* 27 (5)

Lim, D.H. and Oh, B.H. (1999) 'Experimental and Theoretical Investigation on the Shear of Steel Fibre Reinforced Concrete Beams'. *Engineering Structures* 21 (10), 937–944

Limbachiya, M.C., Leelawat, T., and Dhir, R.K. (2000) 'Use of Recycled Concrete Aggregate in High-Strength Concrete'. *Materials and Structures* 33 (November), 574–580

Liu, J. and Chen, B. (2008) 'Mechanical Properties of High Strength Concrete with Field-Demolished Concrete as Aggregates'. *Journal of ASTM International* 5 (10), 1–8

Liu, K., Yan, J., Hu, Q., Sun, Y., and Zou, C. (2016) 'Effects of Parent Concrete and Mixing Method on the Resistance to Freezing and Thawing of Air-Entrained Recycled Aggregate Concrete'. *Construction and Building Materials* [online] 106, 264–273. available from <http://dx.doi.org/10.1016/j.conbuildmat.2015.12.074>

Luo, R. (2008) 'Values of Shear Transfer Coefficients of Concrete Element Solid65 in Ansys'. *Journal of Jiangsu University(Natural Science Edition)* [online] 29 (2), 169–

172. available from <http://zzs.ujs.edu.cn/xbzkb/EN/10.3969/j.issn.1671-7775.2008.02.019>

Mackay, J. and Trottier, J.F. (2004) 'Post-Crack Behavior of Steel and Synthetic FRC under Flexural Creep'. in *Shotcrete, Proceedings 2nd International Conference. on Engineering*. held 2004 at Cairns, Australia. 183–192

Malešev, M., Radonjanin, V., and Broćeta, G. (2014) 'The Properties of Recycled Aggregate Concrete'. *Contemporary Materials* 2, 239–249

Malešev, M., Radonjanin, V., and Marinković, S. (2010) 'Recycled Concrete as Aggregate for Structural Concrete Production'. *Sustainability* 2 (5), 1204–1225

Markovic, I. (2006) *High-Performance Hybrid-Fibre Concrete: Development and Utilisation*. TU Delft, Delft University of Technology

Matias, D., Brito, J. De, Rosa, A., and Pedro, D. (2014) *Durability of Concrete with Recycled Coarse Aggregates : Influence of Superplasticizers*. 26 (7), 1–5

Matias, D., De Brito, J., Rosa, A., and Pedro, D. (2013) 'Mechanical Properties of Concrete Produced with Recycled Coarse Aggregates - Influence of the Use of Superplasticizers'. *Construction and Building Materials* [online] 44, 101–109. available from <http://dx.doi.org/10.1016/j.conbuildmat.2013.03.011>

Megson, T.H.G. (2014) *Structural and Stress Analysis*. 3rd edn. Oxford: Elsevier Ltd.

Michels, J., Christen, R., and Waldmann, D. (2013) 'Experimental and Numerical Investigation on Postcracking Behavior of Steel Fiber Reinforced Concrete'. *Engineering Fracture Mechanics* [online] 98 (1), 326–349. available from <http://dx.doi.org/10.1016/j.engfracmech.2012.11.004>

Moosberg-Bustnes, H., Lagerblad, B., and Forssberg, E. (2004) 'The Function of Fillers in Concrete'. *Materials and Structures/Materiaux et Constructions* 37 (266), 74–81

Mulder, E., de Jong, T.P.R., and Feenstra, L. (2007) 'Closed Cycle Construction: An Integrated Process for the Separation and Reuse of C&D Waste'. *Waste Management* 27 (10), 1408–1415

Nováková, I. and Mikulica, K. (2016) 'Properties of Concrete with Partial Replacement of Natural Aggregate by Recycled Concrete Aggregates from Precast Production'. *Procedia Engineering* 151, 360–367

NSCS (2010) *National Structural Concrete Specification for Building Construction. Technical Committee*. 4th editio.

Ogbologugo, U. (2018) *Investigating the Structural Performance of a New Type of Foamed Lightweight Cementitious Material*. [online] available from <https://curve.coventry.ac.uk/open/items/f8bdcd1b-cb33-4644-8c77-1e9a524f0457/1/Binder1.pdf>

Oikonomou, N.D. (2005) 'Recycled Concrete Aggregates'. *Cement and Concrete Composites* [online] 27 (2), 315–318. available from <https://www.sciencedirect.com/science/article/pii/S095894650400037X?via%3Dihub> [23 March 2018]

Olorunsogo, F.T. and Padayachee, N. (2002) 'Performance of Recycled Aggregate Concrete Monitored by Durability Indexes'. *Cement and Concrete Research* 32 (2), 179–185

Omary, S., Ghorbel, E., and Wardeh, G. (2016) 'Relationships between Recycled Concrete Aggregates Characteristics and Recycled Aggregates Concretes Properties'. *Construction and Building Materials* [online] 108, 163–174. available from <http://dx.doi.org/10.1016/j.conbuildmat.2016.01.042>

Ossa, A., García, J.L., and Botero, E. (2016) 'Use of Recycled Construction and Demolition Waste (CDW) Aggregates: A Sustainable Alternative for the Pavement Construction Industry'. *Journal of Cleaner Production* [online] 135, 379–386. available from <http://dx.doi.org/10.1016/j.jclepro.2016.06.088>

Otsuki, N., Miyazato, S.I., and Yodsudjai, W. (2003) 'Influence of Recycled Aggregate on Interfacial Transition Zone, Strength, Chloride Penetration and Carbonation of Concrete'. *Journal of Materials in Civil Engineering* 15 (5), 443–451

Padmarajaiah, S.K. and Ramaswamy, A. (2002) 'A Finite Element Assessment of Flexural Strength of Prestressed Concrete Beams with Fiber Reinforcement'. *Cement & Concrete Composite* [online] 24, 229–241. available from <www.elsevier.com/locate/cemconcomp>

Padmini, A.K., Ramamurthy, K., and Mathews, M.S. (2009) 'Influence of Parent Concrete on the Properties of Recycled Aggregate Concrete'. *Construction and Building Materials* [online] 23 (2), 829–836. available from <http://dx.doi.org/10.1016/j.conbuildmat.2008.03.006>

Pedro, D., de Brito, J., and Evangelista, L. (2017) 'Structural Concrete with Simultaneous Incorporation of Fine and Coarse Recycled Concrete Aggregates: Mechanical, Durability and Long-Term Properties'. *Construction and Building Materials* [online] 154, 294–309. available from <http://dx.doi.org/10.1016/j.conbuildmat.2017.07.215>

Pepe, M., Koenders, E.A.B., Faella, C., and Martinelli, E. (2014) 'Structural Concrete Made with Recycled Aggregates: Hydration Process and Compressive Strength Models'. *Mechanics Research Communications* [online] 58, 139–145. available from <http://dx.doi.org/10.1016/j.mechrescom.2014.02.001>

Pilakoutas, K., Neocleous, K., and Tlemat, H. (2004) 'Reuse of Tyre Steel Fibres as Concrete Reinforcement'. *Proceedings of the ICE: Engineering Sustainability* 157 (3), 131–138

Poon, C.S., Shui, Z.H., Lam, L., Fok, H., and Kou, S.C. (2004) 'Influence of Moisture States of Natural and Recycled Aggregates on the Slump and Compressive Strength of Concrete'. *Cement and Concrete Research* 34 (1), 31–36

Pradhan, S., Kumar, S., and Barai, S. V. (2018) 'Performance of Reinforced Recycled Aggregate Concrete Beams in Flexure: Experimental and Critical Comparative Analysis'. *Materials and Structures/Materiaux et Constructions* 51 (3)

Pradhan, S., Kumar, S., and Barai, S. V. (2017) 'Recycled Aggregate Concrete: Particle Packing Method (PPM) of Mix Design Approach'. *Construction and Building Materials* [online] 152, 269–284. available from <http://dx.doi.org/10.1016/j.conbuildmat.2017.06.171>

Punmia, B.C., Jain, Ashok K., and Jain, Arun K. (1992) *REINFORCED CONCRETE. STRUCTURES*. fifth. vol. II. Laxmi Publications Ltd

Purkiss, J.A., Wilson, P.J., and Blagojevic, P. (1997) 'Determination of the Load-Carrying Capacity of Steel Fibre Reinforced Concrete Beams'. *Composite Structures* 38 (1), 111–117

Van Der Putten, J., Dils, J., Minne, P., Boel, V., and De Schutter, G. (2017) 'Determination of Packing Profiles for the Verification of the Compressible Packing Model in Case of UHPC Pastes'. *Materials and Structures/Materiaux et Constructions* 50 (2)

Qin, W., Chen, Y., and Chen, Z. (2012) 'Experimental Study on Flexural Behaviors of All-Lightweight Aggregate Concrete Beams and Slabs'. *Applied Mechanics and Materials* [online] 566–169, 1614–1619. available from <http://www.scientific.net/KEM.517.398>

Rahal, K. (2007) 'Mechanical Properties of Concrete with Recycled Coarse Aggregate'. *Building and Environment* 42 (1), 407–415

Ravindrarajah, R.S. (1996) 'Effects of Using Recycled Concrete as Aggregate on the Engineering Properties of Concrete'. *National Symposium on the Use of Recycled Materials in Engineering Construction Journal* 147–152

Ray, S.P. and Venkateswarlu, B. (1991) 'Recycled Aggregate Concrete'. *J. Struct. Eng.* 18 (2), 67–75

Richardson, A.E., Coventry, K.A., and Wilkinson, S. (2012) 'Freeze/Thaw Durability of Concrete with Synthetic Fibre Additions'. *Cold Regions Science and Technology* [online] 83–84, 49–56. available from <http://dx.doi.org/10.1016/j.coldregions.2012.06.006>

Rodrigues, F., Carvalho, M.T., Evangelista, L., and De Brito, J. (2013) 'Physical-Chemical and Mineralogical Characterization of Fine Aggregates from Construction and Demolition Waste Recycling Plants'. *Journal of Cleaner Production* [online] 52, 438–445. available from <http://dx.doi.org/10.1016/j.jclepro.2013.02.023>

Sagoe-Crentsil, K.K., Brown, T., Mak, S.L., and Taylor, A. (1996) 'Engineering Properties and Performance of Concrete Made with Recycled Construction Aggregates'. in *National Symposium on the Use of Recycling Materials in Engineering Construction.* held 1996 at Sydney, Australia

Sagoe-Crentsil, K.K., Brown, T., and Taylor, A.H. (2001) *Performance of Concrete Made with Commercially Produced Coarse Recycled Concrete Aggregate*. 31, 707–712

Salem, R.M., Burdette, E.G., and Jackson, N.M. (2003) 'Resistance to Freezing and Thawing of Recycled Aggregate Concrete'. *ACI Materials Journal* [online] 100 (3), 216–221. available from <http://www.scopus.com/inward/record.url?eid=2-s2.0-0942268512&partnerID=40&md5=748951c2972dd3536f2a78223ef639e5>

Sato, R., Maruyama, I., Sogabe, T., and Sogo, M. (2007) 'Flexural Behavior of Reinforced Recycled Aggregate Concrete Beams'. *Journal of Advanced Concrete*

Technology [online] 5 (1), 43–61. available from <http://koreascience.or.kr/journal/view.jsp?kj=CCRTCN&py=2009&vnc=v21n4&sp=431>

Schubert, S., Hoffmann, C., Leemann, A., Moser, K., and Motavalli, M. (2012) 'Recycled Aggregate Concrete: Experimental Shear Resistance of Slabs without Shear Reinforcement'. *Engineering Structures* [online] 41, 490–497. available from <http://dx.doi.org/10.1016/j.engstruct.2012.04.006>

Senaratne, S., Gerace, D., Mirza, O., Tam, V.W.Y., and Kang, W.H. (2016) 'The Costs and Benefits of Combining Recycled Aggregate with Steel Fibres as a Sustainable, Structural Material'. *Journal of Cleaner Production* [online] 112, 2318–2327. available from <http://dx.doi.org/10.1016/j.jclepro.2015.10.041>

Shima, H., Tateyashiki, H., Matsuhashi, R., and Yoshida, Y. (2005) 'An Advanced Concrete Recycling Technology and Its Applicability Assessment through Input-Output Analysis'. *Journal of Advanced Concrete Technology* [online] 3 (1), 53–67. available from <http://joi.jlc.jst.go.jp/JST.JSTAGE/jact/3.53?from=CrossRef>

Silva, R. V., de Brito, J., and Dhir, R.K. (2017) 'Availability and Processing of Recycled Aggregates within the Construction and Demolition Supply Chain: A Review'. *Journal of Cleaner Production* [online] 143, 598–614. available from <http://dx.doi.org/10.1016/j.jclepro.2016.12.070>

Silva, R. V., De Brito, J., and Dhir, R.K. (2014) 'Properties and Composition of Recycled Aggregates from Construction and Demolition Waste Suitable for Concrete Production'. *Construction and Building Materials* [online] 65, 201–217. available from <http://dx.doi.org/10.1016/j.conbuildmat.2014.04.117>

Silva, R.V., De Brito, J., and Dhir, R.K. (2016) 'Establishing a Relationship between Modulus of Elasticity and Compressive Strength of Recycled Aggregate Concrete'. *Journal of Cleaner Production* [online] 112, 2171–2186. available from <http://dx.doi.org/10.1016/j.jclepro.2015.10.064>

Sim, J. and Park, C. (2011) 'Compressive Strength and Resistance to Chloride Ion Penetration and Carbonation of Recycled Aggregate Concrete with Varying Amount of Fly Ash and Fine Recycled Aggregate'. *Waste Management* [online] 31 (11), 2352–2360. available from <http://dx.doi.org/10.1016/j.wasman.2011.06.014>

Snyder, M.B. (2016) 'Concrete Pavement Recycling and the Use of Recycled Concrete

Aggregate in Concrete Paving Mixtures'. *CP Road Map* [online] (March), 1–7. available from <www.cproadmap.org/publications/MAPbriefMarch2016.pdf>

Soares, D., De Brito, J., Ferreira, J., and Pacheco, J. (2014) 'Use of Coarse Recycled Aggregates from Precast Concrete Rejects: Mechanical and Durability Performance'. *Construction and Building Materials* [online] 71, 263–272. available from <http://dx.doi.org/10.1016/j.conbuildmat.2014.08.034>

Somna, R., Jaturapitakkul, C., and Amde, A.M. (2012) 'Effect of Ground Fly Ash and Ground Bagasse Ash on the Durability of Recycled Aggregate Concrete'. *Cement and Concrete Composites* [online] 34 (7), 848–854. available from <http://dx.doi.org/10.1016/j.cemconcomp.2012.03.003>

Swamy, R.N. and Bahia, H.M. (1985) 'The Effectiveness of Steel Fibers as Shear Reinforcement'. *Concrete International* 35–40

Tabsh, S.W. and Abdelfatah, A.S. (2009) 'Influence of Recycled Concrete Aggregates on Strength Properties of Concrete'. *Construction and Building Materials* [online] 23 (2), 1163–1167. available from <http://dx.doi.org/10.1016/j.conbuildmat.2008.06.007>

Tam, V., Mirza, O., Senaratne, S., and Kang, W.H. (2014) 'Sustainable Structural Material Combining Recycled Aggregate and Steel Fibres'. in *World Construction Symposium*. held 2014 at Colombo, Sri Lanka. Ceylon Institute of Builders, 567–574

Tam, V.W.Y., Gao, X.F., and Tam, C.M. (2006) 'Environmental Enhancement through Use of Recycled Aggregate Concrete in a Two-Stage Mixing Approach'. *Human and Ecological Risk Assessment* [online] 12 (2), 277–288. available from <https://doi.org/10.1080/10807030500531653>

Tam, V.W.Y., Gao, X.F., and Tam, C.M. (2005) 'Microstructural Analysis of Recycled Aggregate Concrete Produced from Two-Stage Mixing Approach'. *Cement and Concrete Research* 35, 1195–1203

Tam, V.W.Y. and Tam, C.M. (2008) 'Diversifying Two-Stage Mixing Approach (TSMA) for Recycled Aggregate Concrete: TSMAsand TSMAsc'. *Construction and Building Materials* 22 (10), 2068–2077

Tam, V.W.Y. and Tam, C.M. (2007) 'Assessment of Durability of Recycled Aggregate

Concrete Produced by Two-Stage Mixing Approach'. *Journal of Materials Science* 42 (10), 3592–3602

Tam, V.W.Y., Tam, C.M., and Le, K.N. (2007) 'Removal of Cement Mortar Remains from Recycled Aggregate Using Pre-Soaking Approaches'. *Resources, Conservation and Recycling* 50 (1), 82–101

Teychenné, D.C., Franklin, R.E., and Erntroy, H.C. (1997) *Design of Normal Concrete Mixes*. Second edi. ed. by Marsh, B.K. vol. 331

Thomas, C., Cimentada, A., Polanco, J.A., Setién, J., Méndez, D., and Rico, J. (2013) 'Influence of Recycled Aggregates Containing Sulphur on Properties of Recycled Aggregate Mortar and Concrete'. *Composites Part B:* [online] 45 (1), 474–485. available from <http://dx.doi.org/10.1016/j.compositesb.2012.05.019>

Thomas, C., Setién, J., and Polanco, J.A. (2016) 'Structural Recycled Aggregate Concrete Made with Precast Wastes'. *Construction and Building Materials* [online] 114, 536–546. available from <http://dx.doi.org/10.1016/j.conbuildmat.2016.03.203>

Tlemat, H. (2004) *Steel Fibres from Waste Tyres to Concrete: Testing, Modelling and Design. Ph.D. Thesis, The University of Sheffield, UK.*

Topcu, I.B. and Sengel, S. (2004) 'Properties of Concretes Produced with Waste Concrete Aggregate'. *Concrete and Concrete Research* 34, 1307–1312

Tu, T.Y., Chen, Y.Y., and Hwang, C.L. (2006) 'Properties of HPC with Recycled Aggregates'. *Cement and Concrete Research* 36, 943–950

Tuyan, M., Mardani-Aghabaglou, A., and Ramyar, K. (2014) 'Freeze-Thaw Resistance, Mechanical and Transport Properties of Self-Consolidating Concrete Incorporating Coarse Recycled Concrete Aggregate'. *Materials and Design* [online] 53, 983–991. available from <http://dx.doi.org/10.1016/j.matdes.2013.07.100>

Vaishali, G.G. and Rao, H.S. (2012) 'Strength and Permeability Characteristics of Fiber Reinforced High Performance Concrete with Recycled Aggregates'. *Asian Journal of Civil Engineering* 13 (1), 55–78

Vasudevan, G., Kothandaraman, S., and Azhagarsamy, S. (2013) 'Study on Non-Linear Flexural Behavior of Reinforced Concrete Beams Using ANSYS by Discrete Reinforcement Modeling'. *Strength of Materials* 45 (2), 231–241

Vázquez, E., Barra, M., Aponte, D., Jiménez, C., and Valls, S. (2014) 'Improvement of the Durability of Concrete with Recycled Aggregates in Chloride Exposed Environment'. *Construction and Building Materials* 67, 61–67

Verian, K.P., Ashraf, W., and Cao, Y. (2018) 'Properties of Recycled Concrete Aggregate and Their Influence in New Concrete Production'. *Resources, Conservation and Recycling* [online] 133 (February), 30–49. available from <https://doi.org/10.1016/j.resconrec.2018.02.005>

Villagrán-Zaccardi, Y.A., Zega, C.J., and Di Maio, Á.A. (2008) 'Chloride Penetration and Binding in Recycled Concrete'. *Journal of Materials in Civil Engineering* 20 (6), 449–455

Wagih, A.M., El-Karmoty, H.Z., Ebid, M., and Okba, S.H. (2013) 'Recycled Construction and Demolition Concrete Waste as Aggregate for Structural Concrete'. *HBRC Journal* [online] 9 (3), 193–200. available from <http://linkinghub.elsevier.com/retrieve/pii/S1687404813000588>

Wang, L., Wang, J., Qian, X., Chen, P., Xu, Y., and Guo, J. (2017) 'An Environmentally Friendly Method to Improve the Quality of Recycled Concrete Aggregates'. *Construction and Building Materials* [online] 144, 432–441. available from <http://dx.doi.org/10.1016/j.conbuildmat.2017.03.191>

Wardeh, G., Ghorbel, E., and Gomart, H. (2015) 'Mix Design and Properties of Recycled Aggregate Concretes: Applicability of Eurocode 2'. *International Journal of Concrete Structures and Materials* 9 (1), 1–20

WBCSD (2012) *The Cement Sustainability Initiative- Recycling Concrete* [online] available from <https://www.wbcsdcement.org/pdf/CSI-RecyclingConcrete-FullReport.pdf> [1 November 2017]

Won, J.-P., Hong, B.-T., Choi, T.-J., Lee, S.-J., and Kang, J.-W. (2012) 'Flexural Behaviour of Amorphous Micro-Steel Fibre-Reinforced Cement Composites'. *Composite Structures* 94, 1443–1449

Won, J.P., Hong, B.T., Lee, S.J., and Choi, S.J. (2013) 'Bonding Properties of Amorphous Micro-Steel Fibre-Reinforced Cementitious Composites'. *Composite Structures* [online] 102, 101–109. available from <http://dx.doi.org/10.1016/j.compstruct.2013.02.015>

WRAP (2007) *Waste Recovery Quick Wins*. (July 2006). 36. available from <http://www.wrapni.org.uk/sites/files/wrap/Waste Recovery Quick Wins FINAL.pdf>

Xiao, J., Li, J., and Zhang, C. (2005) 'Mechanical Properties of Recycled Aggregate Concrete under Uniaxial Loading'. *Cement and Concrete Research* 35 (6), 1187–1194

Xiao, J., Li, W., Fan, Y., and Huang, X. (2012) 'An Overview of Study on Recycled Aggregate Concrete in China (1996-2011)'. *Construction and Building Materials* [online] 31, 364–383. available from <http://dx.doi.org/10.1016/j.conbuildmat.2011.12.074>

Yang, K., Chung, H., and Ashour, A.F. (2008) 'Influence of Type and Replacement Level of Recycled Aggregates on Concrete Properties'. *ACI Materials Journal* 105 (3), 289–296

Yoo, D.-Y., Lee, J.-H., and Yoon, Y.-S. (2013) 'Effect of Fiber Content on Mechanical and Fracture Properties of Ultra High Performance Fiber Reinforced Cementitious Composites'. *Composite Structures* [online] 106, 742–753. available from <http://linkinghub.elsevier.com/retrieve/pii/S0263822313003565>

Younis, K.H., Pilakoutas, K., Guadagnini, M., and Angelakopoulos, H. (2014) 'Feasibility of Using Recycled Steel Fibres To Enhance the Behaviour of Recycled Aggregate Concrete'. *FRC 2014 Joint ACI-Fib International Workshop - Fibre Reinforced Concrete: From Design to Structural Applications* 113–122

Zaharieva, R., Buyle-Bodin, F., and Wirquin, E. (2004) 'Frost Resistance of Recycled Aggregate Concrete'. *Cement and Concrete Research* 34 (10), 1927–1932

Zhang, F., Ding, Y., Xu, J., Zhang, Y., Zhu, W., and Shi, Y. (2016) 'Shear Strength Prediction for Steel Fiber Reinforced Concrete Beams without Stirrups'. *Engineering Structures* [online] 127, 101–116. available from <http://dx.doi.org/10.1016/j.engstruct.2016.08.012>

Appendix A

Design of Conventional Concrete

Design of NAC according to ACI Committee 211 (2009) using the aggregates properties shown in Tables 3.2 and 3.5:

From Table A1.6.3.3, the required water content for $75-100\text{mm}$ slump $= 213\text{kg/m}^3$

From Table A1.6.3.4, water-cement ratio $(^{w}/_{c}) = 0.42$ for concrete of 40MPa strength

Therefore, cement content $= {}^{213}/_{0.42} = 507\text{kg/m}^3$

From Table A1.6.3.6, triple interpolation for fineness modulus of 2.87 gave the dry-rodded volume of concrete as 0.55

Thus, the required dry mass of coarse aggregate $= 0.55 \times 1556 = 856\text{kg/m}^3$

Now, using the absolute volume method:

- Volume of water, $V_w = {}^{213}/_{1000} = 0.213\text{m}^3$
- Solid volume of cement, $V_c = {}^{507}/_{3.15 \times 1000} = 0.161\text{m}^3$
- Solid volume of coarse aggregate, $V_{ca} = {}^{856}/_{2.61 \times 1000} = 0.328\text{m}^3$
- Volume of entrapped air, $V_a = {}^{2.38}/_{100} \times 1.0 = 0.274\text{m}^3$
- Solid volume of fine aggregate, $V_{fa} = 1 - (V_w + V_c + V_{ca} + V_a) = 1 - 0.726$

$$= 0.274\text{m}^3$$

The required volume of fine aggregate $= 0.274 \times 2.58 \times 1000 = 707\text{kg/m}^3$

Hence, the mix proportion for the NAC constituents in dry state is as shown in Table A.

Table A: Mix proportions of NAC (kg/m^3)

Water	Cement	Aggregates	
		Fine	Coarse
213	507	707	856

Appendix B

Equivalent Mortar Volume Mix Proportioning Technique

Design of BAC using the EMV method proposed by Fathifazl et al. (2009a):

Step 1: Proportioning of NAC based on ACI method (ACI Committee 211 2009).

This reference mix was first designed, and the resulting quantity of each constituent is:

$$\text{Water} = 507\text{kg/m}^3$$

$$\text{Cement} = 213\text{kg/m}^3$$

$$\text{Oven} - \text{dry NCA} = 856\text{kg/m}^3$$

$$\text{Oven} - \text{dry NFA} = 707\text{kg/m}^3$$

Step 2: Checking whether complete replacement of NCA with RCA is possible.

The condition for a complete replacement is that the calculated residual mortar content (RMC) must be greater than the actual value obtained as described in Section 3.3 of this paper. The maximum residual mortar content is given by:

$$\text{RMC}_{\text{max}}\% = \left(1 - \text{V}_{\text{DR-NCA}}^{\text{NAC}} \times \frac{\text{S}_{\text{b}}^{\text{NCA}}}{\text{S}_{\text{b}}^{\text{RCA}}}\right) \times 100$$

Where $\text{V}_{\text{DR-NCA}}^{\text{NAC}}$ is the dry-rodded volume of the NCA in NAC, $\text{S}_{\text{b}}^{\text{NCA}}$ is the bulk specific gravity of NCA and $\text{S}_{\text{b}}^{\text{RCA}}$ is the bulk specific gravity of RCA.

By interpolations using Table A1.6.3.6 (ACI Committee 211 2009) with fineness modulus of 2.71,

$$\text{Dry} - \text{rodded volume of NCA} = 0.55$$

Also, from Table 2 of this paper,

$$\text{Bulk specific gravity of RCA} = 2.30$$

and $\text{Bulk specific gravity of NCA} = 2.61$

This implies,

$$\text{RMC}_{\text{max}} = 1 - 0.55 \times \frac{2.61}{2.30} = 37.6\%$$

But from Table 2, the actual RMC of the RCA is 52%, hence it is not feasible to fully substitute NCA with RCA.

Step 3: Checking the minimum quantity of fresh NCA in RAC.

This is given by:

$$R_{min} = 1 - \frac{(1-RMC)}{V_{DR-NCA}^{NAC}} \times \frac{S_b^{RCA}}{S_b^{NCA}}$$

$$R_{min} = 1 - \frac{1-0.52}{0.55} \times \frac{2.30}{2.61} = 23\%$$

To make up for the NCA in RAC mixes in comparison with NAC mixes, the volume of fresh NCA in RAC is assumed to be the equivalent to the volume of the residual mortar. Thus,

$$R = 1 - (1 - RMC) \times \frac{S_b^{RCA}}{S_b^{NCA}}$$

$$R = 1 - (1 - 0.52) \times \frac{2.30}{2.61} = 57.7\%$$

Where R is the volume of fresh NCA in RAC.

Step 4: Calculate the required volume of RCA and NCA in RAC

(i) $$V_{RCA}^{RAC} = V_{NCA}^{NAC} = \frac{W_{OD-NCA}^{NAC}}{S_b^{NCA} \times 1000} = \frac{856}{2.61 \times 1000} = 0.328$$

(ii) $$V_{NCA}^{RAC} = R \times V_{NCA}^{NAC} = 0.577 \times 0.328 = 0.189$$

Where V_{RCA}^{RAC} and V_{NCA}^{RAC} are respectively the volume of RCA and NCA in RAC, V_{NCA}^{NAC} and W_{OD-NCA}^{NAC} are volume of NCA in NAC and oven-dry weight of NCA in NAC, respectively.

Step 5: Calculate the required oven-dry weight of RCA and NCA in RAC.

(i) $$W_{OD-RCA}^{RAC} = V_{RCA}^{RAC} \times S_b^{RCA} \times 1000 = 0.328 \times 2.30 \times 1000 = 754kg$$

(ii) $$W_{OD-NCA}^{RAC} = V_{NCA}^{RAC} \times S_b^{NCA} \times 1000 = 0.189 \times 2.61 \times 1000 = 493kg$$

Where W_{OD-RCA}^{RAC} is the oven-dry weight of RCA in RAC.

Step 6: Calculate the required fresh mortar (FM) and residual mortar (RM) in RAC.

(i) $V_{RM}^{RAC} = V_{RCA}^{RAC} \times \left[1 - (1 - RMC) \times \frac{S_b^{RCA}}{S_b^{NCA}}\right] = 0.328 \times [1 - (1 - 0.52) \times \frac{2.30}{2.61} = 0.189$

(ii) $V_{FM}^{RAC} = V_{M}^{NAC} - V_{RM}^{RAC} = 0.672 - 0.189 = 0.483$

Note: $V_{M}^{NAC} = 1 - V_{RCA}^{RAC} = 1 - 0.328$ and V_{RM}^{RAC}, V_{FM}^{RAC} and V_{M}^{NAC} are volume of RM in RAC, volume of FM in RAC and volume of mortar in NAC, respectively.

Step 7: Calculate the required water, cement, and natural fine aggregate (NFA) in RAC.

$$W_{W}^{RAC} = W_{W}^{NAC} \times \frac{V_{FM}^{RAC}}{V_{M}^{NCA}} = 213 \times \frac{0.483}{0.672} = 153\text{kg}$$

$$W_{C}^{RAC} = W_{C}^{NAC} \times \frac{V_{FM}^{RAC}}{V_{M}^{NCA}} = 507 \times \frac{0.483}{0.672} = 364\text{kg}$$

$$W_{OD-NFA}^{RAC} = W_{OD-NFA}^{NAC} \times \frac{V_{FM}^{RAC}}{V_{M}^{NCA}} = 707 \times \frac{0.483}{0.672} = 508\text{kg}$$

Where W_{W}^{RAC}, W_{W}^{NAC}, W_{C}^{RAC}, W_{C}^{NAC} and W_{OD-NFA}^{RAC} are weight of water in RAC, weight of water in NAC, weight of cement in RAC, weight of cement in NAC and weight of oven-dry NFA in RAC, respectively

Step 8: This is an additional step to incorporate RFA in the mix.

From steps 5 and 7, it can be seen that the required quantity of materials is: Cement (364kg), Water (153kg), RCA (754kg), NCA (493kg) and NFA (508kg). This gives the ratio of RCA:NCA as 1.5:1. Applying this ratio to the fine aggregates as follows:

$$RFA = {}^{1.5}/_{2.5} \times 508 = 305\text{kg}$$

and $$NFA = {}^{1}/_{2.5} \times 508 = 203\text{kg}$$

Appendix C

Compressive Strength Data

The cube compressive strength of concrete for all the investigated mixes at 7, 28, and 56 days:

Mix ID	Specimen No.	Compressive strength (MPa)		
		7 days	28 days	56 days
NAC	1	55.9	69.9	75.8
	2	56.7	65.5	78.2
	3	59.4	63.8	76.2
	4	61.2	67.0	68.2
	5	60.0	66.8	75.7
Average		*58.6*	*66.6*	*74.8*
Std. dev.		*2.21*	*2.25*	*3.81*
RAC	1	45.2	55.7	57.9
	2	44.2	55.9	56.7
	3	46.7	50.7	57.8
	4	46.2	55.4	55.7
	5	41.6	52.4	51.6
Average		*44.8*	*54.0*	*55.9*
Std. dev.		*2.04*	*2.36*	*2.59*
SFRRAC	1	51.2	59.9	64.1
	2	52.5	61.3	63.5
	3	51.0	59.0	64.6
	4	53.1	60.5	63.4
	5	53.7	60.2	67.8
Average		*52.3*	*60.2*	*64.7*
Std. dev.		*1.16*	*0.82*	*1.83*
BAC	1	55.8	63.3	63.5
	2	51.6	58.4	60.6
	3	56.0	60.2	65.7
	4	54.4	63.4	64.6
	5	54.7	63.2	65.2
Average		*54.5*	*61.7*	*63.9*
Std. dev.		*1.76*	*2.28*	*2.03*
SFRBAC	1	47.2	58.0	62.3
	2	47.5	59.1	59.3
	3	45.2	57.3	61.6
	4	45.4	60.0	60.2
	5	44.9	55.8	62.5
Average		*46.0*	*58.0*	*61.2*
Std. dev.		*1.22*	*1.60*	*1.38*

Appendix D

Theoretical Parameters of the Beams

The determination of the theoretical parameters defining the reinforced concrete beams produced from NAC, RAC, SFRRAC, and BAC mixes:

The computation for determining the parameters for the NAC beam are presented here using the following information:

i. Concrete cover, $C = 20mm$
ii. Area of steel reinforcements (2Y10), $A_s = 157.08mm^2$
iii. Width of beam, $b = 80mm$
iv. Overall depth of beam, $h = 180mm$

Hence, the effective depth of beam, $d = h - C - 0.5 \times diameter\ of\ steel = 155mm$

v. Shear span of beam, $a = 400mm$
vi. Elastic modulus for concrete, $E_c = 4700\sqrt{f_c}$ where f_c is the compressive strength of the concrete (MPa)
vii. Elastic modulus of steel, E_s

Hence, the modular ratio, $n = {}^{E_s}/_{E_c} = {}^{210000}/_{34300} = 6.12$

- **Determining the neutral axis depth, y**

Recalling Equation 4.3, the neutral axis depth, y is given by:

$$y = \frac{nA_s}{b}\left(\sqrt{1 + \frac{2bd}{mA_s}} - 1\right)$$

On substituting,

$$y = \frac{6.12 \times 157.08}{80}\left(\sqrt{1 + \frac{2 \times 80 \times 155}{6.12 \times 157.08}} - 1\right)$$

Therefore,

$$y = 50.19mm$$

- **Determining the moment of inertia, I**

Recalling Equation 4.2, the moment of inertia, I is given by:

$$I = \frac{by^3}{3} + nA_s(d-y)^2$$

On substituting,

$$I = \frac{80 \times 50.19^3}{3} + 6.12 \times 157.08\,(155 - 50.19)^2$$

Therefore,

$$I = 13931814.41mm^4$$

- **Determining the moment of resistance, M_R also known as the ultimate moment capacity of the beam**

Recalling Equation 4.4, the moment of resistance, M_R is given by:

$M_R = \frac{f_c}{2} by\left(d - \frac{y}{3}\right)$, where f_c is the cylindrical compressive strength of the concrete.

On substituting,

$$M_R = \frac{53.3}{2} \times 80 \times 50.19\left(155 - \frac{50.19}{3}\right) \times 10^6$$

$$M_R = 14.8kNm$$

- **Determining the ultimate load, P_{ult}**

Recalling Equation 4.6, the ultimate load, P_{ult} is given by:

$$P_{ult} = \frac{2M_R}{a}$$

On substituting,

$$P_{ult} = \frac{2 \times 14.8}{0.4}$$

$$P_{ult} = 74kN$$

Similar procedures were followed to obtain the corresponding values for the RAC, SFRRAC, and BAC beams.

Appendix E

New Compressive Strength Data

The results of the new compressive strength of concrete cubes for all mixes due change of cement:

Table C: "New" compressive strength of concrete measured at 28 days.

Mix ID	Specimen No.	Compressive strength		Average compressive strength (MPa)
		MPa	Std dev.	
NAC	1	56.8		
	2	57.0	0.21	57.0
	3	57.2		
RAC	1	48.9		
	2	54.5	3.57	50.4
	3	47.9		
SFRRAC	1	58.8		
	2	60.0	0.59	59.4
	3	59.4		
BAC	1	52.7		
	2	52.9	1.71	51.9
	3	49.9		
SFRBAC	1	52.2		
	2	51.3	1.13	52.4
	3	53.6		